



UNIVERSIDADE FEDERAL DE SANTA CATARINA
CENTRO TECNOLÓGICO
PROGRAMA DE PÓS-GRADUAÇÃO EM ENGENHARIA QUÍMICA

Danyelle Gurgel

Immobilization of Laccase on Poly(propylene-styrene)/polyacrylonitrile Core-shell Particles for Doxorubicin Degradation

Florianópolis
2024

Danyelle Gurgel

Immobilization of Laccase on Poly(propylene-styrene)/polyacrylonitrile Core-shell Particles for Doxorubicin Degradation

Tese submetida ao Programa de Pós-Graduação em Engenharia Química da Universidade Federal de Santa Catarina como requisito parcial para a obtenção do título de Doutora em Engenharia Química.

Orientador: Prof. Agenor Furigo Júnior, Dr.
Coorientadores: Prof. Bruno Francisco Oechsler, Dr. e Rosana Oliveira Henriques, Dr^a.

Florianópolis

2024

Gurgel, Danyelle

Immobilization of Laccase on Poly(propylene-styrene)/polyacrylonitrile Core-shell Particles for Doxorubicin Degradation / Danyelle Gurgel ; orientador, Agenor Furigo Júnior, coorientador, Bruno Francisco Oechsler, coorientadora, Rosana Oliveira Henriques, 2024.
164 p.

Tese (doutorado) - Universidade Federal de Santa Catarina, Centro Tecnológico, Programa de Pós-Graduação em Engenharia Química, Florianópolis, 2024.

Inclui referências.

1. Engenharia Química. 2. Degradação de fármacos. 3. Doxorubicina. 4. Imobilização de enzimas. 5. Polímeros casca-núcleo. I. Júnior, Agenor Furigo. II. Oechsler, Bruno Francisco . III. Henriques, Rosana Oliveira IV. Universidade Federal de Santa Catarina. Programa de Pós-Graduação em Engenharia Química. V. Título.

Danyelle Gurgel

**Immobilization of Laccase on Poly(propylene-styrene)/polyacrylonitrile Core-shell
Particles for Doxorubicin Degradation**

O presente trabalho em nível de Doutorado foi avaliado e aprovado, em 21 de junho de 2024, pela banca examinadora composta pelos seguintes membros:

Prof^a. Claudia Sayer, Dr^a.

Universidade Federal de Santa Catarina (UFSC)

Martina Costa Cerqueira Pinto, Dr^a.

Universidade Federal do Rio de Janeiro (UFRJ)

Prof. Everton Skoronski, Dr.

Universidade do Estado de Santa Catarina (UDESC)

Certificamos que esta é a versão original e final do trabalho de conclusão que foi julgado adequado para obtenção do título de Doutora em Engenharia Química.

Insira neste espaço a
assinatura digital

Coordenação do Programa de Pós-Graduação

Insira neste espaço a
assinatura digital

Prof. Agenor Furigo Júnior, Dr.

Orientador

Florianópolis, 2024.

AGRADECIMENTOS

A Deus, pela proteção, graça e por ter me concedido tantas oportunidades.

À minha família, que sempre demonstrou muito amor, carinho e incentivo diante de todas as minhas escolhas. Em especial aos meus pais, Francisco das Chagas Gurgel e Antônia Valdirene Gomes, e minha irmã Denise Gurgel, por serem minha base e exemplo de determinação.

Ao meu amado esposo, Alisson Lopes Freire, que acompanhou de perto cada parte da construção do presente trabalho, pelo amor, carinho e parceria de sempre.

Aos meus amigos e colegas de laboratório, pela companhia durante a construção do trabalho, pelos momentos de descontração e por toda ajuda que me deram. Agradeço especialmente: Yago Vieira, Maikon Kelbert, Vitor Conradi, Tamara Agner, Amanda Vasconcelos, Júlia Oliveira, Thayli Araújo e Juliana Zanatta.

Aos meus coorientadores Rosana Oliveira Henriques e Bruno Francisco Oechsler pela paciência e toda a contribuição neste trabalho.

Ao professor Ricardo Antônio Francisco Machado pelo conhecimento e toda ajuda oferecida durante a realização do trabalho.

À professora Débora de Oliveira, que participou ativamente de todas as etapas do trabalho, por compartilhar seu conhecimento e suas ideias.

Ao meu querido orientador, Agenor Furigo Júnior, que acompanhou de perto o desenvolvimento de cada etapa do trabalho, pelos ensinamentos e pelos questionamentos que enriqueceram os resultados da pesquisa.

Aos amigos que me acompanharam fora do ambiente de laboratório pelos momentos de lazer, pelos conselhos, pelas gargalhadas e por me ajudarem a viver outras partes da vida. Agradeço especialmente: Camila Senna, Ana Cláudia da Costa Rocha, Luiz Paulo Soares, Dario Genari, Kassia Kramer, Rafael Amaral, Kamila Ferreira, Joceane Azolim e Lucas Mello.

À Universidade Federal de Santa Catarina, especialmente ao Departamento de Engenharia Química e Engenharia de Alimentos (EQA), por todo suporte e infraestrutura necessária à realização do trabalho.

À Central de Análises do Departamento de Química pela estrutura disponibilizada para a realização de análises de RMN, ao Laboratório Multiusuário de Estudos em Biologia (LAMEB) por disponibilizar sua estrutura e equipamentos na realização do trabalho e à Central de Análises do EQA, especialmente ao Leandro

Guarezi Nandi e à Fernanda Volpato, pela disposição e prontidão na realização das análises solicitadas.

À Termotécnica LTDA pela doação de insumos necessários para a realização do trabalho.

Por fim, gostaria de agradecer à Coordenação de Aperfeiçoamento de Pessoal de Nível Superior (CAPES) e ao Conselho Nacional de Desenvolvimento Científico e Tecnológico (CNPq) pelo auxílio financeiro durante todo o período de doutorado.

“O que é mais importante, a jornada ou o destino?” Perguntou o Grande Panda,

“A companhia.” Disse o pequeno dragão.

O Grande Panda e o Pequeno Dragão

(James Norbury).

RESUMO EXPANDIDO

Introdução

Os fármacos antineoplásicos são muito utilizados no tratamento de diversos tipos de câncer e estão se tornando mais presentes à medida que os casos da doença aumentam mundialmente (VERMETTE *et al.*, 2024). A Doxorrubicina (DOX), por exemplo, foi detectada em águas residuais de hospitais oncológicos e em efluentes de estações de tratamento comuns (KELBERT *et al.*, 2021). Diante disso, há uma crescente preocupação relacionada ao impacto negativo destes compostos ao ecossistema (KELBERT *et al.*, 2021; PEREIRA, 2020). Neste cenário, as lacases são enzimas capazes de catalisar a oxidação de vários substratos (COMAN *et al.*, 2023) e são promissoras para a degradação de compostos farmacêuticos. No entanto, há uma desvantagem na utilização da lacase livre devido à sua inativação em águas residuais e indisponibilidade para reutilização (BHARDWAJ *et al.*, 2022). A imobilização de enzimas em um suporte sólido é uma estratégia comprovada para a reutilização dos biocatalisadores, separação de produtos, reciclagem, e desenvolvimento de processos contínuos. Para isso, o suporte enzimático deve apresentar características e condições de imobilização apropriadas para sustentar a atividade da enzima, como alta estabilidade química e mecânica, elevada área específica, grau de hidrofobicidade adequado e grupos funcionais disponíveis (CHEN; OH; YAP, 2022). Neste contexto, partículas poliméricas com estrutura casca-núcleo oferecem diversas vantagens quando aplicadas como suporte na imobilização de enzimas, como a capacidade de atingir propriedades específicas que não seriam alcançadas por materiais individuais (GURGEL *et al.*, 2022). Dentre os materiais possíveis para a composição da estrutura, a poliacrilonitrila (PAN) tem sido investigada por ser um material de baixo custo e que pode ser facilmente modificada e funcionalizada para interagir bem com a lacase (VIEIRA *et al.*, 2021). O presente trabalho investigou a degradação da doxorrubicina por lacase imobilizada em partículas poliméricas de morfologia específica casca-núcleo compostas por núcleo de polipropileno/poliestireno e casca de poliacrilonitrila.

Objetivos

O principal objetivo deste trabalho é contribuir para a superação de problemas relacionados ao tratamento de águas residuais e efluentes hospitalares por meio de

tecnologia enzimática utilizando lacase imobilizada em suporte polimérico de estrutura casca-núcleo com núcleo de polipropileno/poliestireno e casca de poliácridonitrila.

Materiais e Métodos

O presente trabalho foi realizado em três etapas. A primeira etapa teve como objetivo a síntese e a caracterização de partículas poliméricas de morfologia casca-núcleo. Em seguida, estas partículas foram funcionalizadas e utilizadas como suporte enzimático para a imobilização da lacase e obtenção de um biocatalisador na segunda etapa. A última etapa consistiu em avaliar a degradação da Doxorrubicina, empregando-se o biocatalisador desenvolvido.

Síntese e Caracterização das Partículas de polipropileno (PP) e partículas híbridas de polipropileno/poliestireno (PP/PS)

As partículas comerciais de PP foram caracterizadas em termos de massa específica utilizando a análise picnométrica. A morfologia do PP foi analisada por microscopia óptica e a distribuição de tamanho de partícula (PSD) também foi medida. A análise de solubilidade em xileno (SX) foi realizada para investigar as frações solúveis e insolúveis do polímero. Além disso, foi realizado um teste de intumescimento do PP em estireno e em acrilonitrila (AN) e as curvas termogravimétricas das partículas de PP também foram obtidas. Já as partículas de PP/PS foram sintetizadas por meio de polimerização em suspensão semeada em um reator de 1 L. Estas partículas foram avaliadas quanto às suas características morfológicas, tanto por microscopia óptica, quanto por microscopia eletrônica de varredura (MEV) e foram avaliadas em termos de massa específica por picnometria e composição química por FTIR. A distribuição de tamanho de partículas (PSD) das partículas de PP/PS também foi medida. Além disso, as partículas de PP/PS foram submetidas a uma análise de fracionamento em tolueno para identificar as cadeias de poliestireno na partícula final. As curvas termogravimétricas das partículas de PP/PS também foram obtidas.

Síntese e Caracterização das Partículas casca-núcleo (CS) de PP/PS revestidas com PAN

Partículas CS foram sintetizadas por polimerização da acrilonitrila em suspensão, e precipitação da PAN na presença das partículas previamente preparadas de PP/PS. Estas partículas foram caracterizadas por microscopia para verificar a formação da casca por microscopia óptica e MEV. A área específica foi medida por fisiossorção em nitrogênio (método BET). A análise de FTIR também foi realizada para confirmar a formação de PAN na superfície. Além dessas caracterizações, realizou-se o

fracionamento das partículas PP/PS em dimetilformamida (DMF) para identificar se houve a formação de Copolímeros de Estireno Acrilonitrila (SAN). As curvas termogravimétricas e a distribuição de tamanhos das partículas de CS foram medidas.

Funcionalização da superfície das partículas CS e Imobilização da lacase

As partículas CS obtidas foram avaliadas como suporte para imobilização de lacase. Antes da imobilização, as partículas foram funcionalizadas utilizando quatro etapas, sendo um tratamento alcalino, um tratamento ácido, um tratamento com etilenodiamina e com glutaraldeído. Estas etapas foram baseadas em trabalhos anteriores (TAHERAN *et al.*, 2017a; VIEIRA *et al.*, 2023) e investigou-se a contribuição de cada uma delas para a imobilização da lacase no suporte avaliado. Para investigar a possibilidade de imobilizar a lacase sem funcionalizar o suporte ou reduzindo o número de etapas, foram elaborados cinco suportes diferentes com relação às etapas de funcionalização utilizadas. Após cada etapa de funcionalização, foram retiradas amostras para realização de análises de FTIR e H^1 RMN a fim de avaliar a incorporação de grupos funcionais específicos na superfície do material. Para a imobilização, cada suporte foi tratado com solução de lacase na concentração de $0,25 \text{ mg mL}^{-1}$ e os suportes que ofereceram os melhores resultados no rendimento de imobilização enzimática também foram submetidos a outras concentrações enzimáticas: $0,10$, $0,15$, $0,25$, $0,35$, $0,50$ e $0,60 \text{ mg mL}^{-1}$. Para todos os testes, a cinética de imobilização foi acompanhada durante 7 h, por meio da medição da atividade enzimática da solução na oxidação do ácido 2,2'-azino-bis(3-etilbenzotiazolina-6-sulfônico) (ABTS). Após a imobilização, os biocatalisadores obtidos foram lavados e o rendimento de imobilização foi determinado a partir do decaimento da atividade enzimática no sobrenadante. Para as caracterizações, foi escolhido o suporte com menor número de etapas de funcionalização e que manteve um bom rendimento de imobilização. O derivado enzimático foi então caracterizado quanto à estabilidade térmica (em temperaturas de 30° , 50° , 60° e 70° C), estabilidade em diferentes pHs (3, 5, 6 e 8), estabilidade de armazenamento (em temperatura ambiente e de geladeira), estabilidade operacional e os parâmetros cinéticos da equação de Michaelis-Menten também foram determinados.

Degradação da doxorubicina

Os testes de degradação da doxorubicina foram realizados em condições de temperatura igual a 30° C e pH 6, que são condições próximas às encontradas em

efluentes reais. Foram utilizadas as concentrações de 250 e 500 $\mu\text{g L}^{-1}$. A estabilidade operacional do derivado enzimático na degradação da DOX também foi monitorada.

Resultados e Discussão

As imagens obtidas das partículas CS indicaram a formação de uma casca de PAN uniforme ao redor no núcleo de PP/PS, diferentemente de quando se utilizou o núcleo apenas com PP, o que revelou a importância do intumescimento do polímero em estireno, que para o PP foi de 24%, enquanto para o PP/PS foi de 57%. Pelas imagens por MEV, observou-se a formação de uma casca com superfície porosa. O diâmetro de Sauter das partículas CS foi de $4,54 \pm 1,24$ μm e o fracionamento em DMF demonstrou um total de $15,98 \pm 0,82\%$ (m/m) de PAN na estrutura final. Os resultados de ^1H RMN e das cinéticas de imobilização para cada suporte (tratados com diferentes etapas de funcionalização) permitem observar que os suportes tratados com glutaraldeído ofereceram maior rendimento de imobilização da lacase. A partir destes resultados, o suporte com menor número de etapas (CS-I-IV, tratado apenas com NaOH e glutaraldeído) foi selecionado como o derivado enzimático deste estudo. Com relação à lacase livre, a lacase imobilizada ao suporte CS-I-IV demonstrou maior estabilidade térmica, mantendo mais de 80% da atividade em temperatura de 50° C. Quanto à estabilidade operacional, o derivado enzimático manteve 60% da atividade após cinco ciclos de reutilização. Os valores de parâmetros cinéticos encontrados (K_M e $V_{\text{máx}}$) indicaram alta afinidade entre o derivado e o substrato (ABTS), que foram 61,713 U L^{-1} e 1,0299 mM, respectivamente. Os resultados obtidos para degradação da DOX confirmaram que a degradação ocorreu por ação enzimática. Para testes utilizando concentração de 250 $\mu\text{g L}^{-1}$, a lacase imobilizada foi capaz de degradar aproximadamente 92% da DOX em 180 minutos. Para testes utilizando 500 $\mu\text{g L}^{-1}$, a lacase imobilizada apresentou resultados ainda mais promissores. Em 180 minutos a degradação foi de 91%, chegando a 93% em 240 minutos, enquanto a lacase livre apresentou degradação de 96% em cerca de 480 minutos, indicando que a imobilização da enzima ao suporte foi capaz de melhorar a capacidade de degradação da DOX pela lacase. A lacase imobilizada pôde ser reaproveitada ao menos cinco vezes, quando ainda manteve atividade acima de 60%. Após o sexto ciclo de reutilização, o derivado promoveu 29% de degradação da DOX.

Conclusão

A imobilização da lacase ao suporte polimérico casca-núcleo foi capaz de proporcionar vantagens significativas, incluindo aumento da capacidade de

degradação da DOX, maior estabilidade, além da facilidade de recuperação e reutilização, o que pode contribuir com a viabilidade econômica do processo.

RESUMO

Fármacos anticancerígenos foram recentemente detectados em águas residuais hospitalares, bem como em amostras de águas superficiais. Nesse contexto, a doxorrubicina (DOX), um medicamento frequentemente utilizado no tratamento de câncer, foi encontrada em águas residuais em concentrações de $\mu\text{g L}^{-1}$. Mesmo em baixas concentrações, resíduos de DOX podem oferecer riscos ao ecossistema, tornando imperativa a busca por uma forma eficiente de remover esse composto do meio ambiente, a qual pode ser alcançada por meio de um sistema enzimático utilizando lacase como catalisador. Neste trabalho, a imobilização da lacase em um suporte polimérico de morfologia casca-núcleo foi investigada. Durante o desenvolvimento do trabalho, partículas comerciais de PP e partículas de PP/PS (preparadas por polimerização em suspensão semeada usando estireno) foram testadas como componentes centrais da estrutura final casca-núcleo (CS), enquanto a casca foi preparada por polimerização em solução de acrilonitrila com precipitação. Durante a síntese da casca de poliacrilonitrila (PAN), o grau de inchaço das partículas do núcleo no estireno desempenhou um papel importante na adesão. O grau de intumescimento das partículas de PP foi de 24% (m/m), enquanto as partículas híbridas de PP/PS exibiram um intumescimento de 57% (m/m). Após a síntese, as partículas (PP/PS e CS) foram submetidas à análise de imagens (MEV e microscopia óptica, OM), revelando uma superfície uniforme e lisa para PP/PS e a formação de uma casca porosa uniforme para partículas de CS. A partícula CS obtida com sucesso foi formada por um núcleo de PP/PS e casca de PAN com tamanho de $4,54 \pm 1,24$ μm , área específica de $2,70 \text{ m}^2 \text{ g}^{-1}$ e composição de PAN igual a $15,98 \pm 0,82\%$ (m/m) de partícula total. Este suporte foi submetido a algumas etapas de funcionalização antes da imobilização de lacase. Comprovou-se durante os testes que o tratamento com glutaraldeído foi o mais importante para a imobilização da enzima. Dessa forma, o suporte escolhido como base para o derivado enzimático foi tratado apenas com duas etapas de funcionalização (tratamento no NaOH e glutaraldeído). Os resultados obtidos revelaram um rendimento de imobilização de lacase superior a 50%, com possibilidade de alcançar rendimentos ainda superiores aumentando-se a quantidade de suporte oferecido na solução de imobilização, com uma quantidade aproximada de 1,2 mg de lacase/g de suporte. O derivado enzimático demonstrou maior resistência térmica em relação à lacase livre, além de permitir reaproveitamento do sistema catalítico em mais de cinco ciclos de uso. Nos testes de degradação da DOX foi obtida degradação acima de 92% para todas as concentrações do fármaco avaliadas ($250 \mu\text{g L}^{-1}$ e $500 \mu\text{g L}^{-1}$) em tempo inferior (o suporte com a lacase atingiram a degradação da DOX 40% mais rápido em relação à lacase livre) ao alcançado pela lacase em sua forma livre e com produtos de degradação menos tóxicos do que a DOX em várias concentrações, demonstrando a eficácia do derivado enzimático no processo.

Palavras-chave: Degradação de fármacos. Doxorrubicina. Lacase imobilizada. Partículas casca-núcleo. Poliacrilonitrila.

ABSTRACT

Anticancer drugs have recently been detected in hospital wastewater and surface water samples. In this context, Doxorubicin (DOX), a medicine frequently used to treat various types of cancer, was found in wastewater at concentrations of $\mu\text{g L}^{-1}$. Even in small concentrations, DOX residues can pose risks to the ecosystem, making the search for an efficient way to remove this compound from the environment imperative. This removal can be achieved through an enzymatic (biocatalytic) system using the enzyme laccase. This work investigated the immobilization of laccase on polymeric support with shell-core morphology. During the development of the work, commercial PP particles and PP/PS particles (prepared by seeded suspension polymerization using styrene) were tested as central components of the final shell-core (CS) structure. In contrast, the shell was prepared through seed polymerization of an acrylonitrile solution with precipitation. During polyacrylonitrile (PAN) shell synthesis, the degree of swelling of the core particles in styrene played an important role in adhesion. The degree of swelling of the PP particles was 24% (m/m), while the PP/PS hybrid particles exhibited a swelling of 57% (m/m). After synthesis, the particles (PP/PS and CS) were subjected to image analysis (SEM and optical microscopy, OM), revealing a uniform and smooth surface for PP/PS and forming a uniform porous shell for CS particles. The successfully obtained CS particle was formed by a PP/PS core and PAN shell with a size of $4.54 \pm 1.24 \mu\text{m}$, a specific area of $2.70 \text{ m}^2 \text{ g}^{-1}$, and PAN composition equal to $15.98 \pm 0.82\%$ (m/m) of the total particle. This support was subjected to some functionalization steps before laccase immobilization. During the tests, the treatment with glutaraldehyde was the most important step for immobilizing the enzyme. Therefore, the support chosen as the basis for the enzyme derivative was treated with only two functionalization steps (treatment in NaOH and glutaraldehyde). The results obtained revealed a laccase immobilization yield greater than 50%, with the possibility of achieving even higher yields by increasing the support offered in the immobilization solution, with an approximate amount of 1.2 mg of laccase/g of support. The enzymatic derivative demonstrated greater thermal resistance compared to free laccase, in addition to being able to reuse the catalytic system in more than five cycles of use. In DOX degradation tests, degradation above 92% was obtained for all drug concentrations evaluated ($250 \mu\text{g L}^{-1}$ and $500 \mu\text{g L}^{-1}$) in a shorter time (the support with laccase achieved DOX degradation 40% more faster in relation to free laccase) than achieved by laccase in its free form and with less toxic degradation products than DOX in various concentrations, demonstrating the effectiveness of the enzymatic derivative in the process.

Keywords: Drug Degradation. Doxorubicin. Immobilized laccase. Core-shell particles. Polyacrylonitrile.

LIST OF FIGURES

Figure 1: Graphic summary of this study	22
Figure 2: Mind map of this study.....	24
Figure 3: Graphic summary of chapter two	26
Figure 4: Sequences of procedures adopted in the preparation of core-shell particles.....	32
Figure 5: Schematic representation of the emulsion polymerization process.....	34
Figure 6: Representation of particle synthesis by suspension polymerization	37
Figure 7: Bibliographic survey of polymerization techniques used in the synthesis of core-shell particles (1986 – 2022)	40
Figure 8: Core-shell particle equilibrium morphologies. (a) Core-shell (CS); (b) Inverted Core-Shell (ICS); (c) Janus particle; (d) Separated particles.....	45
Figure 9: Graphic summary of chapter 3	70
Figure 10: Representative scheme of the polymerization apparatus	79
Figure 11: Number size distribution of PP particles (a) and OM micrographs of PP particles (b).....	85
Figure 12: PP swelling curves in styrene (Sty) and acrylonitrile (AN).	87
Figure 13: OM micrographs of PP (a) and PP/PS (b) particles and SEM micrographs of PP/PS particles (c).....	89
Figure 14: Number size distribution of hybrid PP/PS particles.....	90
Figure 15: FTIR spectra of the (a) insoluble fraction PP/PS in toluene and (b) and PP/PS particles	91
Figure 16: Swelling curve of PP/PS particles in styrene	92
Figure 17: OM micrographs of (a) PP particles, (b) particles with PP core and PAN shell, (c) PP/PS particles, (d) particles with PP/PS core and (e) SEM micrograph of the PAN shell.....	94
Figure 18: Number size distribution of CS particles (PP/PS/PAN).....	95
Figure 19: FTIR spectrum of PP/PS/PAN core-shell particles	96
Figure 20: FTIR spectrum of (a) PAN particles, (b) insoluble and (c) soluble fractions of CS beads in DMF.....	97
Figure 21: TG and DTG curves of PP, PP/PS and CS particles	98
Figure 22: Graphic summary of Chapter 4.....	101

Figure 23: Graphical representation of core-shell particles functionalization methodology.....	107
Figure 24: FTIR spectrum of surface samples of CS-I-II-III-IV (a), CS-I-II-III (b), and CS-I-IV (c)	116
Figure 25: ¹ H NMR results after (a) step 1, (b) step 2, (c) step 3 and (d) step 4 of support surface functionalization	117
Figure 26: Immobilization yield as a function of time for supports (using 0.25 g L ⁻¹ initial concentration of laccase, 8 mL of volume and 0.85 g of support), where (●) CS-0, (■) CS-I-II, (▲) CS-I-II-III, (◄) CS-I-II-III-IV and (►) CS-I-IV	118
Figure 27: Maximum laccase (LC) immobilization yield per initial LC concentration for CS-I-IV (A) and CS-I-II-III-IV (B) support, using 0.85 grams of support in a volume of 8 mL of laccase solution.....	120
Figure 28: Thermal stability of the laccase immobilized (▲) and free laccase (●) at 30° C (▲, ●), 50° C (▲, ●), 60° C (▲, ●) and 70° C (▲, ●).....	123
Figure 29: pH stability of the laccase immobilized and free laccase. Free laccase at pH 5.0 (●) and 6.0 (●); Immobilized laccase at pH 5.0 (▲) and 6.0 (▲); and Free and immobilized laccase at pHs 3.0 and 8.0 (●)	124
Figure 30: Reusability of laccase immobilized on CS-I-IV support	126
Figure 31: Residual activity for storage at refrigerator temperature (~8 °C) (▲) and at room temperature (~25 °C) (●).....	127
Figure 32: Substrate concentration and the kinetic parameters, V _{max} (mmol L ⁻¹) and K _M (μmol min ⁻¹ L ⁻¹), obtained from the Michaelis-Menten model	128
Figure 33: DOX concentration calibration curve by fluorescence data	130
Figure 34: DOX removal kinetic curves by: (A) Hydrolysis (●), Adsorption (●), Degradation with immobilized (●) and free laccase (●) at DOX concentration of 250 μg L ⁻¹ ; and (B) Hydrolysis (▲), Adsorption (▲), Degradation with immobilized (▲) and free laccase (▲) at DOX concentration of 500 μg L ⁻¹ (using 1.5 g of enzyme derivative and for the free enzyme assay an amount of 1.7 mg of laccase)	132
Figure 35: Reusability of the enzymatic derivative (CS-I-IV + Lac) in 500 μg L ⁻¹ of DOX solution (Each cycle occurred for 180 min under conditions of pH 6.0 and temperature of 30 °C).....	134

LIST OF TABLES

Table 1: Conceptual diagram of the study	21
Table 2: Core-shell structure materials used in enzyme immobilization	57
Table 3: Interactions, advantages, and disadvantages of immobilization methods	63
Table 4: Chemicals and operating conditions of the core swelling and shell polymerization.	82
Table 5: Measured properties of PP particles	85
Table 6: Measured performance parameters evaluated for PP/PS particles.	89
Table 7: Textural properties of the core-shell particle	95
Table 8: Nomenclature and description of prepared CS supports	107
Table 9: Immobilization yield values for each support (tests carried out using 0.85 grams of support in 8 mL of laccase solution at a concentration of 0.25 mg/mL)	119
Table 10: Laccase immobilization data with different support mass (laccase concentration of 0.25 mg/mL and volume of 8 mL)	121

LIST OF ABBREVIATIONS

Abbreviation	Meaning
ABTS	2,2'-Azino-bis(3-ethylbenzthiazoline-6-sulfonic acid)
AFM	Atomic Force Microscopy
AN	Acrylonitrile
AS	Poly(acrylonitrile-co-styrene) random copolymer
BET	Brunauer, Emmett, and Taller
BJH	Barrett, Joyner, and Halenda
BPO	Benzoyl Peroxide
CAL-B	Lipase B from <i>Candida antarctica</i>
CMC	Critical micellar concentration
CS	Core-shell
DI	Dispersion Index
DLS	Dynamic light scattering
DTG	Derived Thermogravimetry
DOX	Doxorubicin
DMF	Dimethylformamide
DVB	Divinylbenzene
EA	Enzymatic Activity
EMA	European Medical Agency
ETS	Etoposide
EP	Emerging pollutants
EPS	Expanded polystyrene
FTIR	Fourier transform infrared spectroscopy
GLU	Glutaraldehyde
HPLC	High Performance Liquid Chromatography
HRP	Horseradish peroxidase
ICS	Inverted Core-Shell
K _M	Michaelis-Menten constant

KPS	Potassium persulfate
LC	Laccase
LCD	Liquid Crystal Display
MMA	Methylmethacrylate
MMOF	Magnetic metal-organic framework
NMR	Nuclear magnetic resonance
OM	Optical microscopy
PAN	Polyacrylonitrile
PBA	Poly (butyl acrylate) (PBA)
PLLA/PMMA	Poly(L-lactide)/poly (methyl methacrylate)
PMMA	Polymethylmethacrylate
PP	Polypropylene
PP/PS	Polypropylene/polystyrene
PS	Polystyrene
PS-co-DVB	Poly(styrene-co-divinylbenzene)
PS-co-PC	Poly(styrene-co-cardanol)
PSD	Particle size distribution
rpm	Rotation per minute
SAN	Styrene acrylonitrile copolymer
SEM	Scanning electron microscopy
SLS	Static light scattering
SSA	Specific Surface Area
Sty	Styrene
SX	Solubility in xylene
TEM	Transmission Electron Microscopy
TG	Glass Transition Temperature
TMS	Tetramethyl Silane

SUMMARY

CHAPTER 1 – INTRODUCTION AND OBJECTIVES	16
1.1. INTRODUCTION.....	17
1.2. OBJECTIVES.....	20
1.2.1. General Objective.....	20
1.2.2. Specific Objectives	20
2. STRUCTURE OF THESIS	20
CHAPTER 2 – CORE-SHELL POLYMERIC PARTICLES FOR ENZYME IMMOBILIZATION	25
2.1. INTRODUCTION	27
2.2. CORE-SHELL POLYMERIC PARTICLES	28
2.2.1. Synthesis of core-shell polymeric particles	31
2.2.2. Emulsion Polymerization	33
2.2.3. Dispersion Polymerization	35
2.2.4. Suspension Polymerization	36
2.2.5. Other techniques.....	39
2.3. CHARACTERIZATION OF CORE-SHELL PARTICLES	41
2.3.1. Morphology.....	42
2.3.2. Particle size and distribution	47
2.3.3. Specific surface area	49
2.3.4. Hydrophobic surface	49
2.3.5. Surface modification.....	50
2.4. APPLICATIONS	53
2.5. CORE-SHELL POLYMERIC PARTICLES FOR ENZYME IMMOBILIZATION	55
2.6. POLYMERS FOR CORE AND SHELL	61
2.7. IMMOBILIZATION METHODS	62
2.8. CONCLUSION AND FUTURE OUTLOOK.....	67
CHAPTER 3 – FUNCTIONALIZABLE POLY(PROPYLENE-STYRENE)/ POLYACRYLONITRILE PARTICLES WITH CORE-SHELL MORPHOLOGY.....	69
3.1. INTRODUCTION.....	71
3.2. MATERIALS AND METHODS	75

3.2.1.	Chemicals	75
3.2.2.	Polypropylene (PP) particles characterization	76
3.2.4.	PP/PS particles characterization	80
3.2.5.	PAN Shell Preparation through Seeded Dispersion Polymerization	82
3.2.6.	CS particles characterization	83
3.3.	RESULTS AND DISCUSSION.....	84
3.3.1.	PP Particles	84
3.3.2.	PP/PS Particles.....	88
3.3.3.	CS Particles	93
3.4.	CONCLUSIONS.....	98
CHAPTER 4 – DEGRADATION OF ANTICANCER DOXORUBICIN BY LACCASE IMMOBILIZED ON CORE-SHELL POLYMER PARTICLES		100
4.1.	INTRODUCTION.....	102
4.2.	MATERIALS AND METHODS	105
4.2.1.	Chemicals	105
4.2.2.	Functionalization of core-shell particles.....	105
4.2.3.	Laccase immobilization.....	108
4.2.4.	Characterization of the enzyme derivative	110
4.2.5.	Doxorubicin (DOX) degradation assays.....	113
4.3.	RESULTS AND DISCUSSION.....	115
4.3.1.	Functionalization of core-shell particles.....	116
4.3.2.	Laccase immobilization	118
4.3.3.	Characterization of the enzyme derivative	122
4.3.4.	Doxorubicin (DOX) degradation assays.....	129
4.4.	CONCLUSION AND FUTURE PERSPECTIVES.....	135
CHAPTER 5 – FINAL CONSIDERATIONS		136
5.1.	FINAL CONCLUSIONS AND FUTURE OUTLOOK	137
5.2.	REFERENCES.....	138



CHAPTER 1 – INTRODUCTION AND OBJECTIVES

This chapter has a general introduction to the research, the presentation of the main objectives, the document's structure, and the study's conceptual diagram.

1.1. INTRODUCTION

Concerns about emerging pollutants (EP) in the environment have grown exponentially in recent years. Among these, pharmaceutical products are biologically active substances that can negatively affect the environment and cause problems to human health (KELBERT *et al.*, 2021). Furthermore, these products are recalcitrant, that is, they are not efficiently removed by conventional wastewater treatments, in addition to proving to be a challenge for non-conventional water decontamination technologies (BILAL *et al.*, 2019; YADAV *et al.*, 2021; ZOFAIR *et al.*, 2022)

Anticancer drugs have been detected among pharmaceutical products in hospital wastewater and surface water samples. Doxorubicin, etoposide, fluorouracil, cyclophosphamide, tamoxifen, vinblastine, and vincristine are some anticancer drugs that have been detected (KELBERT *et al.*, 2021).

In this context, doxorubicin (DOX) is frequently used in the treatment of various types of cancer, such as breast carcinoma, bone sarcoma, thyroid carcinoma, and gastric carcinoma. However, the wide application of DOX and poor bioavailability inevitably result in its appearance in wastewater at a concentration range of 0.26 – 1.35 $\mu\text{g L}^{-1}$. Even in small concentrations, highly dangerous DOX residues can remain in the environment long and cause harmful effects. From this point of view, the search for an efficient way to treat this compound is essential (KELBERT *et al.*, 2021; ZHAO *et al.*, 2023).

The enzymatic technology appears as an alternative faced with the need for a more effective treatment for the degradation of these drugs. In this sense, laccases are multi-copper oxidases found in plants, fungi, and other microorganisms that catalyze the oxidation of a wide variety of organic and inorganic compounds to form water. These catalysts have been investigated for biotechnological processes,

including dye bleaching, biosensors, applications in the bread industry, plastic degradation, etc. Furthermore, antiproliferative and anticancer activities of different laccase-containing fungal extracts have been reported in recent years (DARONCH *et al.*, 2020; YADAV *et al.*, 2021)

KELBERT *et al.* (2021) evaluated the action of laccase on the degradation of doxorubicin (DOX, a type of anticancer drug). Kinetic studies were performed, varying the enzyme concentration, pH, and temperature. The best degradation results occurred under conditions like those found in effluents present in treatment plants (pH 7 and 30 °C), which showed great potential for application. In particular, the DOX was degraded under these conditions in just 2 hours. In addition, enzymatic degradation reduced the toxicity of DOX by up to 41.4%, indicating that laccase can degrade this drug into non-toxic compounds.

In another study performed by the same research group, PEREIRA *et al.* (2020) managed to evaluate the etoposide (ETS) degradation capacity by laccase. This study evaluated concentrations close to those found in effluents under process conditions that best suit a real effluent treatment. It was possible to observe the degradation of etoposide under all conditions tested. The highest enzyme concentration (1100 U·L⁻¹) degraded 100% of the substrate in one hour. The lowest concentration (55 U·L⁻¹) reached 86% degradation in 6 hours of reaction, demonstrating the potential of laccase in removing anticancer drugs from effluents and wastewater.

Despite these great advances related to the use of laccase in the degradation of anticancer drugs, it is known that enzymes in their free form are economically unfeasible due to their operational instability and high isolation costs (JUN *et al.*, 2019; NGUYEN; KIM, 2017).

In this context, enzymatic immobilization has emerged as a great interest among researchers in developing new, effective, greener, and hybrid strategies for removing toxic contaminants. Immobilization can be considered a biotechnological tool, which binds enzymes to a solid support to increase stability and allow recyclability and reuse, as well as the development of continuous processes, overcoming the economic and operational problems of free enzymes (YAASHIKAA; DEVI; KUMAR, 2022).

In this sense, polymeric materials stand out as supports that can be used to improve the properties of immobilized enzymes, such as reuse and thermal stability. Furthermore, the synthesis of polymers with desired functional groups and other properties that favor the link between the support and the enzyme is possible (VERA et al., 2020; VIEIRA et al., 2021). Within these possibilities, core-shell morphology polymeric materials draw attention due to their controlled structure and unique properties. These particles can have high porosity and, consequently, high surface area. These characteristics can be easily adjusted while synthesizing this structure, making it interesting for bioadsorption and biocatalysis (RAMLI; LAFTAH; HASHIM, 2013; VIEIRA et al., 2021).

Thus, the present work proposes developing a polymeric structure to be used as an enzymatic support for laccase immobilization. In addition, studies that used laccase for the degradation of anticancer drugs obtained satisfactory results but used the enzyme in the free form, which makes the process economically unfeasible. Therefore, this study aims to produce a new biocatalyst based on laccase immobilized on core-shell polymer particles that is effective and viable for the degradation of doxorubicin present in effluents and wastewater.

1.2. OBJECTIVES

1.2.1. General Objective

The main objective of this work is to contribute to overcoming problems related to the treatment of wastewater and hospital effluents through enzymatic technology using laccase immobilized on polymeric support of specific core-shell morphology.

1.2.2. Specific Objectives

- ✓ Synthesize and characterize polymeric supports with core-shell morphology with a polystyrene/polypropylene core and polyacrylonitrile shell;
- ✓ Functionalize the surface of the polymeric particles to obtain specific functional groups;
- ✓ Immobilize laccase on the synthesized support (biocatalyst);
- ✓ Characterize the biocatalysts in terms of immobilization yield, thermal stability, pH stability and storage stability;
 - Evaluate the bioconversion of doxorubicin (DOX) using the immobilized biocatalyst.

2. STRUCTURE OF THESIS

This work is divided into chapters to facilitate reading and understanding. This chapter introduces the research and its objectives. Chapter 2 is a bibliographical survey of the main aspects related to the study, bringing a more in-depth understanding of the characteristics and synthesis of polymeric particles with core-shell morphology and their application for the immobilization of enzymes. This chapter was published and indexed (<https://doi.org/10.1002/slct.202202285>) as a review article entitled "A Comprehensive Review on Core-Shell Polymeric Particles for Enzyme Immobilization." Chapter 3 contains all the methodology and results related to the synthesis of core-shell polymeric particles and was published and indexed

(<https://doi.org/10.1002/app.55667>) in the *Journal of Applied Polymer Science* as a research article titled by “Preparation of functionalizable poly(propylene–styrene)/polyacrylonitrile millimeter-scale particles with core-shell morphology”. Chapter 4, in turn, presents all the methods and results of the application of particles in the immobilization of laccase and degradation of the anticancer doxorubicin. Finally, Chapter 5 contains the final considerations of this work.

Table 1 proposes an overview of the work, the main motivations, what has been done in the literature, and the study's hypotheses. To illustrate the steps of the work, Figure 1 presents the graphic summary of this study. Finally, the mental map can be seen in Figure 2 to represent the steps involved in the work briefly.

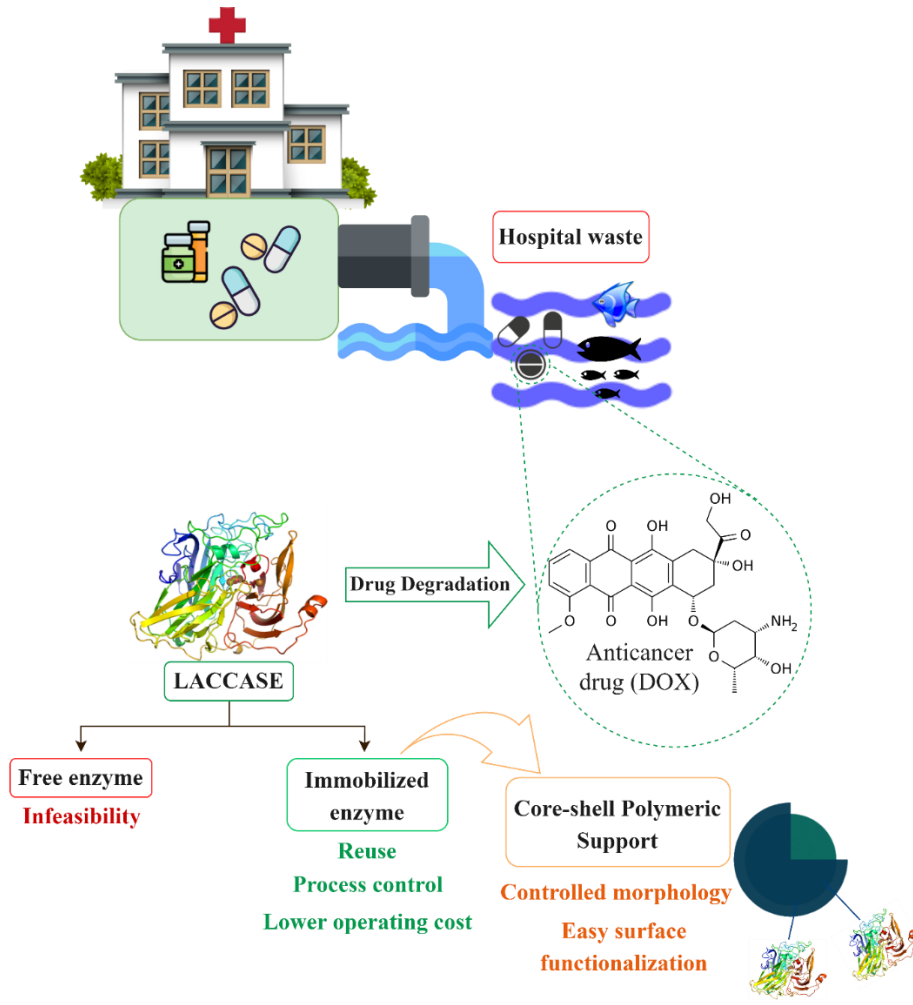
Table 1: Conceptual diagram of the study

Degradation of anticancer drug doxorubicin by laccase immobilized on core-shell particles composed of poly(propylene/styrene) and polyacrylonitrile	
Why?	<ul style="list-style-type: none"> ✓ The degradation of contaminants in environmental matrices and effluents is a process that has drawn attention due to the growing environmental concern; ✓ An efficient alternative for the removal of contaminants is the application of enzymes; ✓ Laccases can catalyze the oxidation of various organic and inorganic products; however, this enzyme in its free form is economically unfeasible due to high instability and difficulty in recovery; ✓ The immobilization of the laccase on insoluble support enables its reuse; ✓ There are no commercial biocatalysts based on immobilized laccase; ✓ Polymeric particles with a core-shell structure offer advantages for the immobilization of enzymes, such as easy surface functionalization and high stability; ✓ The degradation of anticancer drugs by laccase immobilized on core-shell polymer particles is an innovation.
What is being done?	<ul style="list-style-type: none"> ✓ The core-shell polymeric particles have been widely studied in the immobilization of lipases, obtaining very satisfactory results; ✓ Free laccase has already demonstrated potential for the degradation of pharmaceutical compounds, such as those used in cancer treatment.
Scientific method:	<ul style="list-style-type: none"> ✓ Synthesis and characterization of polymeric particles with core-shell structure;

<ul style="list-style-type: none"> ✓ Functionalization on the surface of the particles produced in order to improve the affinity between the support and the enzyme; ✓ Immobilization of laccase on particles; ✓ Characterization of biocatalysts; ✓ Application of biocatalysts in anticancer drug degradation assays.
<p>Research hypothesis:</p> <ul style="list-style-type: none"> ✓ It is possible to synthesize core-shell particles with shell adhesion of PAN on PP or PP/PS core; ✓ It is possible to functionalize these particles to increase the affinity between them and laccase. ✓ It is possible to use the proposed biocatalysts to degrade anticancer drugs.
<p>Answers:</p> <ul style="list-style-type: none"> ✓ Obtaining core-shell polymeric particles by suspension polymerization is well-defined in the literature; ✓ Synthetic polymers are adapted to enzyme immobilization due to the easy modification of their surface; ✓ Laccase can degrade various aromatic and toxic compounds, including Doxorubicin.

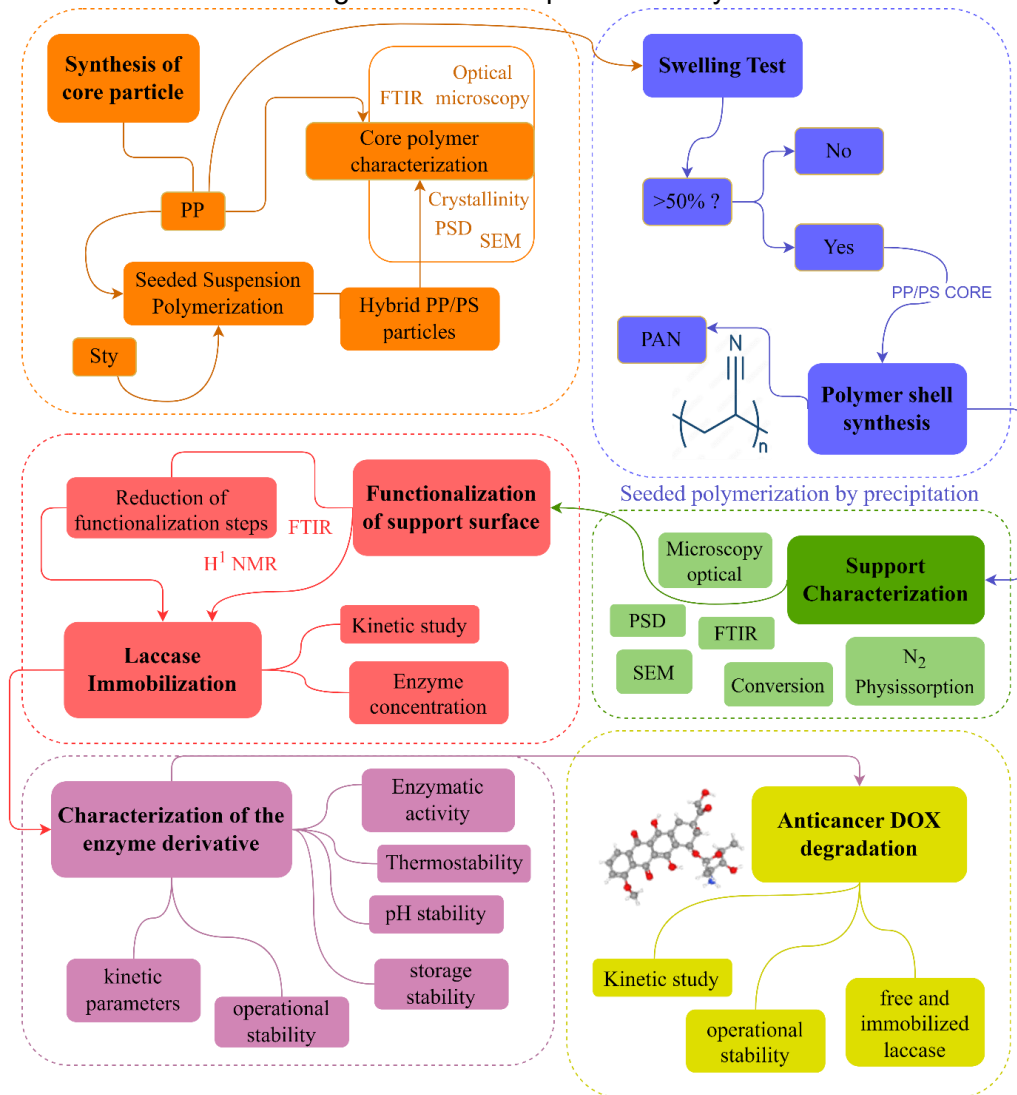
Source: Author's elaboration

Figure 1: Graphic summary of this study



Source: Author's elaboration

Figure 2: Mind map of this study



Source: Author's elaboration

2 CHAPTER 2 – CORE-SHELL POLYMERIC PARTICLES FOR ENZYME IMMOBILIZATION

This section is based on a review article published in Chemistry Select, “A Comprehensive Review on Core-Shell Polymeric Particles for Enzyme Immobilization.” This article was accepted in 2022 and indexed; it can be accessed via the QR Code below. Following Wiley's subscription rules, authors reserve the right to include the article in a thesis if it is not published commercially.

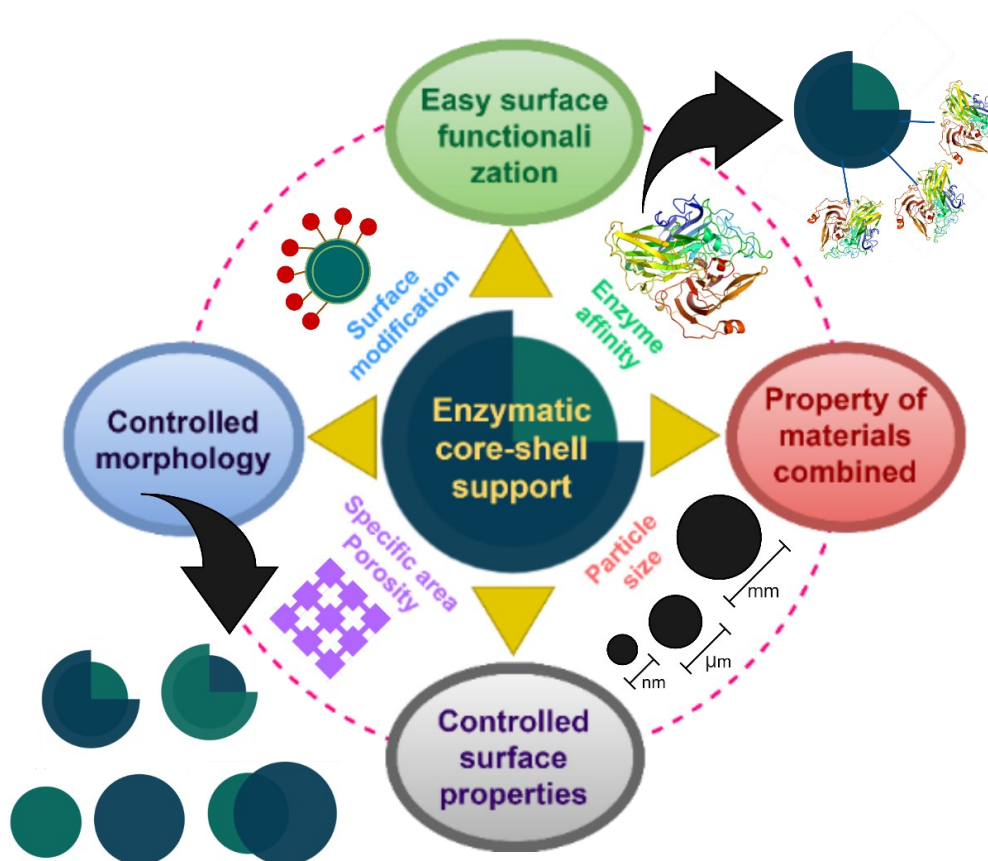


<https://doi.org/10.1002/slct.202202285>

Graphical abstract

Figure 3 below shows the graphic summary of this chapter, designed for quick visualization of the chapter's content.

Figure 3: Graphic summary of chapter two



Source: Author's elaboration

2.1. INTRODUCTION

Enzymes are highly efficient natural catalysts due to their high activity, selectivity, and milder operation conditions. However, their use in free form presents many limitations, including high costs, poor operational stability, and recovery and reuse challenges (CAO *et al.*, 2016). In light of this, enzyme immobilization has become an effective strategy to improve the stability, specificity, and reuse of enzymes, even under adverse reaction conditions and organic solvents, allowing a reduction in the cost of the process by up to 50% (SHARMA *et al.*, 2021).

Using solid support to immobilize proteins is probably the most widespread enzyme immobilization strategy. Enzymatic supports should be: (a) low-cost and ecologically correct (avoiding costs related to environmental problems); (b) inert with the reaction medium (easy recovery); (c) thermally and mechanically resistant; (d) able to improve the interactions between the substrate molecule and the active site of the enzyme (specificity); (e) able to package a large amount of enzyme (desirable surface properties); (f) inert in the conditions of pH and temperature for the enzyme action (DARONCH *et al.*, 2020; SHARMA *et al.*, 2021).

In this context, particles with a core-shell structure are materials composed of two or more layers of different materials (one of them forms the inner core and the others form the outer layers or shell) and offer several advantages when applied as support in enzyme immobilization, such as the ability to achieve characteristics and properties that would not be achieved by individual core and shell materials (GALOGAHI *et al.*, 2020). Furthermore, coating a core particle with a shell material provides increased functionality,

surface modification (controlled surface properties), reduced consumption of precious materials, and improved stability (KURIAN; THANKACHAN, 2021). Core-shell structured polymer particles can be obtained with different morphologies since the equilibrium morphology may not be reached constantly due to the required adjustment of different properties during the particle development. The polymerization techniques play an important role in particle size and in the control of polymerization rates. Various heterogeneous polymerization techniques, such as emulsion, dispersion, and suspension polymerizations or combine processes, can be employed to obtain polymer particles with core-shell structures (SAYER; HENRIQUE; ARAÚJO, 2010).

This review provides an overview of the main elements of polymeric particles with core-shell structure, including the main synthesis techniques, their properties, and characterizations techniques, with particular emphasis on the advantages and ease of using these structures as enzymatic support as well as the possible application as effective biocatalysts. Several works that investigated the application of these materials in the immobilization of some enzymes are discussed in the present work, which makes it possible to notice a deficiency in the investigation of these materials in the context of enzyme immobilization.

2.2. CORE-SHELL POLYMERIC PARTICLES

Particles with core-shell morphology can be formed by a core consisting of inorganic nanoparticles (SiO_2 , TiO_2 , CaCO_3 , ZnO , etc.) or organic polymers (MA *et al.*, 2013), and a shell solid of another material, which involves the entire surface of the core and can add new properties to the structure, improving its stability and chemical affinity with the enzyme (HE *et al.*, 2019; MA *et al.*, 2013).

According to the composition of these two materials of the core-shell particles, they can be classified into four groups: inorganic/organic, organic/inorganic, organic/organic, and inorganic/inorganic. As it is a hybrid particle, it combines the desired properties of both polymers that form it, thus aiming to improve the physical and chemical properties of the final material (CAPELETTO *et al.*, 2014). In this sense, they cover a wide range of applications, such as enzymatic support, biomarkers, catalysts, electronic components, sensors, and optical materials, among others (BESTETI; FREIRE; PINTO, 2011).

The fit of shell and core materials can affect the chemical, biological, magnetic, and optical functions of core-shell particles. This type of design allows the choice of material to change the final characteristic of the core-shell particle since it will have properties that are not achievable by the materials alone (GALOGAHI *et al.*, 2020). In other words, the morphology of these particles tends to have the inherent advantages of each component material. For example, Uliana and collaborators (2014) suggested that modifying the impact strength of polymeric materials could be acquired by synthesizing particles with core-shell morphology. They produced a particle whose core consisted of a rubberized phase of a styrene-butadiene copolymer and the shell in a glassy phase of polystyrene (PS). The authors demonstrated that the addition of 30 wt% of the core-shell particles increased the mechanical strength of PS by 70% (ULIANA *et al.*, 2014).

Thus, it is possible to think of this type of material as a two-way street, where the choice of component material for the shell and core strongly interferes with the application, as well the properties of the final material can be tailored to the intended application. The core-shell polymerization makes it possible to

obtain two incompatible monomers in the same particle. In addition, it is possible to functionalize groups of both the shell polymer and the core (SAYER; HENRIQUE; ARAÚJO, 2010), thus covering a wide list of applications.

Among the techniques used for synthesizing particles with core-shell morphology, the most used are emulsion, dispersion, and suspension. The technique used can play an important role in the final characteristics of the particle. The influence of the polymerization method was addressed by Peres and collaborators (2017). The authors evaluated the effect of the technique and the mixing ratio on the morphology and miscibility of the particles. Among the three techniques used, the miniemulsion followed by solvent evaporation showed greater flexibility for the formation of poly(L-lactide)/poly(methyl methacrylate) (PLLA/PMMA) nanoparticles. PLLA was produced by ring-opening polymerization of L-lactide, and then this was dissolved in MMA.

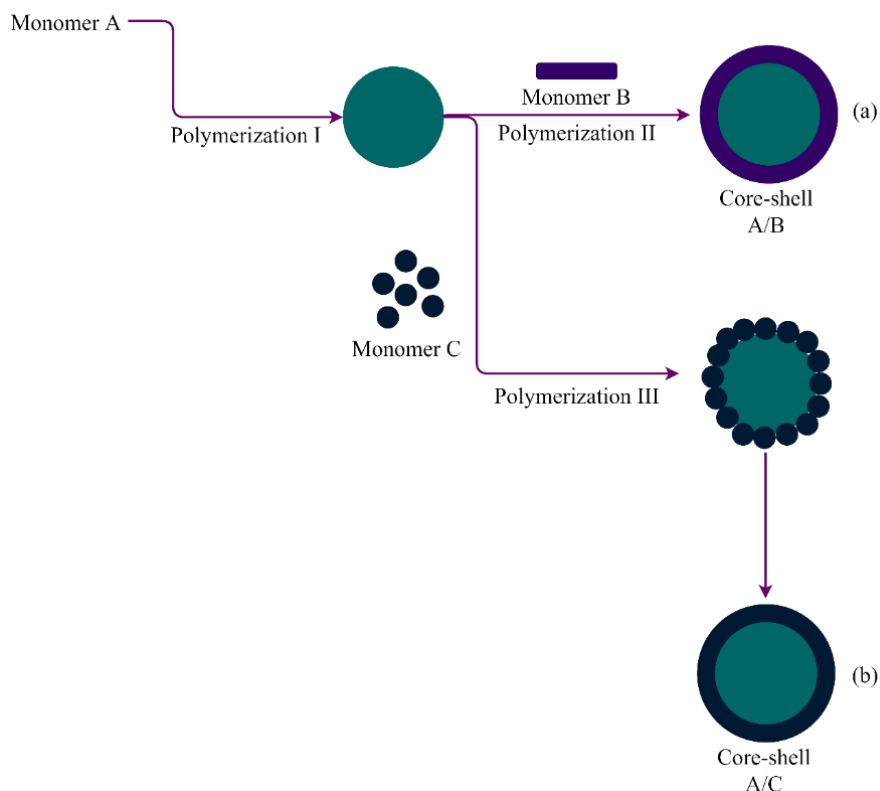
Using only the miniemulsion technique, the authors could produce immiscible and amorphous particles with a core-shell morphology, where a PLLA shell covered the PMMA core. According to the authors, these particles showed efficiency above 85% for carrying a hydrophobic drug (PERES *et al.*, 2017).

The production of core-shell polymer particles for biotechnological applications, especially those involving enzymatic immobilization, must consider biocompatibility (WANG *et al.*, 2022), equilibrium morphology, synthesis method, particle size, and surface functionalization of the shell polymer (RAMLI; LAFTAH; HASHIM, 2013; SU *et al.*, 2020). Therefore, the main synthesis techniques used to produce core-shell polymer particles and their characteristics will be discussed below.

2.2.1. Synthesis of core-shell polymeric particles

Polymeric particles with core-shell morphology are generally synthesized using a consecutive sequence of heterogeneous polymerization techniques such as emulsion, dispersion, precipitation, and suspension polymerizations using different morphology (RAMLI; LAFTAH; HASHIM, 2013; SAYER; HENRIQUE; ARAÚJO, 2010). Typically, the adopted methodologies use two-stage polymerization, initially preparing the core particles, and then the shell formation procedure can be performed (Fig. 4-a). Usually, the methodologies adopted use two-stage polymerization, initially preparing the core particles. Then the shell formation procedure can be performed using a soluble monomer in the continuous phase (monomer B) (Fig. 4-a). The formation of these structures also occurs by heterocoagulation of smaller polymer particles into larger polymer particles employing heat treatment (RAMLI; LAFTAH; HASHIM, 2013; SU *et al.*, 2020), as shown in Figure 4-b.

Figure 4: Sequences of procedures adopted in the preparation of core-shell particles



Source: Author's elaboration

In Figure 4, polymerization route I is typically a suspension reaction. In contrast, polymerization routes II and III can be an emulsion, mini-emulsion, or solution reaction with polymer precipitation (dispersion), with polymerization III generally being an emulsion reaction of an insoluble monomer in the continuous phase (monomer C). After the reaction, the heat treatment allows the temperature to rise above the T_g of the shell polymer, which allows the shell formed to take the form of a film.

However, it is important to know that in any technique, applying a two-step strategy to build a second-stage polymer shell on the first-stage polymer core will not necessarily result in obtaining particles with core-shell morphology due to factors such as the surface tension of the materials used (SAYER; HENRIQUE; ARAÚJO, 2010).

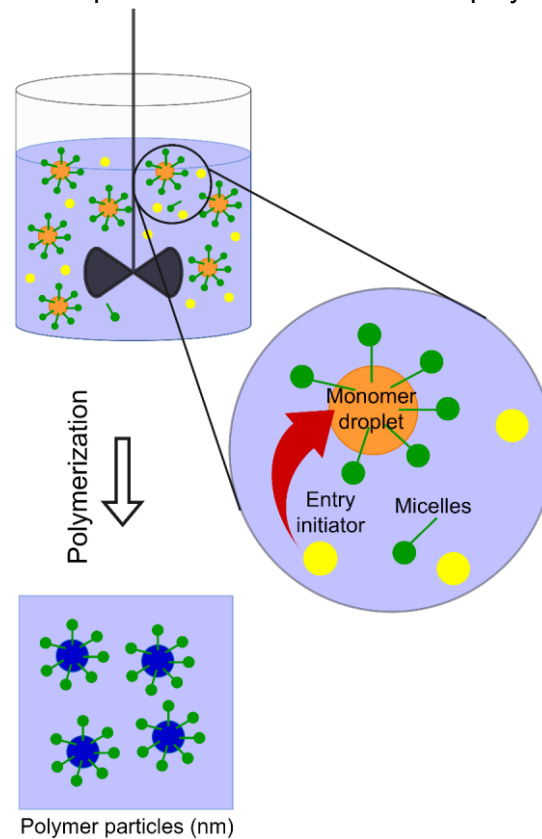
The choice of the technique to be used depends on the desired characteristics of the final polymer. The techniques can produce particles of different sizes, for example. Dispersion polymerization produces polymer particles in the range of 1-15 μm (RAMLI; LAFTAH; HASHIM, 2013), while the emulsion, miniemulsion, and microemulsion lead to the formation of submicrometric particles (10-800 nm) (SAYER; HENRIQUE; ARAÚJO, 2010). In addition to particle size, the morphology, porosity, pore size, and surface modification can be controlled during the polymerization process (HAYES *et al.*, 2014). These parameters will be discussed in more detail later.

The main techniques used to synthesize polymeric core-shell particles will be discussed in the following subtopics, addressing their most important conditions and characteristics.

2.2.2. Emulsion Polymerization

Emulsion polymerization is a technique performed in a heterogeneous medium (RUDIN; CHOI, 2013). The system is characterized by the presence of monomer droplets dispersed in a continuous aqueous phase with the help of a surfactant (Fig. 5). There may also be swollen monomer micelles as long as the surfactant concentration in the continuous phase is above its critical micellar concentration (CMC) (RAMLI; LAFTAH; HASHIM, 2013).

Figure 5: Schematic representation of the emulsion polymerization process



Source: Author's elaboration

Seeded emulsion polymerization is the most common technique for synthesizing core-shell particles, which can occur either in batch or semi-continuous mode, with or without previous swelling of the seed particles. The basic strategy for the formation of the core-shell structure is that the core nucleus polymer is formed in the first stage. Then the shell polymer is synthesized by emulsion polymerization from a continuous feeding of the second-stage monomer to a pre-specified rate to allow the second-stage polymer to accumulate on the core surface, obtaining a uniform and continuous shell (MA *et al.*, 2013; SAYER; HENRIQUE; ARAÚJO, 2010).

Huang and collaborators (2019) synthesized particles of core-shell morphology through emulsion polymerization using a semi-continuous pre-emulsion method. Polymer particles of different sizes (100-450 nm) of the cross-linked poly (butyl acrylate) (PBA) were prepared as the inner core and the hard shell using the poly (acrylonitrile-co-styrene) random copolymer (AS). In the study, they investigated the influence of the feeding mode on the particle size, concluding that the feeding rate increases the microsphere size of the PBA seed in the semi-continuous pre-emulsion polymerization but not by the batch polymerization (HUANG *et al.*, 2019).

Cunha and collaborators (2014) synthesized different core-shell morphology particles for lipase immobilization (CALB) and compared the results with the CALB immobilization performance of Accurel MP[®]. The authors used a combined suspension and emulsion polymerization process to produce the particles, with the core formed by the suspension polymerization process and the shell formed by polymer particles nucleated by the emulsion polymerization process. Their work shows that final particle morphology and molecular weight distribution depend significantly on emulsion feed flow rates and initial feed time (CUNHA *et al.*, 2014). Thus, we understand that feeding polymerization components are a crucial factor in forming the core-shell morphology when using emulsion polymerization processes.

2.2.3. Dispersion Polymerization

Dispersion polymerization is another alternative for synthesizing polymer particles with a core-shell structure. In this type of polymerization, the monomer and the initiator are completely soluble in the continuous phase, which can also be made up of other non-reactive components. Due to the miscibility of these

components, dispersion polymerization starts as a homogeneous process. Still, with the formation of the polymer, which is not soluble in the continuous phase, it is precipitated, forming colloidal particles that are stabilized by the added dispersant. Thus, polymerization occurs both in the continuous phase and in the particulate phase, in different degrees, depending on the monomer partition and the radicals between the phases (RUDIN; CHOI, 2013; SAYER; HENRIQUE; ARAÚJO, 2010).

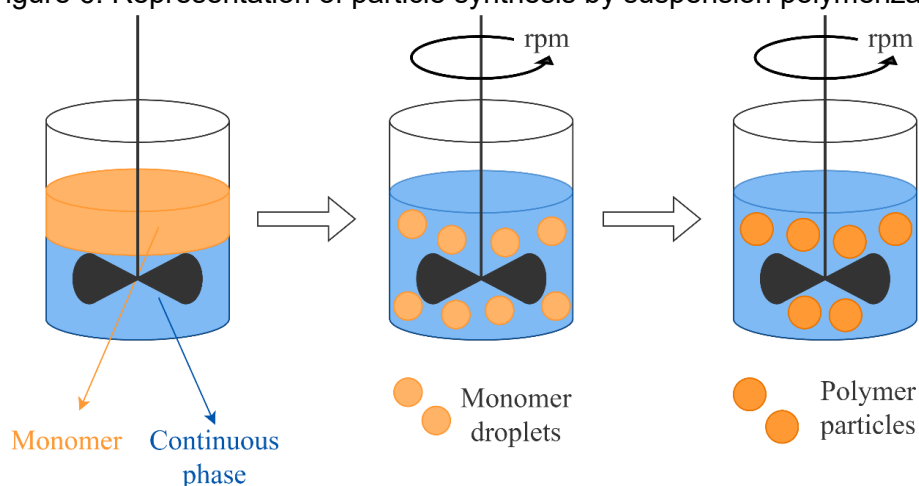
One of the reported advantages of the dispersion polymerization technique compared to emulsion polymerization is that emulsifiers used in emulsion polymerization often pollute subsequent compounds and affect the morphology of the core-shell particles. It can be overcome through dispersion polymerization without emulsifiers, as the monomers are dissolved in water or organic solvent and polymerized in the presence of a stabilizer (WANG *et al.*, 2007). However, some negative effects can also occur in dispersion polymerization, such as difficulty in controlling the particle size distribution and instability due to adding extra agents at the beginning of the polymerization. These problems can be avoided when "two-stage" polymerization occurs, that is, when functional agents (such as crosslinkers, chain transfer agents, or polymerizable dyes) are added after the nucleation stage. In this case, the morphology of the final particles is also affected by the addition time of extra agents to the reaction. (WANG *et al.*, 2013b).

2.2.4. Suspension Polymerization

Suspension polymerization processes are characterized by heterogeneous, in which the reactive phase (monomer) is insoluble or partially soluble, like MMA, in the continuous phase (usually water). During the process,

the monomer droplets are dispersed in water, acting as micro-sized reactors (Fig. 6). In free-radical polymerization reactions, an organic initiator is added, such as a miniature bulk free-radical polymerization. Its proper dispersion is ensured through agitation (generated by a mechanical impeller) and by the presence of a suspending agent. As the monomer is converted to polymer, the droplets are transformed into dense and sticky monomer/polymer particles that become spherical solid polymer particles (JENSEN *et al.*, 2017; ZHU; HAMIELEC, 2012).

Figure 6: Representation of particle synthesis by suspension polymerization



Source: Author's elaboration

Suspension polymerization is suitable for fabricating large polymer particles. In suspension polymerization, relatively water-insoluble monomer droplets are formed by vigorous stirring and polymerize in the presence of a steric stabilizer, which leads to an aqueous dispersion of polymeric particles in the size range of 50 to 3500 μm . (SAYER; HENRIQUE; ARAÚJO, 2010). These relatively large particles (compared to emulsion particles) can be isolated by filtration and/or sedimentation, which is a clear distinction between the terms "suspension," "emulsion," and "dispersion" (VIVALDO-LIMA *et al.*, 1997).

The main advantages of suspension polymerization compared to other polymerization processes are easy to heat removal and temperature control, low dispersion viscosity, low levels of impurities in the polymer product, low separation costs, and the final product in the form of particles. On the other hand, some disadvantages can also be mentioned, such as lower productivity for the same reactor capacity (volume) and accumulation of polymer on the reactor wall, baffles, agitators, and other surfaces, when compared to the mass polymerization process (VIVALDO-LIMA *et al.*, 1997).

Suspension polymerization is a promising technique for controlling particle morphology. Recent studies have evaluated the improvement of particle morphology and shape by controlling operating parameters such as mixing rate, pH, temperature, and feed rate (JAYAWEERA; WICKRAMASINGHE; NARAYANA, 2021). A two-step procedure must be employed for synthesizing particles with a core-shell structure, where the core particles can be obtained by suspension polymerization and the second step monomer added afterward. It is also possible to obtain this type of morphology from seeded suspension polymerization, which uses polymer particles as seeds and adds the components of suspension polymerization to form the shell (JAYAWEERA; NARAYANA, 2021).

Gonçalves and collaborators (2008) synthesized core-shell particles of suitable sizes for rigid foams from seeded suspension polymerization of methyl methacrylate (MMA) using polystyrene (PS) particles as seeds. In this study, three synthetic strategies were implemented, differing in how the monomer was fed into the system. For this, the monomer and the initiator were fed in different ways at a constant rate of 0.9 g/min. In the first strategy, they were added when

the reactor was already at the reaction temperature (70 °C), and in the other strategies, when the reactor was still at a temperature of 50 °C and left at different times before increasing the temperature to 70 °C. This time that the PS and MMA seeds were in contact before reaching the reaction temperature (90 min and 130 min, for the second and third strategies, respectively) was called the swelling time, where the core should "swell" before the formation of the PMMA shell. As a result, it was observed that the longer the swelling time, the greater the shell thickness and the fraction of PMMA formed inside the seeds as a shell (GONÇALVES *et al.*, 2008).

2.2.5. Other techniques

Other techniques can also be used to synthesize polymers with core-shell morphology, such as miniemulsion, microemulsion, and precipitation polymerization. The miniemulsion process is based on the generation of nanometer-sized monomer droplets by high-shear rates devices (sonifier, rotor-stator system, high-pressure homogenizer), which can be converted into nanoparticles with narrower particle size distribution during polymerization. Unlike the emulsion process, there is no coexistence of micelles and monomer droplets at the beginning of the miniemulsion process (JENJOB; SEIDI; CRESPIY, 2018).

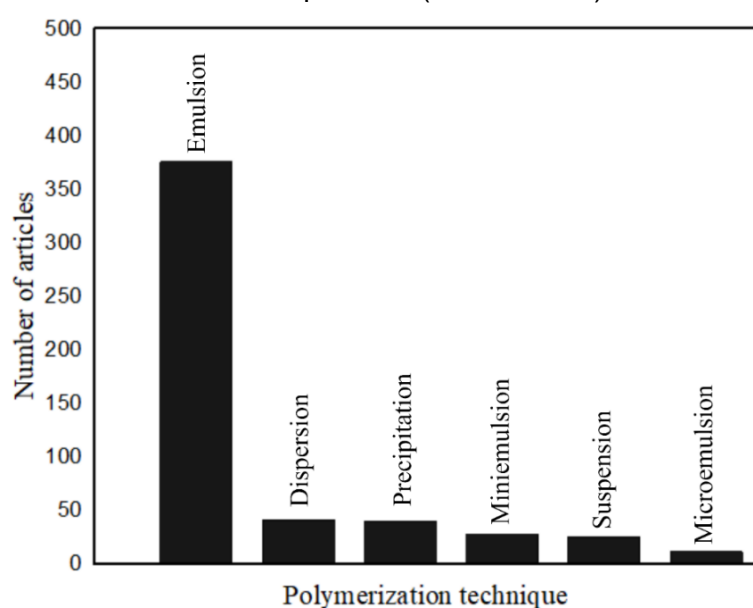
In microemulsion polymerization, large amounts of surfactants are required to form micrometre-sized monomer droplets, provide rapid nucleation, and stabilize the particles during polymerization and storage (XU; GAN, 2005). The main difference between the emulsion and microemulsion process is the amount of surfactant needed to stabilize the systems, which is much higher for

the microemulsion. It is a disadvantage because high and low amounts of solids and surfactants are desired in most applications (YILDIZ; CAPEK, 2003).

In the case of polymerization by precipitation, it is not necessary to use surfactants or stabilizers during the process (SUN *et al.*, 2021). Precipitation polymerization starts as a homogeneous mixture of monomer, initiator, and solvent. The growing polymer chains separate from the continuous phase during the process by enthalpic precipitation (in the absence of a crosslinker) or entropic precipitation (when cross-linking prevents polymer and solvent from mixing freely) (ZHANG, 2013).

The bibliometric survey (Fig. 7), carried out on the Scopus platform on a time scale from 1986 to 2022, with different keywords, showed the predominance of emulsion techniques (~72%) in the preparation of materials with a core-shell structure, mainly applied for the formation of the shell around the previously synthesized core particles (seeded emulsion).

Figure 7: Bibliographic survey of polymerization techniques used in the synthesis of core-shell particles (1986 – 2022)



Source: Author's elaboration

Two modes of operation (batch and semi-batch), with or without pre-swelling of the seed particles, are commonly used in seeded emulsion polymerizations (SAYER; HENRIQUE; ARAÚJO, 2010). The main difference between batch and semi-batch emulsion polymerization is that polymerization ingredients (surfactant, monomer, water, and initiator) can be fed into the system during semi-batch polymerization. Thus, the residence time and particle nuclei distribution in this process are wider, and these characteristics make the polymerization kinetics and mechanisms more complicated compared to the batch process (RAMLI; LAFTAH; HASHIM, 2013). The main advantage of semi-batch processes is that some properties can be controlled during polymerization, for example, composition drift can be reduced by feeding the monomer mixture into the reactor at the same rate, and it is also possible to produce emulsions with non-uniform size (RAMLI; LAFTAH; HASHIM, 2013; URREA-QUINTERO; HERNANDEZ; OCHOA, 2020).

2.3. CHARACTERIZATION OF CORE-SHELL PARTICLES

The characterization of polymeric particles with core-shell structure includes, in addition to determining the shape of the particle, also evaluating the composition of the surface and interior of the particle. Although very important, microscopic images are not enough to provide all relevant details about the particles' structure; therefore, different techniques are needed to characterize the morphology of these materials properly.

In addition to morphology, other characteristics of the polymeric structure are crucial for the analysis of its final application, especially regarding enzyme immobilization. The most observed characteristics of particles with a core-shell

structure are particle size, surface area, hydrophobicity, and morphology. All these characterizations are important to analyze the potential of polymer particles as enzymatic support for synthesizing a biocatalyst (SU *et al.*, 2020).

2.3.1. Morphology

Various characterization techniques can be used to determine particle morphology, such as microscopic techniques: optical microscopy, TEM (transmission electron microscopy), AFM (atomic force microscopy), and SEM (scanning electron microscopy) (SAYER; HENRIQUE; ARAÚJO, 2010). However, it is important to know that it is only possible to visually identify and differentiate the core and shell components in some cases. In most cases, the justification for the core structure is based on the thermodynamic incompatibility between the polymers or their different solubility in the continuous phase (TKACHENKO *et al.*, 2020).

Synthesis of core-shell materials often does not lead to an ideal core-shell morphology with complete phase separation. The components at the interface will mix in different ways depending on the compatibility of the two polymers involved and the reaction conditions (LANDFESTER *et al.*, 1996). Interfacial tensions determine the morphology of the final particle to minimize the total interfacial energy; that is, the incompatibility between the seed particle and the secondary formed polymer results in phase separation (VATANKHAH *et al.*, 2020).

Before applying the synthesis method of a core-shell particle composed of two distinct polymers, it is necessary to know about the equilibrium morphology, that is, that morphology in which it is possible to obtain a clear distinction between the shell and the core. The polymeric components should be arranged so that the

shell covers the core as evenly as possible. This equilibrium morphology is subject to the kinetic aspects determining the rate at which this equilibrium will occur and to the thermodynamic aspects involved in particle synthesis (TAKUYA TANAKA, REIKO NAKATSURU, YOSHIMI KAGARI, NAOHIKO SAITO, 2008). Briefly, the equilibrium morphology reduces the interfacial free energy. From a kinetic perspective, it depends on the relative polymerization rates and the diffusion rate inside the particles during the second polymerization phase (STUBBS; SUNDBERG, 2006). However, obtaining this type of particle is challenging and may often not be achieved.

According to Gonzalez-Ortiz and Asua (1996), the interaction between kinetics and thermodynamics that determine the morphology of the polymeric particle is given in three main processes: (A) the polymeric chains of the shell are formed in an established position in a polymer particle seed; (B) phase separation can occur if the newly formed polymer is incompatible with the seed polymer that will serve as the core. Thus, there is the formation of agglomerates, called clusters, due to this phase separation; (C) these clusters migrate towards the equilibrium morphology to minimize the Gibbs free energy. The size of the clusters during migration varies due to three factors: (i) the clusters can coagulate with each other, (ii) there can be polymerization within the clusters, and (iii) the polymer chains can diffuse from the clusters. The phase viscosities strongly influence coagulation and diffusion in these cases (GONZÁLEZ-ORTIZ; ASUA, 1996).

When the shell and core polymers are incompatible, and there is a low viscosity in the particle, the polymer chains are mobile, and the equilibrium morphology is instantly achieved when the chemical composition of the shell is


gradually varied at the beginning of the reaction, causing the monomer moves towards the periphery of the particle (KOSKINEN; CARL-ERIC WILÉN, 2009). For these cases, thermodynamic considerations are the basis for the developed models, and the total variation of the Gibbs free energy is equal to the variation of the interfacial energy. Thus, the thermodynamically preferred morphology is given by the change in the minimum interfacial energy (GONZALEZ-ORTIZ; ASUA, 1995). The combination of terms involving entropy, enthalpy, and interfacial energy changes describe the change in Gibbs free energy. In this sense, the minimum interfacial energy can be expressed as (Eq. 1):


$$\phi = \frac{1}{2} \sum_{i=1}^3 \sum_{\substack{j=1 \\ i \neq j}}^3 a_{ij} \theta_{ij} \quad \text{Eq. 1}$$

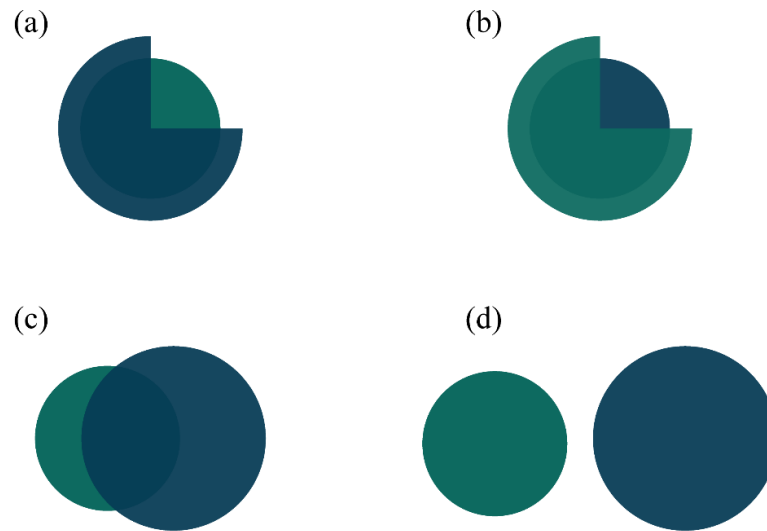
Where, θ_{ij} e a_{ij} represent the interfacial tension and the interfacial area between phases i and j, respectively.

The interfacial tensions in the polymer-polymer and polymer-aqueous phases and the cross-link density are the dominant factors in the control of equilibrium morphology (SUNDBERG; DURANT, 2003). According to Sayer and Araujo (2010), it is possible to mention four types of equilibrium morphology (Figure 8) when the components of interfacial tensions in a system based on two polymers and an aqueous medium, represented as polymer 1 (core), polymer 2 (shell), and phase 3 (aqueous phase), are taken into account:

Figure 8: Core-shell particle equilibrium morphologies. (a) Core-shell (CS); (b) Inverted Core-Shell (ICS); (c) Janus particle; (d) Separated particles

Polymer 1 

Polymer 2 



Source: Author's elaboration

1. Core-shell (CS): In this type of morphology, polymer 2 continuously covers polymer 1. It is possible to obtain this type of particle in two ways. The first is when the core polymer is more hydrophobic than the shell polymer ($\sigma_{13} > \sigma_{23}$), while the shell polymer has more affinity with the core polymer than the aqueous phase ($\sigma_{12} < \sigma_{23}$). The second mode is when the core polymer has more affinity with the shell polymer ($\sigma_{12} < \sigma_{13}$) than with the aqueous phase ($\sigma_{12} > \sigma_{23}$).
2. Inverted Core-Shell (ICS): This happens when polymer 1 forms a shell around polymer 2. So, this second polymer has more affinity for polymer 1 than it does with the aqueous phase ($\sigma_{12} < \sigma_{23}$), and polymer 2 is more hydrophobic than polymer 1 ($\sigma_{23} > \sigma_{13}$).

3. Janus: This morphology can be obtained in three ways - I: the affinities of polymer 2 with the aqueous phase and polymer 1 are similar ($\sigma_{12} \approx \sigma_{23}$); II:
 4. polymer 2 has less affinity with the aqueous phase than with polymer 1 ($\sigma_{12} < \sigma_{23}$), while both polymers have similar affinities with the aqueous phase ($|\sigma_{23} - \sigma_{12}| \leq \sigma_{13}$); III: Polymer 2 has more affinity with the aqueous phase than with polymer 1 ($\sigma_{12} > \sigma_{23}$), while polymer 1 has similar affinities with
 5. the aqueous phase and polymer 2 ($|\sigma_{23} - \sigma_{12}| \leq \sigma_{13}$).
6. Separated particles: It is not exactly a core-shell morphology. It can be understood as the simultaneous polymerization of two distinct polymers. It is obtained when there are similar affinities between each polymer and the aqueous phase, and this affinity is greater than that they have for each other ($\sigma_{13} < \sigma_{12}$) and ($\sigma_{23} < \sigma_{12}$).

The distribution of clusters formed by the polymer of the shell around the seed particle that forms the nucleus describes the type of final morphology. However, the literature does not present any simple technique to characterize this distribution accurately.

As can be seen, the equilibrium morphologies are obtained by three values of interfacial tension: between polymer 1 and the aqueous phase, between the two polymers, and between polymer 2 and the aqueous phase. Compatibilizing agents can strongly influence the interfacial tension between polymers 1 and 2, and surfactants and initiators can influence the tension between each polymer and the aqueous phase (LOVELL; SCHORK, 2020).

Molecular weight also becomes an important parameter for obtaining equilibrium morphology in seeded emulsion polymerization, as it determines the diffusion of polymers that form in the second polymerization step and thus influences the interfacial tension between the polymers and the aqueous phase (KARLSSON; HASSANDER; WESSLÉN, 2000). In summary, the equilibrium morphology in an emulsion system can be predicted by analyzing the contact angles, propagation coefficients in the three phases (polymer 1, polymer 2, and aqueous phase), and interfacial tensions (AHANGARAN; HAYATY; NAVARCHIAN, 2017). In addition, the equilibrium morphology analysis becomes even more complex when using copolymers in the shell or core so that the interfacial tensions depend not only on the characteristics of two polymers that would form the structure but, on a polymer, and a copolymer.

Besteti and collaborators (2014) report the production by combined suspension and emulsion of particles with polystyrene (PS) core and poly(methyl methacrylate) (PMMA) shell and that the low compatibility between PMMA and PS negatively affected the coating efficiency of the seed particles, resulting in some particles seemingly without a shell or that the shell formed is too thin. The poor compatibility of PMMA with PS makes it more difficult to capture and fix the emulsified particles in the PS core, especially when the suspension polymerization has a longer duration and the PS core becomes more rigid.

2.3.2. Particle size and distribution

The particle size distribution (PSD) strictly means the particle diameter distribution. The size distribution of polymeric particles is an extremely necessary parameter in determining suspension stability and product quality attributes, significantly influencing several fundamental properties of the final product, such

as viscosity, the maximum content of solids, adhesion, polymer rheology, optical properties, mechanical strength (MACHADO *et al.*, 2000; ZHANG *et al.*, 2021a). Many methods have been developed to calculate this parameter, and angular scattering is widely used due to its advantages of real-time measurement, non-contact method, and high sensitivity (MA *et al.*, 2021).

Light scattering measurement of the PSD is based on the scattering light principle. When a beam of light strikes a particle, the beam of light is absorbed and scattered by the particle, and then the outgoing light will deviate from the direction of propagation of the incident light and scatter around (ZHANG *et al.*, 2021a). Light scattering measurements include classical static light scattering (SLS) and dynamic light scattering (DLS).

When emulsions are formed from very small particle sizes, they can generate very high viscosities, while very large particle sizes can lead to unstable emulsion particles. Dynamic light scattering (DLS) particle size determination gives a mean size (Z-average) value based on a detector angle (173° or 90°). It is a quick and simple way to determine the hydrodynamic radius of colloidal species (MAKAN *et al.*, 2016). Recently, most works involving synthesizing materials with core-shell structures sought to obtain submicron-sized particles (CIPOLATTI *et al.*, 2016; JIN *et al.*, 2018; TKACHENKO *et al.*, 2020).

An index of great importance in particle size distribution analysis is the dispersion index (DI), defined as a measure of dispersion. It means that when DI is equal to 1, all particles are equal in size and the standard deviation is zero. For some polymers, such as polystyrene, it is common for the dispersion index to be around 2 (MACHADO *et al.*, 2000).

2.3.3. Specific surface area

Determining surface properties is becoming increasingly important for different types of materials. The main property is the Specific Surface Area (SSA), which is the area available for the adsorption of molecules, especially liquids and gases. One way to increase surface area in polymer particles is to reduce particle size by crushing and grinding, for example, or changing its porosity by heat treatment. This property is usually determined by physically adsorbing a gas on the material surface and measuring the amount of adsorbed gas. SSA of materials is usually calculated using the Brunauer-Emmett-Teller (BET) method or modifications thereof (GIBSON *et al.*, 2019; NADERI, 2015).

Cunha and collaborators (2014) synthesized core-shell particles from suspension polymerization (core formation) and emulsion (shell formation) combined. The results show a relationship between the specific surface area and the suspension time (when the emulsion starts for the shell polymerization). The authors produced core-shell particles with different materials for the core and shell, including inverting the position between them. Still, regardless of the polymer involved, the suspensions of up to 2 hours provided a final structure with a larger specific area (around 2 times more than particles synthesized with a suspension of 4 hours).

2.3.4. Hydrophobic surface

The hydrophobicity of a material means that water does not spread over it. On the contrary, when water is in contact with a hydrophobic surface, it forms droplets, and a contact angle from the surface plane can be measured. Thus, hydrophobic surfaces are characterized by high contact angles with water, usually 40 to 110 degrees, and low immersion heat (ZETTLEMOYER, 1968).

Hydrophobic polymers have been extensively studied, especially when the intention is to immobilize lipases, as it is reported that these enzymes show interfacial activation in the presence of hydrophobic surfaces, which a conformational modification can explain in the structure of the enzyme, which causes exposure of the enzyme active center (phenomenon observed for lipases from CAL-B) (PINTO *et al.*, 2020).

2.3.5. Surface modification

The use of synthetic polymers for enzymatic immobilization is extensive in the literature. It is necessary to evaluate the functionalizable groups in the polymer chain whenever this type of support is considered, especially when the immobilization method involves the covalent bond between enzyme and support. In general, synthetic polymeric structures are inert. They do not have a group capable of chemically reacting with the enzyme. Thus, some reactions are performed to activate the groups of these polymers and make them covalently bind to the amino acid residues present in the enzyme's three-dimensional structure, aiming to avoid binding to residues in its active site.

In this sense, the frequent amino acids in the enzyme to be covalently attached to the support should not be essential to its activity. Among these, cysteines and lysins are possibly the most applied for this type of binding. However, it is still possible to point out glutamic and aspartic acids (DAS; DWEVEDI; KAYASTHA, 2021), and there are still works in the literature in which the enzyme is linked to support through the phenolic groups of tyrosine residues (CATAPANE *et al.*, 2013). There is a certain challenge in reaching cysteine residues in enzymatic immobilization since these are rare and commonly buried in hydrophobic sites or involved in disulfide bonds (RODRIGUEZ-ABETXUKO *et*

al., 2020). In summary, the main functional groups of amino acids involved in covalent coupling are the amino, hydroxyl, thiol, phenolic, carboxylic, sulfhydryl, imidazole, thiol, and indole groups (NGUYEN; KIM, 2017).

A polymer must have reactive functional or functionalizable groups to covalently bind an enzyme, which must exhibit stability in reaction environments. The main side groups of the polymer chain involved in linking with enzymes are amino, carboxyl, hydroxyl, sulfhydryl, imidazole, phenolic hydroxyl, and epoxy (BILAL *et al.*, 2018; MARTINOVÁ; NOVÁK, 2018). The support material must therefore have inert characteristics whose enzymatic immobilization is strong enough to avoid the leaching of the biomolecule during application (PEDROCHE *et al.*, 2007).

Furthermore, when choosing the shell material, it is necessary to consider that the coupling of the enzyme to the polymeric matrix is developed in two steps: the activation of the particle surface through functionalization and the activation of the particle surface through functionalization immobilization in the activated matrix. Several literature reports point to functionalization steps and their applications, generally achieved through bifunctional agents (RUDAKIYA; GUPTA, 2019). The large surface area and surface functionality allow the application of polymeric shell-core particles for large-scale enzymatic immobilization (HO *et al.*, 2010). Each enzymatic immobilization method may require a different functionalization condition on the shell polymer.

Aggarwal and collaborators (2021) state that polymeric nanomaterials are usually highly adaptable if reactions with glutaraldehyde, ethylenediamine apply activation processes, carbodiimide, or even by silanization, sulfonation, phosphorylation, and acylation/alkylation (AGGARWAL; CHAKRAVARTY;

IKRAM, 2021). It can be applied to other polymeric morphologies, such as the core-shell, since polymers such as polyacrylonitrile, for example, present characteristics such as easy functionalization (VIEIRA *et al.*, 2021). Reactive copolymers can also be used for immobilization by covalent bonding when functionalized by amination. This type of functionalization should not change the physical parameters of the support, including its topography and surface area (CORDEIRO *et al.*, [s.d.]).

Despite the almost absolute need for functionalization in polymeric matrices, there is still a great risk of denaturation of the enzyme throughout the immobilization process because the chemical modifications of the functional groups involve the use of several steps and reagents (DAS; DWEVEDI; KAYASTHA, 2021).

In this sense, the choice of the shell material and the immobilization method is fundamental and must be done with a due theoretical foundation. It is because both the nature of the support and the conditions of immobilization of the enzyme in the catalytic process must be evaluated. Depending on the compounds and functional groups present on the surface of the support, the immobilization of the enzyme will be given differently (DARONCH *et al.*, 2020). For example, in the covalent bond immobilization method, the functional groups of the support surface should be compatible with the functional groups available in enzymes, allowing that covalent bond occurs. In contrast, the textural properties of support as its surface area will be more important for the immobilization method by adsorption.

2.4. APPLICATIONS

Considering all the properties presented so far, particles of core-shell morphology are the target of studies in various scientific areas, with applications in the cosmetic and food industries, the biomedical area, electronics, and, particularly, in the production of catalysts (GALOGAHI *et al.*, 2020; SU *et al.*, 2020). As they have an excellent specific area, porous structure, and easy functionalization of the shell, several kinds of research have focused on synthesizing nanoporous core-shell particles with applications such as bioadsorbents and biocatalysts (SU *et al.*, 2020). In the case of nanoporous particles, pore size control is performed by changing the agitation rate or the surfactant content used in the synthesis. In this sense, a higher surface-to-volume ratio can be controlled in the polymerization process (PANDAY *et al.*, 2018). Depending on the pore size, these particles can adsorb cells, macromolecules (such as proteins and enzymes), and small molecules (such as drugs and amino acids) (SU *et al.*, 2020). This interaction with molecules most commonly occurs through physical adsorption and chemical bonding.

From this perspective, the particle size distribution is important for specific applications. For Sarnello and collaborators (2021), using heterogeneous catalysts in industry demands larger particles to facilitate product separation at the end of the process. The accepted range for particle sizes for biomedical applications is around 100 nm (SARNELLO; LI, 2021). Regardless of the application, the use of core-shell particles allows the use of enzymes efficiently in different environments (SARNELLO *et al.*, 2020).

Concerning the application of core-shell particles as a support for making heterogeneous biocatalysts, the possibilities are as vast as those that employ

other inorganic and polymeric structures as enzymatic support. For example, the use of lipase for biodiesel production is widely discussed in the literature, generally showing good results both in free and immobilized form. Paitaid and H-Kittikun (2019) used magnetic nanoparticles coated with polyacrylonitrile to immobilize this enzyme. The results proved the biocatalyst's efficiency in converting biodiesel and showed high immobilization rates. In this study, the high surface area of polyacrylonitrile provided greater lipase carrying, and by using a magnetic nanoparticle as a core, the separation of the biocatalyst at the end of the transesterification reaction was facilitated (PAITAIID; H-KITTIKUN, 2020).

Enzyme catalysis is the main feature of applications of immobilized enzymes in core-shell structures. On the other hand, using these catalysts as biosensors has aroused interest in the scientific community. Although most studies involve magnetic core-shell particles (CHAPA GONZALEZ *et al.*, 2014; MAGRO *et al.*, 2020; YUAN *et al.*, 2019), interest in polymeric particles has increased in the last few years. Recently, a study was developed to detect glucose by photoelectrochemical biosensors formed by the enzyme glucose oxidase immobilized in a structure composed of a titanium dioxide core and a polydopamine shell (XU *et al.*, 2020). In addition, core-shell particles of carbon and polyaniline were identified as support for the immobilization of acetylcholine esterase and applied as a biosensor for insecticide detection (HE *et al.*, 2018).

Environmental legislation worldwide has sparked interest in environmentally adequate, low-cost solutions that are operable under milder conditions. In this sense, the treatment of effluents by biotechnological processes has gained prominence in recent years since enzymes are efficient catalysts in the degradation of recalcitrant compounds discarded in public sewage networks

or by the food, pharmaceutical, and textile industries. The application of enzymes immobilized on core-shell particles finds a solid space in this niche. It is possible to find in the literature on the removal of difficult-to-degrade compounds such as Methyl Orange Dye (WANG *et al.*, 2021b), Malachite Green Dye, Bisphenol A, and Bisphenol F (RAN *et al.*, 2019) or Triclosan and Remazol Brilliant Blue R (LE *et al.*, 2016).

2.5. CORE-SHELL POLYMERIC PARTICLES FOR ENZYME IMMOBILIZATION

The core-shell morphology particles demonstrate advantageous characteristics compared to other supports aiming to polymerize supports for enzymatic immobilization (GALOGAHI *et al.*, 2020; HE *et al.*, 2019; MA *et al.*, 2013; PINTO *et al.*, 2019). It is known that supports for enzymatic immobilization must present some desired characteristics, such as insolubility in water, high capacity to interact with the enzyme, chemical stability, mechanical resistance, hydrophobic or hydrophilic surfaces, preferentially porous morphology, storage capacity, and low costs. Moreover, the chosen material should present functional groups (or that can be adequately functionalized) to interact with enzymes (BESTETI *et al.*, 2014b). In this sense, the desirable characteristics and those made available by the core-shell morphology are in harmony.

One of the advantages of using materials with a core-shell structure in enzyme immobilization is that the combination of two polymers (or materials) is usually sought to enhance the properties of one or both components and to achieve superior properties. Using the core-shell structure is a strategy that has been used to combine two different materials to achieve properties that are

difficult to achieve just by mixing them (RAMLI; LAFTAH; HASHIM, 2013). Table 2 shows several works using polymeric materials with core-shell structures in enzyme immobilization.

1

Table 2: Core-shell structure materials used in enzyme immobilization

Support								
Core/Shell materials*	Size	Specific area (m ² /g)	Support modification	Enzyme	Immobilization method	η (%)**	Protein loading (mg/g _{support})	Reference
PS/PS; PS/PS-co-PC; PS/PMMA; PMMA/PS; PMMA/PMMA; PS-co-DVB/PS-co-DVB ⁴ ; PS/PS-co-DVB; PS-co-DVB/PS; PMMA-co-DVB/PMMA-co-DVB; PMMA/PMMA-co-DVB; PMMA-co-DVB/PMMA	-	7.9; 6.2; 36.7; 8.7; 5.0; 28.9; 9.5; 10.9; 12.6; 11.3; 8.7	Without chemical modification on the support surface	Lipase (CAL-B)	Physical adsorption	52; 63; 23; 75; 47; 98; 74; 83; 75; 57; 83	3.4; 3.5; 0.8; 6.0; 1.5; 17.4; 10.7; 13.4; 11.4; 7.4; 6.8	(BESTETI <i>et al.</i> , 2014a; CUNHA <i>et al.</i> , 2014)
PS/PS; PS-co-DVB/PS-co-DVB	114.6 ± 1.3 μm; 65.8 ± 18.6 μm	27.3; 33.4	Without chemical modification on the support surface	Lipases (RML ⁶ ; TLL ⁷); CAL-B; LU ⁸)	Physical adsorption	-	55 - 120	(MANOEL <i>et al.</i> , 2016)
Sodium alginate /Calcium alginate	20 - 40 mesh	112.93	Without chemical modification on the	Lipase on the bamboo carrier	Physical adsorption	≈ 80	-	(DENG <i>et al.</i> , 2019)

PMMA/Chitosan	275 - 324 nm	-	support surface Without chemical modification on the support surface	Lipase from <i>Candida rugosa</i>	Physical adsorption	80 - 93	-	(JENJOB <i>et al.</i> , 2012)
Fe ₃ O ₄ /Poly(MMA-co-DVB)	10.0 μm	12.0	Without chemical modification on the support surface	Lipase	Physical adsorption	-	15.0	(MENG <i>et al.</i> , 2013)
Pyrene-poly(styrene-acrylamide-acrylic acid)	111.5 nm	107.96	Without chemical modification on the support surface	Peroxidase enzyme conjugated antibodies	Crosslinking	95 - 98	-	(JAIN <i>et al.</i> , 2013)
Poly(styrene)-b-poly(styrene-alt maleic anhydride)	20-30 nm	-	Nitrilotriacetic acid-modified polymer in the presence of Ni ²⁺ Without chemical modification on the support surface	Two His6-tagged endoglucanases, CelA and CelF	Covalent bonding	-	-	(LU <i>et al.</i> , 2019)
P(S-co-DVB)/P(S-co-DVB)	-	43.4	Without chemical modification on the support surface	Lipase from <i>Candida rugosa</i>	Physical adsorption	97.8	17.5	(PINTO <i>et al.</i> , 2019)

*The first name is the core composition, and the second is the shell composition.

**η - Immobilization efficiency.

¹PS - Polystyrene; ²PS-co-PC - Poly(styrene-co-cardanol); ³PMMA - Poly(methyl methacrylate); ⁴PS-co-DVB - poly(styrene-co-divinylbenzene); ⁵CAL-B - Lipase B from *Candida antarctica*.

Source: Author's elaboration

Other advantages and discussions can also be added for using core-shell polymeric structures as support for enzymatic immobilization. First, the interaction between the enzyme and support should be strong when discussing enzyme immobilization, as previously discussed. In addition, there is a need for the enzymatic system to be stable; that is, the catalytic activity must be maintained for a few cycles (LUO *et al.*, 2022).

The main stabilizing effects of an enzyme are caused by the simple fact that it is inside/bound to a solid particle. But there are also advantages related to the stability of the enzyme system when using polymers and the core-shell structure. This polymeric structure can generate more stable enzymatic conformations or rigidity via covalent bonding (RODRIGUES *et al.*, 2021; WANG *et al.*, 2021a).

Studies report that these supports can maintain excellent catalytic capacity in the microenvironment, high water tolerance, and good stability (CAI *et al.*, 2021; FARHAN *et al.*, 2021; TAHERI; CLARK, 2021). Other studies identified that using core-shell polymeric particles in the immobilization of enzymes such as lipase can alter the diffusion rates of substrates depending on physical changes that may occur on the surface of the support. In this case, some properties such as shell porosity and thickness can affect the diffusion rates of substrates through the polymeric support and, consequently, the enzymatic reaction rates (CUNHA *et al.*, 2014; DENG *et al.*, 2019; PINTO *et al.*, 2019). Therefore, the apparent kinetic parameters (K_m and V_{max}) of enzymatic reaction are correlated with support properties in the case of reaction rates controlled by internal diffusion. In this sense, the main piece of information regards the possibility of adjustment of shell porosity and thickness from the polymerization technique used in the production of the core-shell support, as well as the choice of polymers. The use of a thin shell thickness in which the enzyme is

immobilized can decrease the internal diffusion rates, increasing the enzymatic reaction rates.

2.6. POLYMERS FOR CORE AND SHELL

The coating material directly interferes with the shell's chemical, physical and biological properties. In this regard, polymers have advantages over other materials, such as oxides and metallic salts, because particle size and surface area are very difficult to control when using inorganic materials, and the enzyme can be easily leached from the system. In contrast, polymers (mainly synthetics) can offer a wide range of uses, proper specific surface area, and available functional groups, which can be selected according to each enzyme (LUO *et al.*, 2022).

This great flexibility in choosing polymers for shell composition allows synthesizing of core-shell particles with diverse functionalities and properties. It implies that the shell materials can be selected according to the enzyme to be immobilized. In addition, the shell increases biocompatibility and dispersibility and provides greater chemical and mechanical resistance to the final support (GALOGAHI *et al.*, 2020).

In studies involving these structures, core materials are mainly concentrated in inorganic nanoparticles or organic polymers. When it comes to polymers and enzyme immobilization, thermoplastics are the most explored polymers to form the shell and the core. However, the core polymer is generally a low-cost synthetic polymer, such as polystyrene, which appears in most works that involve this morphology in enzyme immobilization (SU *et al.*, 2020).

The polymers used in the shell formation are chosen to resist the support and direct interaction with the enzyme. In this context, synthetic polymers receive special emphasis because they are easily produced and modified, with functional groups that interest the enzyme. In general, they have a low cost (PINTO *et al.*, 2020).

For lipase, hydrophobic polymers have been widely studied due to the interfacial activation that many lipases show in the presence of hydrophobic surfaces, a phenomenon justified by a conformational modification in the structure of the enzyme, exposing its active center, as occurs for CAL-B (CUNHA *et al.*, 2014; MANOEL *et al.*, 2016; PINTO *et al.*, 2020). In the case of laccases, it is reported on the functional groups present on the surface of the support. Depending on the group, the fixation of the enzyme will be given differently. When the groups -OH, C=O, and -NH₂ are present, only the trapping methods can be applied, but on a surface with -OH, COOH, C=O, -SH, -NH₂, adsorption of the enzyme may occur, and the formation of the covalent bond (DARONCH *et al.*, 2020). Thus, looking at the enzyme you want to immobilize is necessary for the ideal choice of support polymers.

2.7. IMMOBILIZATION METHODS

If well-chosen, the immobilization technique gives the enzyme greater thermal and chemical stability, allowing its reuse in several cycles and long storage periods, as long as they are kept under favorable conditions (ALMEIDA *et al.*, 2021). Polymeric materials have been extensively investigated as enzyme support because they have several practical advantages (ZHANG *et al.*, 2021b). Among these advantages is that they are insoluble, resistant, malleable, functional, and generally of low cost.

After considering the choice of materials that will compose the core-shell particle that will be applied as enzymatic support, identifying the functional groups of the polymer, and the functionalization methods, the choice of the immobilization method is also a very important step.

In this sense, it is worth mentioning that the characteristics of the support can define which immobilization method to use. For example, a controlled porosity

facilitates immobilization by physical adsorption. Likewise, if the porosity on the surface of the support is insufficient, immobilization by covalent bonding may be more suitable.

The most used immobilization methods in the literature are adsorption, covalent bonding, trapping, cross-linking, and encapsulation (DARONCH *et al.*, 2020). Each method has particularities, advantages, and disadvantages that must be considered. There are still reports in the literature on combining more than one method, aiming at improving immobilization and supplying the disadvantages that each method can have individually (JUN *et al.*, 2019; ZHOU; ZHANG; CAI, 2021). In Table 3, it is possible to observe a summary of the best-known methods.

Table 3: Interactions, advantages, and disadvantages of immobilization methods

Immobilization method	Interaction	Advantages	Disadvantages
Adsorption	Ionic, hydrogen, or Van der Waals bond	Simple and accessible process	Low stability
Covalent bond	Covalent bond with the functional groups of the enzyme	Stronger and more stable connection	May cause loss of enzyme activity
Entrapment	Entrapment in the porous matrix	High strength and stability	Complex and irreversible process
Encapsulation	Immersion in selectively permeable membranes	Simple and low cost	Restricted substrate flow and low stability
Crosslinking	Enzymes are linked to each other	Large contact surface	Complex, high-cost, and irreversible

Source: Author's elaboration

In adsorption immobilization, the enzyme is generally reversibly bound to insoluble support through weak forces such as ionic, hydrogen, or Van der Waals bonds. The set of these interactions allows just enough stability to keep the enzymes adhered to the support for some cycles, especially when the reactions are carried out in an organic medium, given that under these conditions, the enzyme is insoluble in

non-polar systems (DE OLIVEIRA *et al.*, 2021). However, the stability of the bonds is not observed when one wants to reuse the biocatalyst for many cycles since the desorption of the enzyme is noticed with reuse or washing (JESIONOWSKI; ZDARTA; KRAJEWSKA, 2014). It is a widely used immobilization method due to its simple operation, low cost, reproducibility, and practically no changes in the enzyme (AGGARWAL; CHAKRAVARTY; IKRAM, 2021).

Glucose Oxidase (GOx) has been immobilized by physical adsorption on a poly(methyl methacrylate) structure in the core and BSA protein in the shell. In this research, it was observed that the influence of ionic strength and pH played a fundamental role in immobilization that occurred by electrostatic interactions. By comparing the activities of the enzyme immobilized in the core-shell structure and the free enzyme, the researchers found that the immobilized GOx retained 80% of the free enzyme activity, in addition to having superior stability under high-temperature conditions (HE *et al.*, 2009).

Immobilization by covalent bonds is one of the most used methods. As the name suggests, it involves the covalent bonding of functional groups on the support with the functional groups present in the amino acid residues that compose the enzyme's surface (FERNÁNDEZ-FERNÁNDEZ; SANROMÁN; MOLDES, 2013). Because it is a stronger bond, the enzyme does not easily decouple from the support, as in immobilization by adsorption, and, for this reason, the bond resists extreme operating conditions. The counterpoint of this type of method is the decrease in enzymatic activity. It can occur due to some possible damage caused to the structural conformation of the enzyme (DAMIN *et al.*, 2021) or the connection between the support and the amino acid residues in the active site.

Regarding covalent bond immobilization, horseradish peroxidase (HRP) was immobilized on core-shell particles composed of expanded polystyrene (EPS) in the core and bio-adhesive polydopamine in the shell. The immobilization had an efficiency of 46% and provided stability of the enzyme at high pH (pH 10) and temperature (60°C) compared to free enzyme. Immobilized HRP was also tested on Gentian Violet dye degradation, resulting in 96% degradation in 120 minutes. Additionally, it was reported that immobilized peroxidase showed 80% of its initial activity in the tenth cycle and 60% in the fifteenth (YASSIN; GAD, 2020).

Trapping is based on literally trapping the enzyme in a porous matrix, commonly in polymers and gelatins, which allows the substrates to pass through the support, but the enzyme does not escape (REN *et al.*, 2020). This method results in excellent thermal resistance and high stability, allowing multiple biocatalyst reuse cycles. Among the disadvantages are the complexity of the immobilization operation, little control over the size of the pores, which must not be large enough for the enzymes to escape, and the increase in the Michaelis-Menten constant. Trapping is an irreversible process (JUN *et al.*, 2019); once a certain enzyme is immobilized, it is impossible to reuse the support after enzymatic inactivation.

A method of immobilizing laccase by entrapment in a core-shell structure formed from metallic nanoparticles coated with silica was developed through dopamine self-polymerization. In practice, the laccase adhered to the surface of the core particle formed by iron and silica and was covered with a polydopamine shell. The study results showed an enzyme activity recovery of approximately 43%, greater stability, and resistance to pH changes, in addition to the retention of the initial activity after 10 cycles (65%) of use and 70 days of storage (80%). Of the main advantages of the process,

the authors point out its low cost, sustainability, and high catalytic activity (DENG *et al.*, 2015).

The encapsulation immobilization method envelops the enzyme in selectively permeable membranes, allowing substrates to flow through the immobilized enzyme. This process provides a protective environment for the enzyme, either through adhesion or binding of the enzyme to the main structure of the polymer (JEYARAMAN; SLAUGHTER, 2021). Despite similar problems to the trapping method, such as the diffusion-controlled rate of substrates and the diffusion of enzymes through the pores, it is a simple and low-cost method (FERNÁNDEZ-FERNÁNDEZ; SANROMÁN; MOLDES, 2013; JUN *et al.*, 2019). Many studies deal with encapsulating anticancer drugs (AL-SHALABI; ALKHALDI; SUNOQROT, 2020; BOURGAT *et al.*, 2021; HONG *et al.*, 2018) and food products (CASTRO COELHO; NOGUEIRO ESTEVINHO; ROCHA, 2021). However, few works have been found for enzyme immobilization. Recently, urease has been encapsulated in two core-shell nanoparticles, an iron-alginate, and an iron-nickel-alginate composite. The immobilization yield in the two systems was approximately 98%. In addition, the thermal and pH stability was improved, and the enzymatic activity with reuse for the two types of particles was high up to 27 cycles (İSPIRLI DOĞAÇ; TEKE, 2021).

Unlike the other methods presented above, immobilization by cross-linking does not necessarily use support but cross-linking agents. This method links the enzymes, forming a network structure with a large contact surface through a complex and costly process. So, these cross-linked enzymes may or may not be attached to a support. A major disadvantage of this method is the possible loss of enzymatic activity when enzymes are cross-linked in a configuration that prevents substrate contact with the active site, which is not easily controllable (JUN *et al.*, 2019).

In obtaining a heterogeneous biocatalyst, the most important factors are the specific area to promote a good interaction between the enzyme and the substrate and the pore volume of the support (DARONCH *et al.*, 2020; ZHOU; ZHANG; CAI, 2021). These factors strongly influence how the support will interact with the enzyme and substrate, thus enabling a better choice of immobilization method. Generally, the larger the pores and the specific area, the higher the adsorption rates due to the more active functional groups. In addition, a larger area and properly sized pores maximize enzyme loading in immobilization and prevent enzyme inactivation. In this sense, polymeric core-shell particles stand out since the specificities above can be controlled in the polymerization process.

2.8. CONCLUSION AND FUTURE OUTLOOK

This review article summarizes the research on polymeric particles with core-shell structures applied in the immobilization of enzymes, which some researchers in recent decades have studied. It was possible to see that the main advantage of core-shell particles is their versatility in terms of their properties and preparation techniques, emphasizing various ideas, methodologies, materials, and characteristics. In addition, various polymers can be exploited according to their affinity with the enzyme and thermal, chemical, and mechanical properties that offer stability to the support against adversities in the reaction medium, improving the enzyme's performance in the desired application. The core-shell architecture is fascinating in composite materials because they combine the excellent functions of the constituents.

There are still few polymers studied in the formation of shell-core structures in the immobilization of enzymes, and the studies focus on the immobilization of lipases with a polystyrene core (or copolymers derived from styrene) and poly(methyl

methacrylate) shells and copolymers, or polystyrene itself. Furthermore, these works were focused on the immobilization of lipases.

Therefore, future scientific research must be designed to meet the demands for different enzymes that have been drawing attention for their performance in the degradation of toxic compounds, such as laccase, and which also offer great immobilization challenges to enable their application.

3 CHAPTER 3 – FUNCTIONALIZABLE
POLY(PROPYLENE-STYRENE)/
POLYACRYLONITRILE PARTICLES WITH CORE-
SHELL MORPHOLOGY

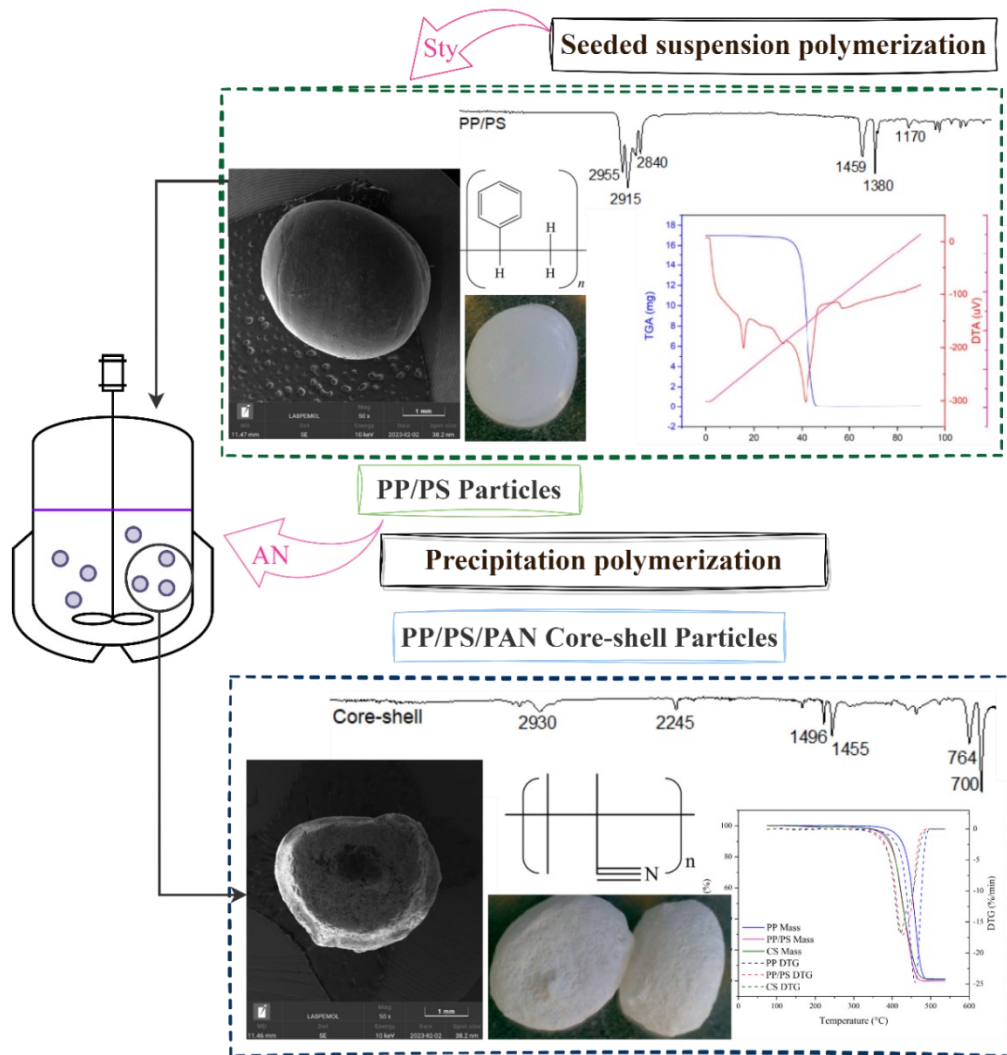
This chapter deals with the entire study behind the synthesis of particles with core-shell morphology and the physicochemical characterization of the material obtained. This chapter has been published and indexed (<https://doi.org/10.1002/app.55667>) in the Journal of Applied Polymer Science titled "Preparation of Functionalizable Poly(propylene-styrene)/Polyacrylonitrile Millimeter-Scale Particles with Core-Shell Morphology". To access, scan the QR Code below. Following Wiley's subscription rules, authors reserve the right to include the article in a thesis if it is not published commercially.



Graphical Abstract

Figure 9 below shows the graphic summary of this chapter, designed for quick visualization of the chapter's content.

Figure 9: Graphic summary of chapter 3



Source: Author's elaboration

3.1. INTRODUCTION

Core-shell (CS) particles constitute a class of particles formed by two or more layers of different materials (the innermost material forms a core and the outermost material(s) form the shell). In some situations, the core and shell may be composed of the same material, but with different properties (GURGEL *et al.*, 2022; HAYES *et al.*, 2014). This type of structure has attracted broad interest from the scientific community, as these particles can find applications in several areas, such as support for heterogeneous catalysts (including enzyme immobilization, for example) (CHEN *et al.*, 2023; GURGEL *et al.*, 2022), carriers for targeted drug delivery (YANG; XIE, 2021), solid substrates for bioadsorption and biocatalysis (SU *et al.*, 2020), vehicles for high energy storage (EZZAHRA; RAIHANE; AMEDURI, 2020), among others.

The wide range of CS application is mainly due to the flexibility of the structure, which allows the combination of two components (core and shell), providing simultaneously high structural strength, good dimensional and chemical stability, excellent anti-corrosion property, among other special functions, when compared to the properties of a commoner single-phase material (GONZALEZ-ORTIZ; ASUA, 1995; MA *et al.*, 2013).

Particles with a core-shell structure can be prepared with various materials. Among these, polymers (mainly synthetic ones) can offer several advantages to constitute the structure, as they are extremely versatile, allowing the incorporation of desired functional groups on the particle surfaces, and providing high specific surface area (SARNELLO *et al.*, 2020; WANG *et al.*, 2013b).

CS polymer particles are generally synthesized through sequential heterogeneous polymerization techniques, such as emulsion, suspension, dispersion, and precipitation polymerizations. Consequently, polymer particles with different

morphologies and sizes can be obtained. In general, the preparation of CS polymer particles involves two steps: (i) the core particle synthesis and (ii) the shell formation (GURGEL *et al.*, 2022; SAYER; HENRIQUE; ARAÚJO, 2010).

During a standard suspension polymerization process, monomer droplets are dispersed in water and act as microsized reactors. Suspension polymerization is the most used technique when it is desired to manufacture larger polymer particles. At the end of the reaction, polymer particles with diameters ranging from 50 to 3500 μm can generally be obtained. The prepared particles can then be easily separated by filtration and/or sedimentation, which is an important feature of this technology (GURGEL *et al.*, 2022). Additionally, suspension polymerizations present other competitive advantages when compared to other heterogeneous polymerization techniques, such as the better temperature control, the low dispersion viscosity, the low levels of impurities in the polymeric product, the low separation costs, and the particulated form of the final product (DOS SANTOS SILVA *et al.*, 2024; DUTRA *et al.*, 2020; PINTO *et al.*, 2013).

In standard bead suspension polymerizations, the produced polymer is soluble in its monomer, and normally smooth spherical particles are produced (PINTO *et al.*, 2013). On the other hand, seeded suspension polymerizations make use of polymer seeds that are initially swollen with monomer. Swollen seeds then are transformed into finely structured composite polymer particles through in-situ polymerization inside the previously swollen seeds. This process typically comprises two stages. In the first stage, monomer is added under stirring into a reaction vessel that contains water, seed particles, and suspending agents, allowing the swelling of polymer seeds. Then, *in situ* polymerization takes place through addition of initiator and monomer, normally following a free radical polymerization mechanism. This process has been used to produce hybrid polystyrene beads from polyolefin seeds (LIN; BIEGLER; JACOBSON,

2010). In particular, seeded suspension polymerization can result in different degrees of polymer penetration in seeds and particle properties depending on operation mode (batch or semi-batch) and reaction conditions (GONÇALVES *et al.*, 2008).

In the case of precipitation polymerization, the reaction begins as a homogeneous mixture of monomer, initiator and solvent. Subsequently, the growing polymer chains separate from the continuous phase during the polymerization by enthalpic precipitation (in the absence of a cross-linker) or entropic precipitation (when cross-linking prevents the polymer and solvent from freely mixing) (GURGEL *et al.*, 2022; VIEIRA *et al.*, 2023). For the formation of the shell in the CS structure, as the polymer forms and precipitates, precipitated particles can agglomerate on the surfaces of the previously prepared particle cores (WAN *et al.*, 2021).

Still, the synthesis of CS polymer particles demands further investigations, as several challenges related to the adhesion of the shell to the core must be faced and remain open. Particularly, the reaction conditions can certainly affect the final characteristics of the obtained structure (GURGEL *et al.*, 2022), including reaction time, agitation and temperature. Besides, this type of reaction allows the combination of different polymers through the addition of distinct monomers, providing means for manipulation of the final characteristics of the particles. This way, the CS properties and morphology tends to incorporate the inherent features of each component (BERG *et al.*, 2023; KARTSONAKIS *et al.*, 2023).

Polyacrylonitrile (PAN) is a synthetic polymer that can be represented by the linear formula $(C_3H_3N)_n$ and is available commercially in granulated or powdered forms, obtained through the polymerization of acrylonitrile monomer (KAUSAR, 2019; VIEIRA *et al.*, 2023). The main characteristic of PAN is the presence of highly polar nitrile groups due to the higher electronegativity of the nitrogen atom in respect to the carbon

atom (VIEIRA *et al.*, 2021). The presence of the nitrile group can provide chemical versatility when PAN is used for the preparation of core-shell particles. For example, the nitrile group can be easily modified and replaced by new functional groups of interest, depending on the desired application (AGRAWAL; CHATURVEDI; VERMA, 2018). Moreover, PAN can keep its structure and composition essentially constant when subjected to extreme conditions and in the presence of alkaline compounds, oxidants, and organic solvents, which indicate its potential utility for various applications (MINET *et al.*, 2010; WU *et al.*, 2017).

Conversely, polypropylene (PP), represented by the chemical formula $(C_3H_6)_n$, is regarded as an excellent material due to its low cost, easy processing, high chemical resistance, and good mechanical properties (ZHAO *et al.*, 2021). Polystyrene (PS) is also one of the most important commodity thermoplastics mainly due to its low cost, low density and excellent electrical properties (such as low electrical conductivity), transparency, high gloss, and good resistance to strong solvents (BESTETI *et al.*, 2014b; MANOEL *et al.*, 2016).

In this context, previous works have already manufactured core-shell materials with these polymers. Gonçalves *et al.* (2008) produced polymer particles with core-shell morphology composed of PS core and poly(methyl methacrylate) (PMMA) shell through seeded suspension polymerization. In this study, the increase of the swelling time resulted in higher incorporations of PMMA and thicker shells (GONÇALVES *et al.*, 2008). Ribeiro *et al.* (2017) produced similar core-shell particles through seeded suspension polymerizations, showing that the styrene conversions of the PS core affected the final polymer properties and that the use of PS seeds with lower styrene conversion allowed the production of higher amounts of poly(styrene-co-MMA) chains, as it might be expected (RIBEIRO *et al.*, 2017).

Some works in the literature have used monomers such as styrene in seeded suspension polymerization reactions to produce particles with core-shell morphology (HAYNE; MARGEL, 2023; MANOEL *et al.*, 2016; PINTO *et al.*, 2019), and in studies that reported the use of polyacrylonitrile, it appears on the surface of the structure due to its contribution of functionality to add and form new chemical groups in the shell of the structure (FAN *et al.*, 2012; GAO *et al.*, 2021; WANG *et al.*, 2013a). Although these polymers (PP, PS and PAN) have already been used to produce core-shell structures, their combination in the same structured core-shell particles has not been described in the open literature yet. Furthermore, few studies in the literature reported the manufacture of core-shell structures in the millimeter scale. Based on the previous remarks, the present study investigated for the first time the manufacture of core-shell particles composed of hybrid poly(propylene-co-styrene) millimeter-scale particle cores (produced through seeded suspension polymerization) and coated with poly(acrylonitrile) particles (synthesized by precipitation polymerization). In particular, the following properties of the obtained CS particles were investigated: particle size distribution, thermal degradation, chemical structure, textural properties, and final particle composition. In addition, the following intrinsic factors related to formation of core-shell structures were also investigated: the swelling degree of core PP particles, the grafting degree between polystyrene and polypropylene in the core structure, and formation of styrene-acrylonitrile copolymers in the shell.

3.2. MATERIALS AND METHODS

3.2.1. Chemicals

Polypropylene particles (PP, Braskem) and styrene (Sty, with 14 ppm of p-tert-butyl-catechol as inhibitor provided by Termotécnica LTDA, 98%) were used to synthesize the core polymer particles. Acrylonitrile monomer (AN, Vetec, 98%) was

used to prepare the polyacrylonitrile shell. Potassium persulfate (KPS, Vetec, 99%) was used as the aqueous phase initiator and benzoyl peroxide (BPO, Akzo Nobel, 99%) was used as the organic phase initiator. Ascorbic acid (Labsynth, 99%) and sodium chloride (Neon, 99%) were also added to the reactor during the PAN shell synthesis. Xylene (Synth, 98.5%), toluene (Dinamica, 99.5%) and dimethylformamide (DMF, Dinamica, 99.8%) were used to fractionate the polymer samples in different analyses. Unless stated otherwise, materials were used as received.

3.2.2. Polypropylene (PP) particles characterization

The commercial PP particles were characterized in terms of specific mass using a pycnometer with cyclohexane as a reference solvent (density = 0.78 g. mL⁻¹). This analysis was performed in triplicate. The morphology of polypropylene was analyzed by optical microscopy using an LCD Microscope (DM4, HD1080P). Particle size distribution (PSD) was evaluated using the Image J software from a sampling of 250 particles. The individual diameters of each particle in the sampling set was counted and measured.

The solubility in xylene (SX) can be considered a fractionation technique that evaluates the relative degrees of crystalline and amorphous fractions of the PP sample, based on its soluble and insoluble fractions (MELO; PESSOA; PINTO, 2023). In summary, the procedure consisted of weighing the sample (about 3 grams) and solubilizing it in 250 g of xylene stabilized with 1 g.L⁻¹ of 2,6-ditert-butyl-4-methylphenol. The sample solubilization was carried out at 135 °C under stirring rate of approximately 200 rpm for 30 minutes, using a heating magnetic stirring plate (ETS-D5 S032, IKA®) and an oil bath. The polymer sample and xylene were added to a round-bottom flask connected to a condensation system. Then, the system was cooled to 25 °C by removing heat from the system using an ice bath. During cooling, the crystalline

polymer fraction precipitates. Then the precipitate is separated through vacuum filtration, constituting the insoluble fraction. The contents of the filter paper (which contains the insoluble fraction) are then placed in an oven at 60 °C for 2 hours. A 50 mL aliquot was collected from the filtrate to remove the solvent by evaporation under heating at 80 °C, thus providing the soluble fraction (LIMA *et al.*, 2014). SX was performed in triplicate and the fractions were calculated with Equations 2 and 3:

$$\% \text{ Soluble} = \left[\frac{(m_2 - m_1)}{V_{\text{filtrate}}} \times V_{\text{xylene}} \right] \left(\frac{1}{m_{\text{PP}}} \right) \times 100 \quad (2)$$

$$\% \text{ Insoluble} = 100 - \% \text{ Soluble} \quad (3)$$

where m_2 is the mass of soluble polymer fraction and crucible after solvent evaporation, m_1 is the mass of crucible, V_{xylene} is the initial xylene volume used in fractionation, V_{filtrate} is the filtrate volume aliquot and m_{PP} is the initial mass of polypropylene.

Furthermore, as PP particles were used to synthesize the polymer core, swelling tests were carried out with styrene. The degree of swelling (solvent or monomer absorption) can be expressed in terms of volume or weight increase (GOKMEN; DU PREZ, 2012). In the second case, swelling is achieved by measuring the sample mass as it swells in a solvent or monomer (such as styrene). Excess monomer on the particle surface must be removed before measuring the mass of the swollen polymer particles through careful paper drying. The degree of swelling is defined as the ratio of the swollen weight in respect to the dry weight. The absorption of styrene then leads to modification of the properties of the swollen polymer particles (CUNHA *et al.*, 2014).

The swelling tests were carried out in test tubes inserted in a thermostatic bath with a controlled temperature of 85 °C. 0.2 g of polypropylene (PP) particles were placed in test tubes with 0.5 g of styrene. Each test tube was removed 15 minutes apart until the degree of swelling became constant, indicating the equilibrium swelling degree of the particles. The assay was performed in duplicate. The swelling degree can be calculated with Equation 4:

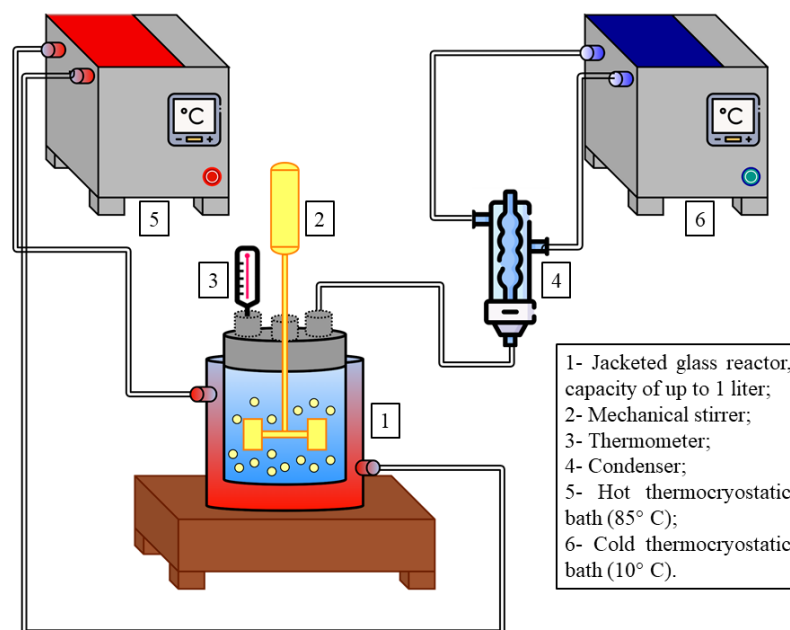
$$\% \text{ Swelling} = \left(\frac{Mass_{final} - Mass_{initial}}{Mass_{initial}} \right) \times 100 \quad (4)$$

Swelling tests of PP particles were also carried out with acrylonitrile. PP particles were characterized through thermogravimetry (TGA) using the Simultaneous Thermal Analysis (STA 449 F3 Jupiter, Netzsch) equipment. This analysis involved heating samples of approximately 6.0 mg from 20 to 600 °C with a heating rate of 10 °C.min⁻¹ under nitrogen atmosphere (at a flowrate of 60 mL.min⁻¹).

3.2.3. Preparation of Polypropylene/Polystyrene (PP/PS) Hybrid Particles

Polypropylene/polystyrene (PP/PS) particles were synthesized through seeded suspension polymerization. Figure 10 presents a schematic representation of the batch reactor used to produce the hybrid PP/PS particles, consisting of two thermocryostatic baths (MQBTC99-20, Microquimica) and a mechanical stirrer (RW20D, IKA).

Figure 10: Representative scheme of the polymerization apparatus



Source: Author's elaboration

For these reactions, 100 g of PP particles and deionized water (approximately 500 g) were placed inside a 1 L reactor. Afterwards, 25 g of styrene were added at 85 °C and stirred at 480 rpm (the amount of styrene added corresponds to the maximum swelling of the particles, as shown in the next section). After 1 hour of contact between the PP and the styrene (also according to swelling tests), the initiator (BPO, 0.5 g) was added in pure powder form, mixed with approximately 25 mL of deionized water to aid in the addition of the compound to the reactor. Suspension polymerization was performed for 4 hours under the same temperature and stirring conditions of the swelling step. At the end of 4 hours, the particles were separated by filtration, washed with deionized water and dried in an oven at 60 °C for 24 hours until constant weight.

At the end of the reaction, weighing of the particles mass allowed to obtain the styrene conversion. This measure represents the mass composition of PP and PS and the calculation was performed using Equation 5:

$$X (\%) = \frac{(m_{Final} - m_{Initial})}{m_{Styrene}} \times 100 \quad (5)$$

where X is the styrene conversion, m_{Final} is the dried mass of hybrid PP/PS particles, $m_{Initial}$ is the initial mass of PP particles and $m_{Styrene}$ is the mass of styrene added in the polymerization reaction.

3.2.4. PP/PS particles characterization

The PP/PS particles were characterized according to their morphological aspects, both by optical microscopy (as described above) and by scanning electron microscopy (SEM) (TESCAN MIRA 4 microscope) with approximation of 50 and 100x, after particles coating with gold before analysis. Similarly to the PP particles, the PP/PS particles were also characterized in terms of specific mass by pycnometric analysis and chemical composition by FTIR. PSD of hybrid PP/PS particles was also evaluated as discussed in previous sections.

PP/PS particles were also submitted to fractionation analyses in toluene for evaluation of particles composition and occurrence of grafting (chemical bond between the polypropylene and polystyrene chains) during the suspension polymerization of styrene in the swollen PP particles. For these analyses, 1.5 g of the polymer were initially weighed in each of two sample holders prepared with filter paper. Analyses were conducted in duplicates. The fractionations apparatus consisted of a 1 L round-bottom glass flask, a Soxhlet extractor, a ball condenser, and a heating mantle (~130 °C). The sample holders were placed in the extractor and kept under toluene reflux for 4 complete cycles (approximately 5 hours). After fractionation, the sample was vacuum filtered to separate the soluble and insoluble fractions. The insoluble polymer fraction retained in the paper filter was dried in a circulation oven at 60 °C for 12 h (LIMA *et al.*,

2014). Next, the dried insoluble polymer fraction was weighted and the experimental insoluble fraction (IF^{exp}) was calculated with the following equation:

$$IF^{exp} (\%) = \frac{m_{dried}}{m_{polymer}} \times 100 \quad (6)$$

where m_{dried} is the dried mass of insoluble polymer fraction after the fractionation procedure and $m_{polymer}$ is the initial mass of hybrid PP/PS particles. Soluble fraction in absence of grafting (covalent bonds between PP and PS), SF^{ag} , was calculated under the assumption that the particle comprised a physical mixture of PP and PS, where PP is insoluble in toluene, while PS is completely soluble.

$$SF^{ag} (\%) = \frac{m_{PS}}{m_{PS} + m_{PP}} \times 100 \quad (7)$$

$$m_{PS} = m_{styrene}X \quad (8)$$

$$IF^{ag} (\%) = 100 - SF \quad (9)$$

The thermogravimetric curves and the PSD of the PP/PS particles were obtained as already described for PP particles. FTIR spectrophotometry analysis was performed using a Cary 600 Series Spectrometer (Agilent Technologies) equipped with ZnSe crystal. The analysis was performed by transmittance mode in the region of 4000-400 cm^{-1} (resolution of 4 cm^{-1}) and reported as average of 32 scans. The samples were macerated together with KBr to prepare the pellet for analysis.

3.2.5. PAN Shell Preparation through Seeded Dispersion Polymerization

The core-shell particle production started with the swelling stage of the particles that compose the core (produced according the protocol discussed in Section 2.3), whose conditions were based on the swelling tests previously discussed in Section 2.2. Then, the components required for the shell formation were added to the reactor. In the case of the acrylonitrile dispersion polymerization, an aqueous phase soluble initiator (potassium persulfate) was added due to the high solubility of acrylonitrile in water. Ascorbic acid was used to prevent the inhibition of free-radical reactions caused by oxygen, and sodium chloride was used to decrease the solubility of monomer in water (BESTETI *et al.*, 2014b; CUNHA *et al.*, 2014; RIBEIRO *et al.*, 2017). The conditions and chemicals used in each process are listed in Table 4.

At the end of the reaction, the particles were filtrated, washed several times with deionized water and then dried in an oven at 60 °C for 24 hours until constant weight.

Table 4: Chemicals and operating conditions of the core swelling and shell polymerization.

Core swelling		Shell formation	
Chemical	Amount	Chemical	Amount
Particles (PP or PP/PS)	50 g	KPS	1 g/20 g de H ₂ O
Deionized water	400 g	BPO	0.37 g
Styrene	25 g	Acrylonitrile	15 g
		Ascorbic acid	0.35 g
		Sodium chloride	5 g
Operating conditions		Operating conditions	
	80 °C		85 °C
	400 rpm		600 rpm
	1 hour		4 hours

*Kindly provided by Termotecnica LTDA (Joinville, SC, Brazil)

Source: Author's elaboration

3.2.6. CS particles characterization

The core-shell particles were initially characterized by optical microscopy to verify the presence and formation of the shell around the core of the structure. The particles were also analyzed by SEM at the same conditions described previously to evaluate the presence and morphology of the shell.

The specific surface area was measured using the Brunauer-Emmett-Teller (BET) method with relative pressure (P/P_0) of approximately 0.99584, through a surface area analyzer (Nova 1200e, Quantachrome Instruments – Autosorb-1, USA). Pore volumes were determined by nitrogen physisorption isotherms at -195.8°C under a critical pressure of 33.5 atm, while the pore size distribution was obtained from the adsorption branch of Barrett-Joyner-Halenda (BJH) isotherms (VIEIRA *et al.*, 2023). These experiments were carried out using approximately 100 mg of particles after drying in a circulation oven until constant mass.

FTIR analyses were also performed to confirm the formation of the PAN shell, as described before. To investigate the possible formation of acrylonitrile/styrene copolymer chains in the core-shell structure, particle fractionation was carried out in dimethylformamide (DMF), as it is known that PAN is completely soluble, while PS has low solubility and PP is highly insoluble in DMF (JING; DU; ZHANG, 2018; KAUR; GAUTAM; KHANNA, 2009; KHANNA; KAUR; KUMAR, 2010; WOLF; ECKELT; ECKELT, 2011). Initially, the sample (approximately 4 g, $m_{initial}$) was kept in 200 mL DMF for 30 min at 250 rpm and 150°C . After the specified time, the system was cooled to room temperature, and the solid content was vacuum filtrated to separate the insoluble fraction. Then, the insoluble fraction was placed in an oven for about 2 hours at 60°C (LIMA, 2015) and the mass was weighed again (m_{final}). Finally, the solvent was evaporated in a petri dish with sample paper in a forced convection oven at a

temperature of 60° C. from the filtrate to obtain the soluble fraction. The soluble PAN fraction of the core-shell particles was calculated with the following equation:

$$\%PAN = 1 - \frac{m_{final}}{m_{initial}} * 100\% \quad (11)$$

To specify the incorporation of acrylonitrile in the formation of the PAN shell, the degree of incorporation can be calculated with Equation 12:

$$\% Incorporation = \frac{m_{shell}}{m_{PAN}} * 100 \quad (12)$$

where m_{AN} is the mass of acrylonitrile added into the polymerization reactor, while m_{shell} is the polyacrylonitrile mass adhered to core particles.

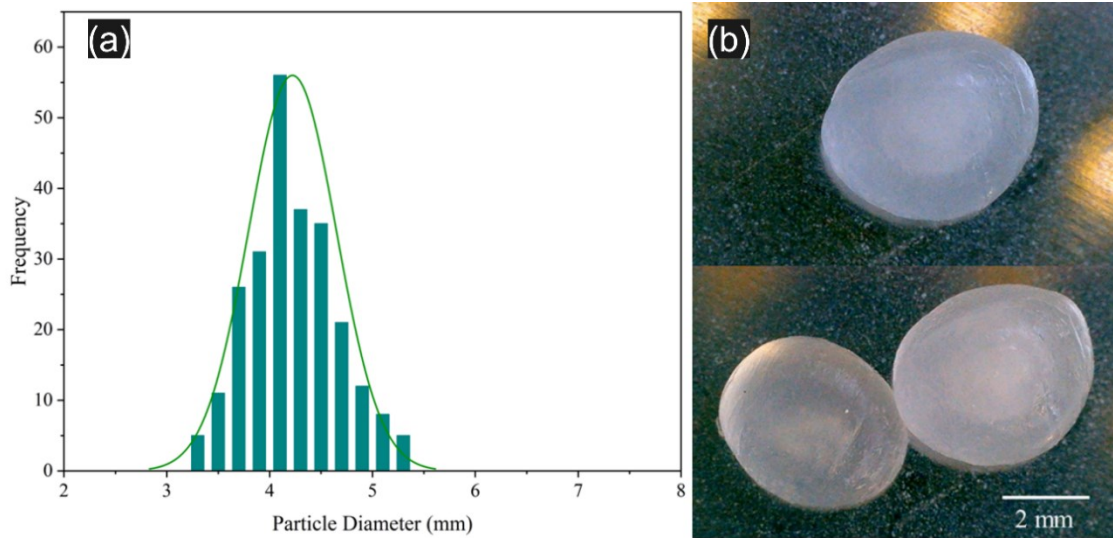
FTIR analyses of the soluble and insoluble fractions were performed to identify whether SAN copolymer chains were formed. The thermogravimetric curves and the PSD of the obtained CS particles were obtained as already described for PP particles.

3.3. RESULTS AND DISCUSSION

3.3.1. PP Particles

Initially, the morphological and structural characteristics were evaluated through micrographs obtained by optical microscopy, as one can see in Figure 2. In addition, the Sauter mean diameter of PP particles was evaluated as 4.309 μ m, as indicated through the particle size distribution (PSD) analysis.

Figure 11: Number size distribution of PP particles (a) and OM micrographs of PP particles (b).



Source: Author's elaboration

Figure 11(b) shows that PP particles are oval and non-porous. The particles are translucent because of the semi crystalline nature of PP(LIN *et al.*, 2020). The XS analysis provides us with the soluble fraction, which corresponds to the oligomers and atactic material of the polymer. The insoluble fraction (approximately 77 wt%) can be a measure of the crystalline fraction of PP, as presented in Table 5, corroborating the qualitative results observed in the images obtained by optical microscopy. Table 5 also shows the average diameter and specific mass of the PP particles.

Table 5: Measured properties of PP particles

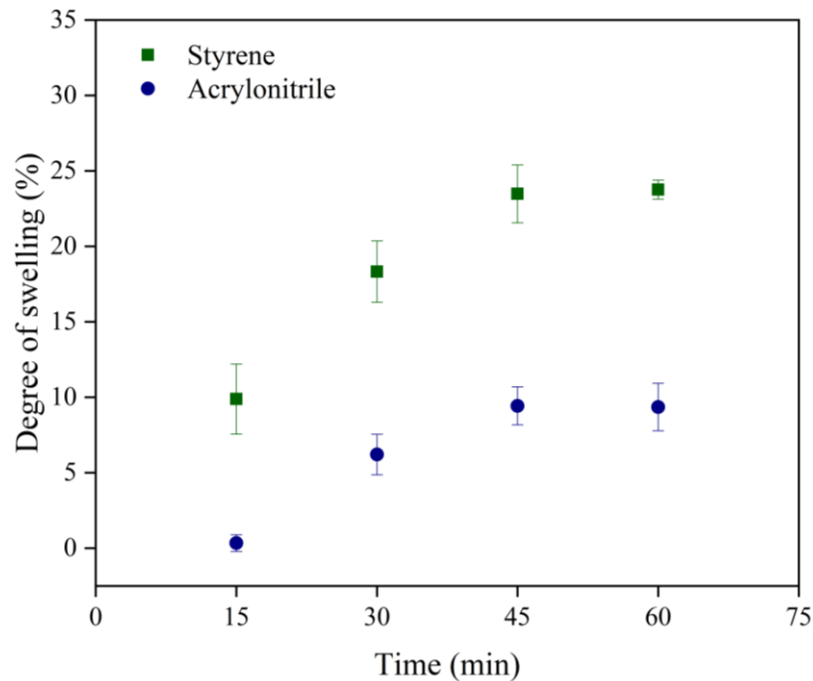
Parameter	Value
Sauter mean diameter (mm)	4.309
Specific mass (g/cm ³)	0.862 ± 0.084
Insoluble Fraction (wt%)	76.73 ± 0.27

Source: Author's elaboration

The specific mass observed in Table 5 is in accordance with data provided by Braskem (0.905 g/cm^3) for PP particles. The degree of crystallinity refers to the degree of structural order of a solid. PP beads presented a high crystalline fraction (77 wt% of xylene solubles). In terms of mechanical properties, crystalline regions provide higher toughness, wear resistance, stiffness, and strength when compared to amorphous polymers. Besides, amorphous thermoplastics gradually soften when subjected to temperatures above the glass transition temperature, while crystalline and semi-crystalline polymers kept their orderly structure up to the melting point. At temperatures higher than the melting point, these polymers present a transition to molten state. Furthermore, the semi-crystalline structure provides excellent chemical resistance and biocompatibility, as solvents and chemicals preferentially solubilize or react with non-crystalline regions (VAES; VAN PUYVELDE, 2021).

Figure 12 presents the PP swelling degrees (in styrene and acrylonitrile) as functions of time in the analyzed batch experiments. 60 minutes was sufficient for PP beads to reach the maximum swelling degree in both monomers. The maximum swelling degrees of PP beads were equal to $9.43 \pm 1.25 \text{ wt\%}$ and $23.76 \pm 0.62 \text{ wt\%}$ in acrylonitrile and styrene, respectively. Therefore, the PP beads preferentially absorbed styrene than acrylonitrile.

Figure 12: PP swelling curves in styrene (Sty) and acrylonitrile (AN).



Source: Author's elaboration

The polar characteristics of acrylonitrile can explain the lower swelling degree of PP beads in this monomer, while the higher swelling degree of PP beads in styrene is attributed to its apolar characteristics (SENICHEV; TERESHATOV, 2014; XIAO; SUN, 2016). The swelling of core beads is required during shell polymerization to ensure its adhesion. In particular, the higher the degree of swelling of the core, the lower its viscosity becomes. Lower viscosities of core beads are essential for enabling the adherence of the shell, because the rates of particle agglomeration on the surface increase (although other physical properties, such as the interfacial tension, can also affect the shell formation process) (LENZI *et al.*, 2002). However, the PP seeds cannot be completely dissolved by the monomer in the swelling step, in order to prevent massive particle agglomeration. Therefore, the ratio between the monomer and seeds in the swelling stage should be used to prevent the loss of the hydrodynamic stability of the reaction medium (GONÇALVES *et al.*, 2008; LIN; BIEGLER; JACOBSON,

2010). Since PP beads have some crystallinity, styrene can be used to swell the core beads, resulting in hybrid PP/PS beads. Particularly, in the case of non-porous polymers (as seen in Figure 11), diffusion rates of living chains and monomers are controlled by core viscosity. Therefore, incorporation of polystyrene in the core beads only occurs if PP beads swell reasonably in styrene (GOKMEN; DU PREZ, 2012).

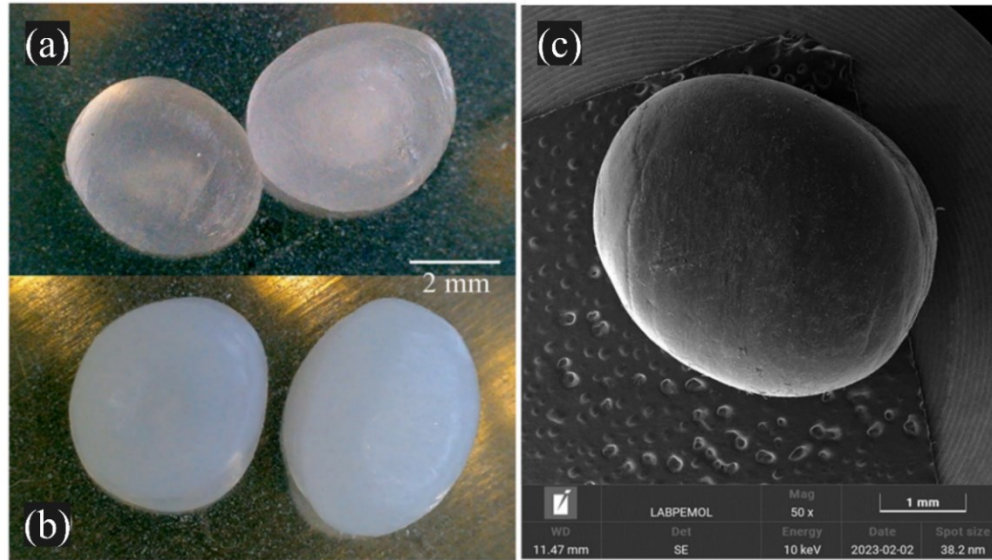
Therefore, the high swelling of the PP particles is desired to facilitate the formation of the core-shell structure. Still, with a low degree of swelling, an attempt was performed to synthesize particles with a core-shell structure, comprising only the PP core and the PAN shell. The result will be shown in the next section, but due to poor adherence of the shell onto the particles surfaces, hybrid PP/PS particles were prepared and used as the core of the proposed structure.

3.3.2. PP/PS Particles

Hybrid PP/PS particles were significantly different from PP particles, as one can observe in the OM micrographs shown in Figure 13(a) and (b). While PP particles are translucent, hybrid PP/PS particles have a non-translucent appearance and a more whitish color, indicating the incorporation of PS, which can form semi-crystalline domains inside the mostly amorphous PP regions where styrene is absorbed. SEM micrographs are also shown in Figure 13(c). PP/PS particles exhibited smooth, non-porous and uniform surfaces.

In addition, hybrid PP/PS particles presented a slight increase in particle size due to PS incorporation into swollen beads during the seeded suspension polymerization. Particularly, PSD analyses (Figure 14) indicated the Sauter mean diameter of 4.612 μm as shown in the Table 6. The remaining performance parameters, such as conversion, fractionation results, and specific mass, are also presented in Table 6.

Figure 13: OM micrographs of PP (a) and PP/PS (b) particles and SEM micrographs of PP/PS particles (c).



Source: Author's elaboration

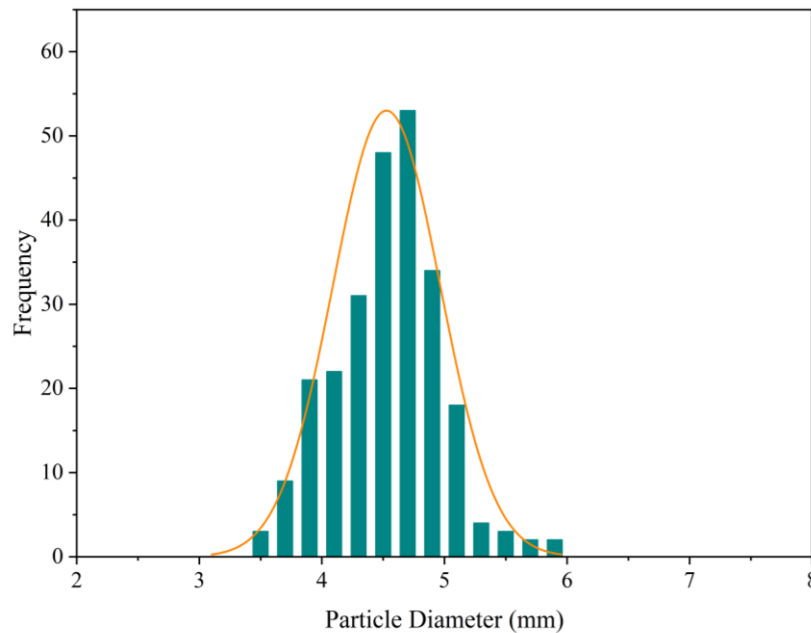
Table 6: Measured performance parameters evaluated for PP/PS particles.

Parameter	Value
Sauter mean diameter (mm)	4.612
Specific mass (g/cm^3)	0.877 ± 0.065
Insoluble in toluene ^a (%)	95.58 ± 1.32
Insoluble in toluene ^b (%)	85.57 ± 1.43
Conversion (%)	67.41 ± 1.16

^aExperimental value (Equation (5)) and ^bReference value (Equation (8))

Source: Author's elaboration

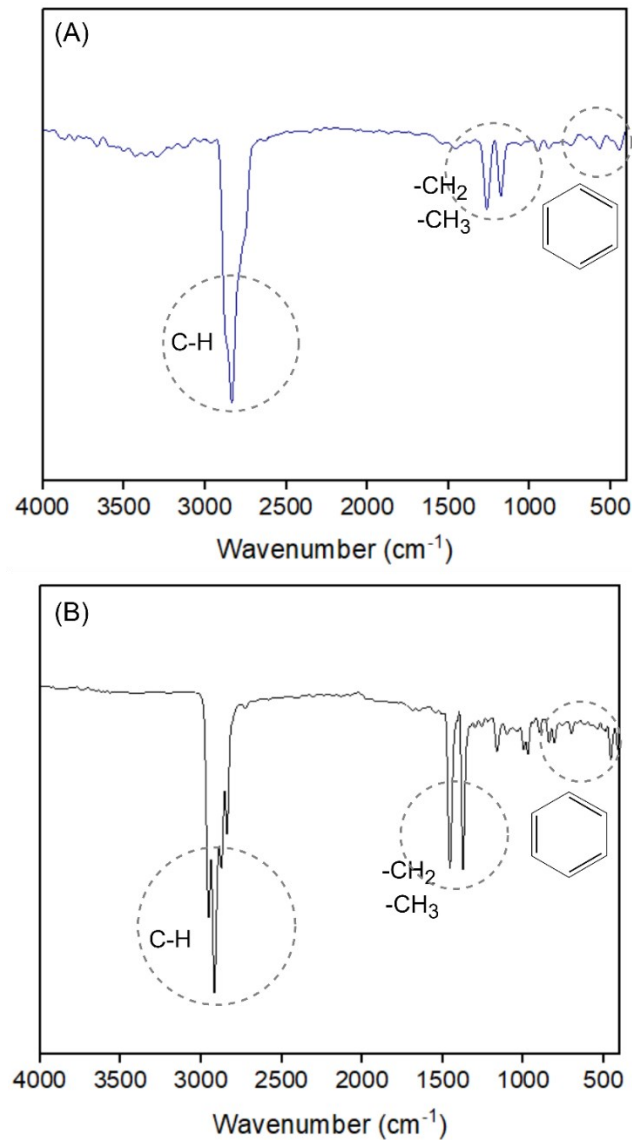
Figure 14: Number size distribution of hybrid PP/PS particles



Source: Author's elaboration

As for the other physical properties shown in Table 3, one can observe that the specific mass of the PP/PS particles was slightly increased after incorporation of PS. Besides, the fractionated materials were analyzed through FTIR to verify whether polystyrene was grafted (chemical bonding) onto polypropylene. The insoluble fraction content of PP/PS beads in toluene (measured through fractionation tests) was approximately equal to 95.6%; however, based on swelling results, PP beads absorbed around 20-25% in styrene. Considering the measured conversion of styrene monomer, the reference polypropylene fraction in PP/PS beads was equal to 85.6%. This value should correspond to the insoluble fraction in toluene in the absence of grafting. The higher insoluble fraction content in toluene suggests the occurrence of grafting reactions between PS and PP (LIMA *et al.*, 2014), and also explains the similar values of specific mass of PP and PP/PS particles. The FTIR spectrum of the PP/PS fraction insoluble in toluene (a) and PP/PS particles (b) are shown in Figure 15.

Figure 15: FTIR spectra of the (a) insoluble fraction PP/PS in toluene and (b) and PP/PS particles



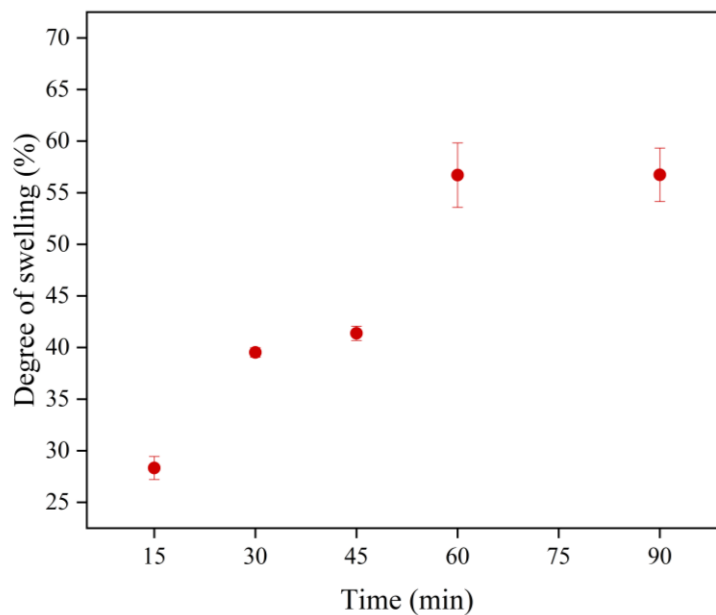
Source: Author's elaboration

In particular, characteristic peaks of both PP and PS can be seen in the spectra. The peaks placed between 900 and 500 cm^{-1} can be attributed to C-H groups present in the aromatic rings, which are present in the chemical structure of PS. The characteristic CH₂ and CH₃ peaks that can be observed at 1457 and 1375 cm^{-1} and the CH peak located at 2920 cm^{-1} (MOHAMED *et al.*, 2017) are present in the structures of PP and PS, respectively.

Although the peaks related to polystyrene appeared with lower intensity in the samples after toluene fractionation, there is still evidence of polystyrene (indicated by the presence of aromatic chains) in the insoluble fraction of the polymer in toluene. Therefore, FTIR results indicated that PS was incorporated into the PP particles by grafting, due to the free-radical reaction mechanism and physical mixture. However, the incorporation of PS into the particles can be seen more clearly in the swelling results of the PP/PS particles in styrene.

The swelling curve of the PP/PS particles in styrene is shown in Figure 16. Particularly, the incorporation of PS into PP particles led to increase of the swelling degree by styrene. The higher swelling degree of the beads can lead to lower viscosity in the polymeric cores during the formation of the shell and enhancing adhesion conditions for the precipitating particles to form the final core-shell structure of the support (BESTETI *et al.*, 2014b; PINTO *et al.*, 2020).

Figure 16: Swelling curve of PP/PS particles in styrene



Source: Author's elaboration

As previously discussed, the maximum degree of swelling for the PP particles in styrene was equal to 23.8%. However, the swelling degree of PP/PS beads in styrene was equal to 56.7%, as presented in Figure 16; that is, there was considerable increase of the swelling degree for hybrid particles. Moreover, 60 minutes were sufficient for these particles to reach the maximum degree of swelling. The difference in the degree of swelling was expected, as well as the higher swelling degrees of particles that contained polystyrene in their composition. As the monomer used to swell the particles was styrene, the absorption of styrene in PP/PS beads increased because the known solubility of polystyrene in its monomer.

Despite the previous results that favor the use of PP/PS hybrid particles for manufacture of core-shell materials, both PP and PP/PS beads were used as cores during the acrylonitrile dispersion polymerization reactions to form core-shell structures to evaluate the influence of swelling on the adhesion of the PAN shell.

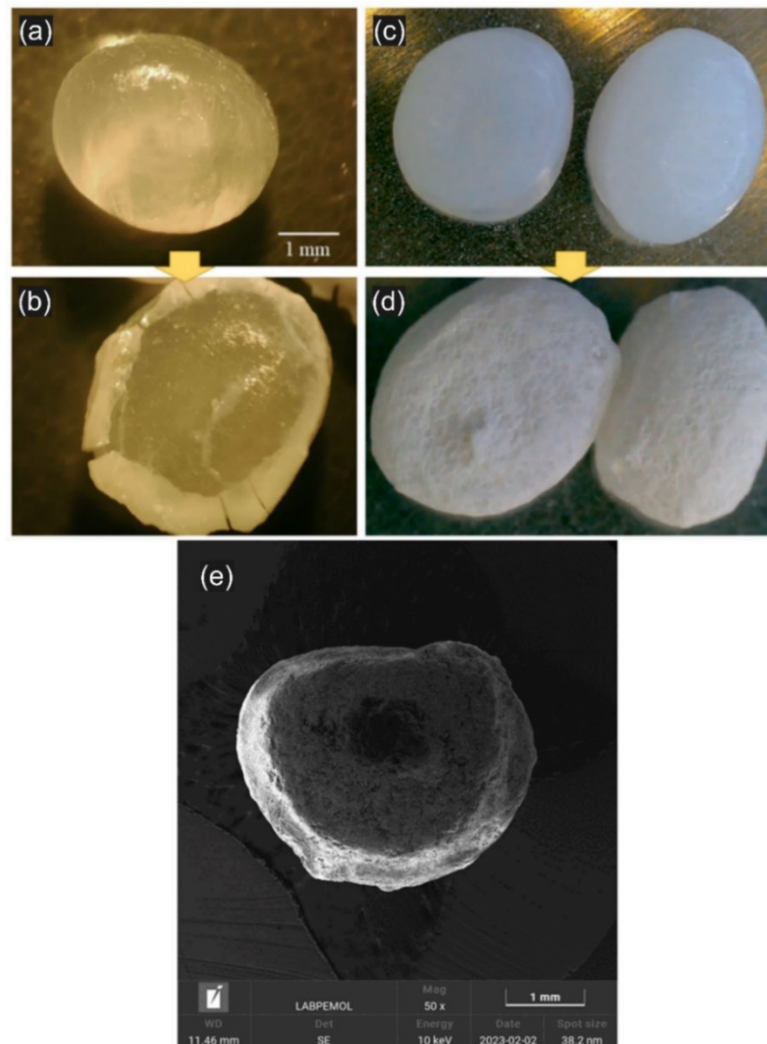
3.3.3. CS Particles

OM micrographs were taken to evaluate the formation of the core-shell structure, as shown in Figure 17. The micrographs show the uniform formation of the shell around the PP/PS core, which did not occur when the PP core was used. For core-shell particles prepared with the PP core, PAN adhesion did not take place onto the PP surfaces. When the polymerization reactor was discharged, the PAN particles were suspended in the medium. However, when PP/PS particles were used as the core, it was possible to obtain particles with the expected core-shell structure. The enhanced adhesion in this case can be attributed to the presence of the hybrid polymer with higher capacity to absorb styrene before the shell forming reactions.

The viscosity and sticky nature of the PP/PS core due to styrene swelling can promote the agglomeration of PAN particles generated during dispersion

polymerization, resulting in particles with the desired core-shell morphology (BESTETI *et al.*, 2014a; DAI *et al.*, 2022). Thus, this work selected the core-shell (PP/PS)/PAN particles for evaluation of the textural and morphological properties and of the chemical structure. As a matter of fact, the PAN particles formed during the dispersion polymerization stage are deposited around the core, forming a porous surface, as corroborated by the results obtained through BET and BJH analyses (shown in Table 8).

Figure 17: OM micrographs of (a) PP particles, (b) particles with PP core and PAN shell, (c) PP/PS particles, (d) particles with PP/PS core and (e) SEM micrograph of the PAN shell.



Source: Author's elaboration

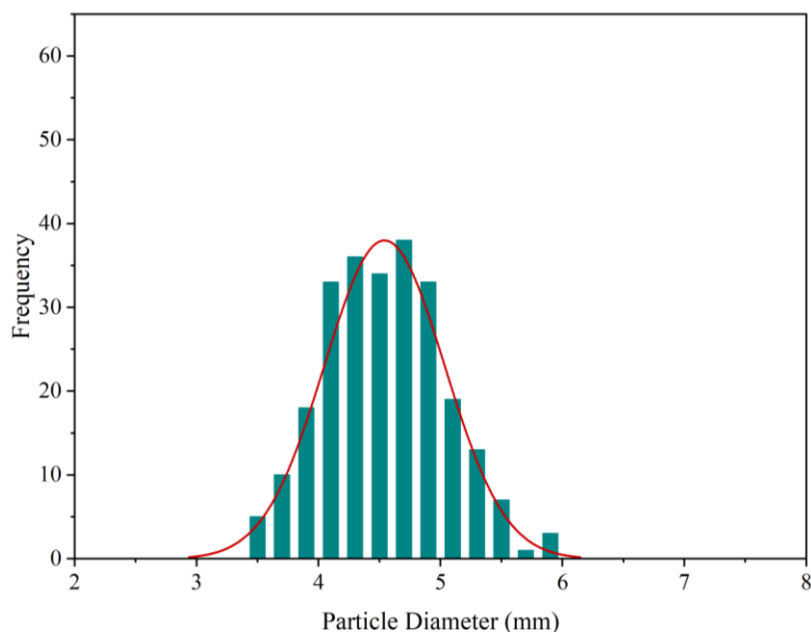
Table 7: Textural properties of the core-shell particle

Parameter	Value
Surface area (BET)	2.70 m ² /g of PAN shell*
Total pore volume (BJH)	0.028 cm ³ /g of PAN shell*
Average pore diameter	0.28 Å

*Textural properties were calculated using the mass of PAN porous shell
Source: Author's elaboration

Based on the PSD analyses of the core-shell particles (PP/PS/PAN), the Sauter mean diameter was 4.647 mm. This result indicates that a thin shell layer was formed around the core, as the PSD was shifted towards larger diameters in the case of PP/PS/PAN particles, as shown in Figure 18. Particularly, the uncontrolled agglomeration of PAN particles produced through dispersion polymerization onto de PP/PS particles can explain the widening of the particle size distribution of the CS particles (SELVARAJ; SAKTHIVEL; RAJENDRAN, 2015; ZHANG *et al.*, 2022).

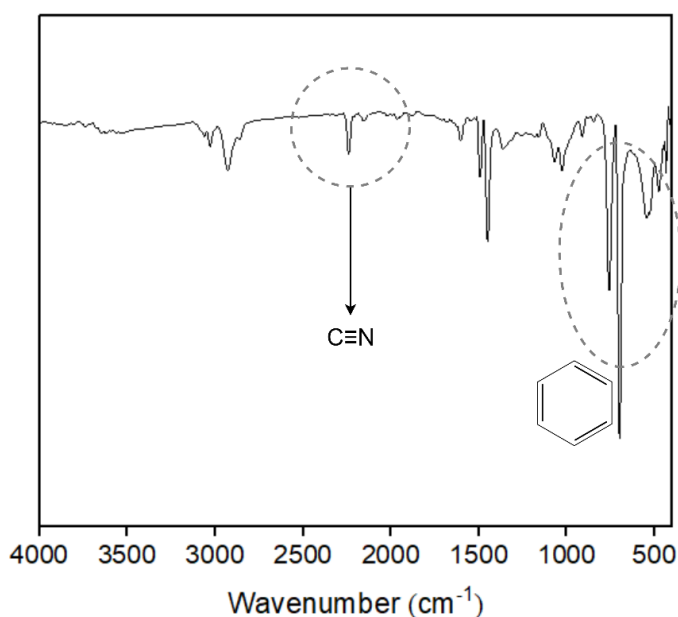
Figure 18: Number size distribution of CS particles (PP/PS/PAN)



Source: Author's elaboration

The FTIR spectrum of the prepared core-shell particles is shown in Figure 19. In this spectrum, it is possible to observe the characteristic peak of the nitrile group located at 2245 cm^{-1} , proving the presence of the polyacrylonitrile shell in the polymeric structure (VIEIRA *et al.*, 2023).

Figure 19: FTIR spectrum of PP/PS/PAN core-shell particles



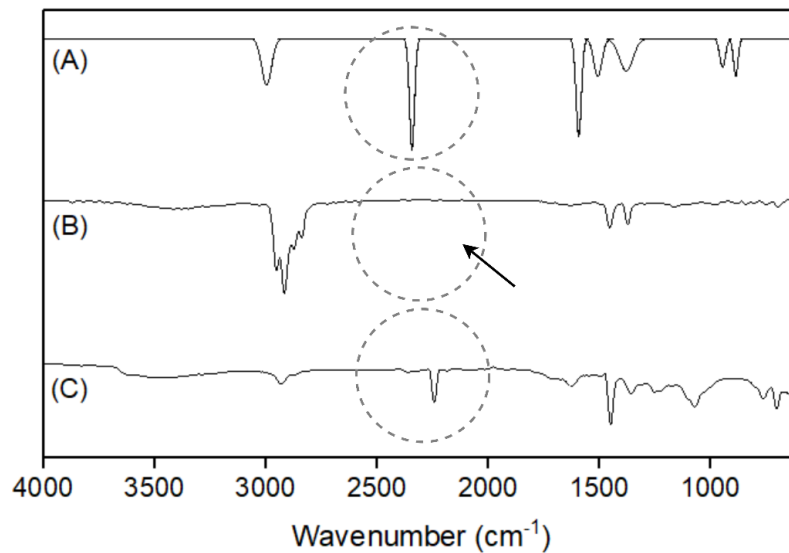
Source: Author's elaboration

After fractionation of CS particles in DMF (PINTO *et al.*, 2013), 15.98 ± 0.82 wt% of soluble fraction was obtained, which represents the polyacrylonitrile content of the core-shell structure. In addition, the degree of PAN incorporation into the final particles was equal to 54 wt%. The remaining amount of 46 wt% of acrylonitrile that was not incorporated onto the CS particles formed PAN particles that remained suspended in the aqueous phase (GONÇALVES *et al.*, 2009).

FTIR analyses of the DMF-soluble and DMF-insoluble fractions are shown in Figure 20. It can be observed that the insoluble fraction did not show any evidence of PAN, as no peaks were detected around 2245 cm^{-1} (which represents the nitrile group

$C\equiv N$, characteristic of PAN). On the other hand, the FTIR spectrum of the soluble fraction is extremely similar to the spectrum that characterizes PAN (VIEIRA *et al.*, 2023). Therefore, it is possible to conclude that there was no formation of SAN copolymer chains and that the shell is formed exclusively by agglomerated PAN particles. Furthermore, this result also indicates that the polymerization of acrylonitrile occurred only in the aqueous phase.

Figure 20: FTIR spectrum of (a) PAN particles, (b) insoluble and (c) soluble fractions of CS beads in DMF.

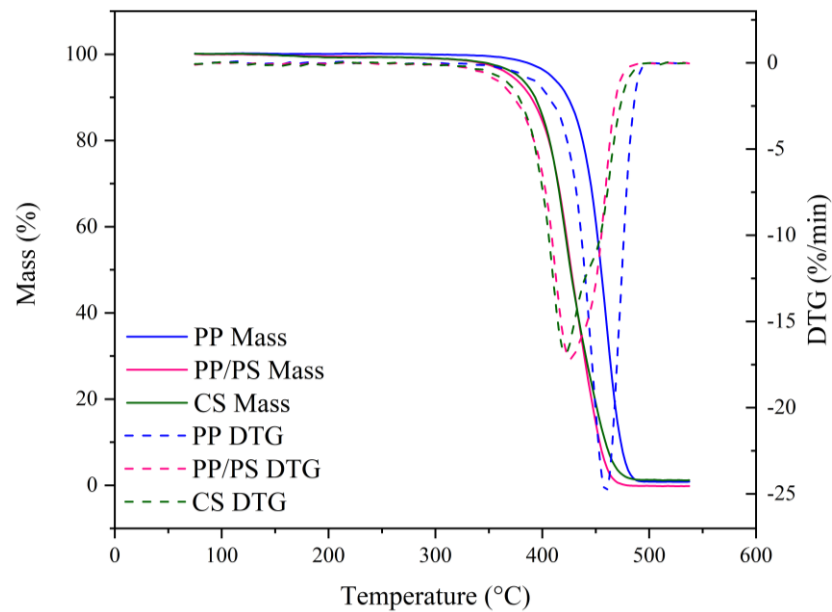


Source: Author's elaboration

TG and DTG curves of all particles prepared in the present study are shown in Figure 21. Despite the different compositions, similar mass loss behaviors could be observed, indicating the absence of copolymers on hybrid PP/PS core particles and core-shell particles. All particles presented a single mass loss peak that can be observed in the DTG curves. The mass loss starts at lower temperatures and extends to higher temperatures ($\sim 350 - 500$ °C) in these cases. Conversely, pure PP presents mass loss in a narrower temperature range (400 – 500 °C) (MIANDAD *et al.*, 2019; RIVERA-ARMENTA *et al.*, 2022; SILVA *et al.*, 2022). The incorporation of the shell

exerted little effect on the thermal behavior. However, it is important to observe that the thermal behavior of produced CS particles is compatible with several catalytic processes, conducted at milder temperatures, such as most enzymatic reactions.

Figure 21: TG and DTG curves of PP, PP/PS and CS particles



Source: Author's elaboration

3.4. CONCLUSIONS

Particles with core-shell (CS) morphology were efficiently synthesized through sequential seeded suspension and dispersion polymerizations. The particles produced with a polypropylene (PP) core did not allow the homogeneous formation of the polyacrylonitrile (PAN) shell through *in situ* dispersion polymerization. However, obtained micrographs confirmed that the particles produced with a polypropylene/polystyrene (PP/PS) core (previously manufactured through seeded suspension polymerization) allowed the formation of uniform PAN shells on their surface through dispersion polymerization.

The obtained results indicated that adhesion of the shell to the core was associated with the degree of swelling of the particle that constitutes the core of the structure. Fractionation of CS particles also indicated that styrene and acrylonitrile did not copolymerize during the shell forming reactions, confirming that the shell was formed only by PAN. In addition, the particle core presented some degree of grafting between PP and PS, as indicated by toluene extraction analyses. In this context, the particles were produced with a core formed by low-cost commodity polymers and a shell formed by PAN, making the surface of the final particle chemically functionalizable. Furthermore, as they have a relatively large size (millimeter scale). Therefore, the CS particles described here are interesting for several applications that require reuse due to the easy recovery of these particles through filtration or settling.

4

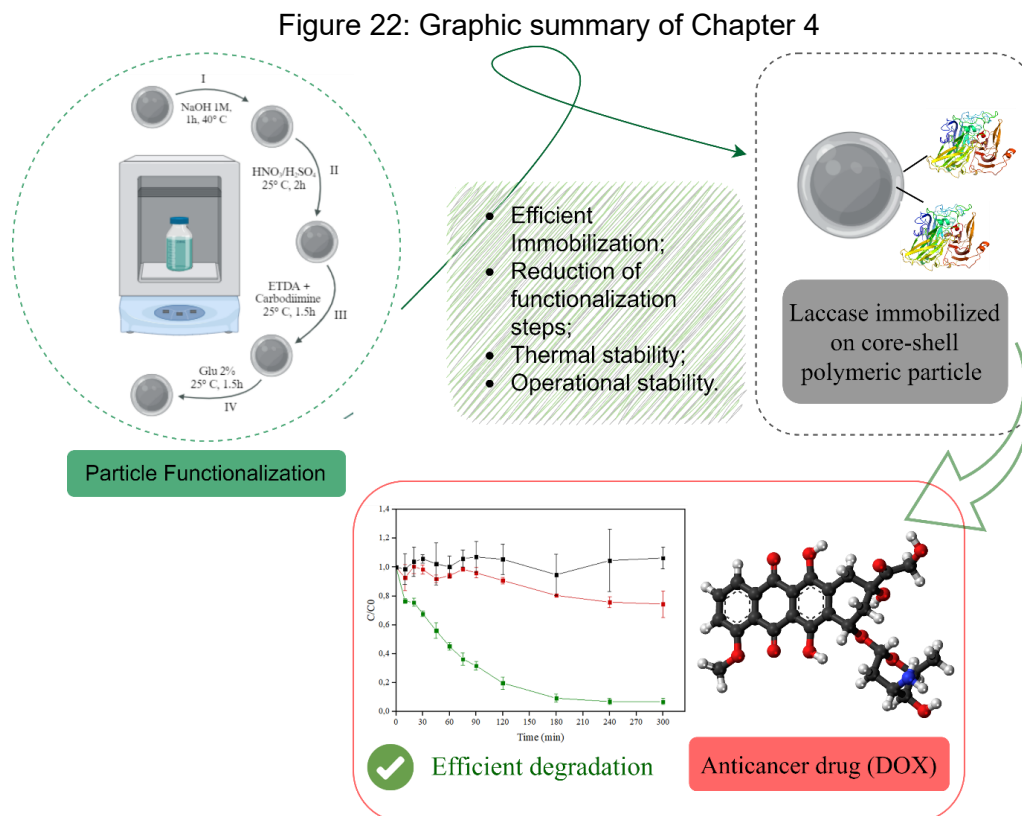
CHAPTER 4 – DEGRADATION OF ANTICANCER DOXORUBICIN BY LACCASE IMMOBILIZED ON CORE-SHELL POLYMER PARTICLES

This chapter presents the entire methodology and results of laccase immobilization in polymeric particles with core-shell morphology synthesized and characterized in the previous chapter, and the application of the enzymatic derivative in the degradation of the anticancer drug doxorubicin. This chapter is submitted to the Journal of Environmental Chemical Engineering and titled "Immobilization of Laccase in Core-Shell Polymer Particles for Degradation of Anticancer Doxorubicin" and using the QR Code below you can visit the journal's website.



Graphical abstract

Figure 22 shows the graphic summary of this chapter, designed for quick visualization of the chapter's contents.



Source: Author's elaboration

4.1. INTRODUCTION

Doxorubicin (DOX) is an effective chemotherapy agent and is widely used in the treatment of metastatic breast cancer, sarcomas, lymphomas, and other human neoplasms. This drug can be eliminated by urine (3–10%) and feces (40–50%). Studies report that DOX and its degradation products have been detected in concentrations ranging from nanograms to micrograms per liter in wastewater samples. In this scenario, there are uncertainties about the environmental effects that can be caused by the drug and its metabolites, even at low concentrations. Long-term exposure raises deep concern, as this can generate chronic effects related to cardiotoxicity, the development of drug resistance, and the risk of bioaccumulation (FERREIRA GARCIA *et al.*, 2020; KELBERT *et al.*, 2021, 2023).

Therefore, the development of alternatives processes or the improvement of the processes currently applied in wastewater treatment is required, aiming at degrading these anticancer compounds. Direct application of laccase for doxorubicin removal was recently reported. In particular, JINGA; TUDOSE; IONITA (2022) investigated an catalytic degradation of doxorubicin (DOX) in presence of laccase and an organic nitroxide free radical. This study obtained up to 100% removal results for pH 5 and 7 conditions and used different proportions among doxorubicin, laccase, and TEMPO (JINGA; TUDOSE; IONITA, 2022). KELBERT *et al.* (2021) evaluated the potential of free laccase to degrade doxorubicin under different conditions of enzyme concentration, pH, and temperature. In addition, the kinetic parameters of degradation were estimated, and the environmental implications of DOX degradation products were also evaluated. The greatest degradation rate of doxorubicin was achieved at pH 7 and 30 °C, and the results indicated that laccase degrades DOX into non-toxic compounds (KELBERT *et al.*, 2021).

In this sense, laccase - an oxidoreductase enzyme belonging to a multi-copper oxidase - has been explored as a promising alternative for removing unwanted compounds (such as DOX) in wastewater streams. However, the use of laccase in enzymatic processes for effluents and wastewater treatment presents significant challenges, which deserve careful attention to optimize their effectiveness and practical implementation (DEHGHANIFARD *et al.*, 2013; PEREIRA, 2020). One of the main challenges is the stability of laccase in adverse conditions, such as variations in pH and temperature. This instability can compromise its catalytic activity over time, limiting its effectiveness in effluent and wastewater treatment plants, which are subject to transitions in pH and temperature conditions. Another problem to be overcome is the high cost related to the use of laccase in homogeneous processes (GURGEL *et al.*, 2022).

An advantageous approach capable of overcoming these challenges is the use of enzymes immobilized on solid supports, as this technique provides greater stability and durability to the enzymes, making them more resilient in adverse conditions, such as pH variations, temperature, and presence of toxic compounds. Furthermore, immobilization allows the recovery and reuse of enzymes after treatment, reducing operational costs (DARONCH *et al.*, 2020; VIEIRA *et al.*, 2023).

In this context, the use of polymeric materials as solid support for the immobilization of laccase offers several advantages, such as a high surface area, versatility in the choice of polymer, mechanical and chemical stability, and adjustable porosity (PEIXOTO *et al.*, 2009; RIBEIRO *et al.*, 2017; WANG *et al.*, 2013a). Among the possible morphologies, polymer particles with core-shell structure present a morphology where an outer layer (shell) surrounds a central core. This specific architecture offers advantages in adjusting surface properties, as well as offer excellent

mechanical stability, and high chemical resistance, such as a result of the combination of the characteristics of the polymers that form the core and shell of the structure (GALOGAHI *et al.*, 2020; GURGEL *et al.*, 2022). In this context, when the core has a base of polymers such as polypropylene and polystyrene, there is an increase in the thermal and mechanical resistance of the structure as a whole; while for the surface, polyacrylonitrile is a polymer that allows functionalization with the addition of desirable functional groups for the immobilization of enzymes, and also presents interesting surface properties, such as the specific area of the shell (GURGEL *et al.*, 2022, 2024). Additionally, the size of the support needs to be sufficient to promote easy recovery.

Therefore, in this study we used the polymeric support synthesized by GURGEL *et al.* (2024) to immobilize laccase, investigating functionalization steps necessary for binding the enzyme to the support (TAHERAN *et al.*, 2017b; VIEIRA *et al.*, 2023), evaluating after immobilization the characteristics of the biocatalyst, as well as stability at different pHs, thermal and storage stability. The present study also aimed to evaluate the efficacy of the degradation of the anticancer doxorubicin using the biocatalyst obtained.

To our knowledge, few studies have investigated the ability of these already known core-shell particles to immobilize laccase, and this work is pioneering in evaluating the applicability of the enzymatic derivative in the removal of anticancer compounds such as doxorubicin. The results of this study can significantly contribute to the development of more efficient and sustainable methods for the degradation of pharmaceuticals in aquatic environments.

4.2. MATERIALS AND METHODS

This section presents the specific materials, equipment, and software used, together with an explanation of the experimental methods adopted.

4.2.1. Chemicals

Laccase from *Trametes versicolor* (≥ 0.5 U/mg), ABTS (2,2'-Azino-bis(3-ethylbenzothiazoline-6-sulfonic acid, $\geq 98\%$) and doxorubicin hydrochloride suitable for fluorescence ($\geq 98\%$) were provided by Sigma-Aldrich. Sodium hydroxide (Dinamica, $\geq 97\%$), sulfuric acid (Dinamica, $\geq 98\%$), nitric acid (Dinamica, 54%), ethylenediamine (Neon, 99.0%), carbodiimide (N-(3-Dimethylaminopropyl)-N'-ethyl carbodiimide hydrochloride, Sigma Aldrich, $\geq 98.0\%$) and glutaraldehyde (Sigma-Aldrich, 25%) were used to functionalize the surface of core-shell particles. Citric acid ($\geq 98\%$) and dibasic sodium phosphate ($\geq 98\%$) were purchased from Neon (Brazil). Dimethyl sulfoxide (DMSO, 99%) was purchased from Sigma-Aldrich. Unless otherwise noted, materials were used in their original state.

4.2.2. Functionalization of core-shell particles

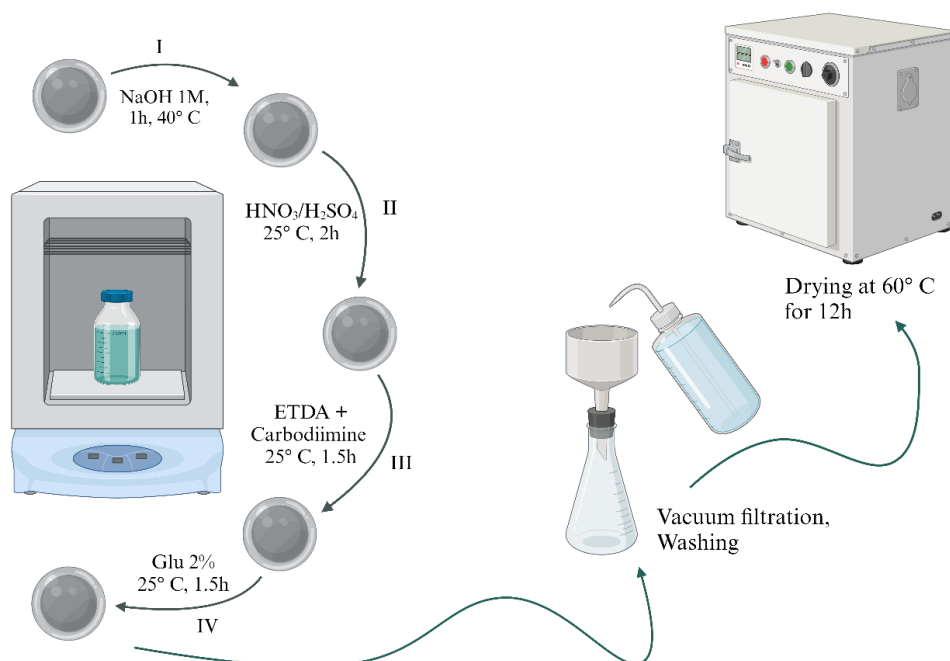
The core-shell particles (with polypropylene/polystyrene core and polyacrylonitrile shell) obtained by seeded suspension polymerization described by GURGEL *et al.* (2024) were evaluated as a support for laccase immobilization. Before immobilizing the laccase, four different supports were prepared based on the functionalization steps previously described by VIEIRA *et al.* (2023) and TAHERAN *et al.* (2017).

Adapting the methodology proposed by VIEIRA *et al.* (2023) the functionalization steps of core-shell polymer particles consisted of:

- ✓ Step I – Weighing of approximately 2 grams of core-shell particles (CS), followed by immersion in 100 mL of NaOH solution (1 mol L^{-1}) in an incubator (Tecnal, TE-424) maintained at $40 \text{ }^{\circ}\text{C}$ for 1 h. After this time, the samples were washed with distilled water and sent to the second stage;
- ✓ Step II – After being washed, CS particles were immersed in 100 mL of 10% v/v $\text{HNO}_3/\text{H}_2\text{SO}_4$ solution (50:50 v/v) for 2 h at $25 \text{ }^{\circ}\text{C}$. The main objective of these first two steps is the formation of $-\text{COOH}$ groups;
- ✓ Step III – After being washed again with distilled water, the particles were then immersed in 100 mL of ethylenediamine (1 mol L^{-1} , pH 4.7)/carbodiimide (0.1 mol L^{-1}) solution at $25 \text{ }^{\circ}\text{C}$ for 1.5 h for the amination of protein carboxylic groups;
- ✓ Step IV – After washing again in distilled water, the fourth step consisted of immersing the particles in a solution containing 2% (v/v) of glutaraldehyde for 1.5 h at $25 \text{ }^{\circ}\text{C}$ (TAHERAN *et al.*, 2017a; VIEIRA *et al.*, 2023).

After all steps, the particles are washed again with distilled water and dried in an oven at 60°C for 12 h. Figure 23 illustrates the processes involved in the functionalization of CS particles.

Figure 23: Graphical representation of core-shell particles functionalization methodology



Source: Author's elaboration

Five different supports were prepared to investigate the possibility of immobilizing laccase without functionalizing the support or with fewer steps, aiming to reduce costs in the process, as described in Table 8 below.

Table 8: Nomenclature and description of prepared CS supports

Support	Description
CS-0	Core-shell particles without any functionalization step
CS-I-II	Core-shell particles functionalized with steps I and II
CS-I-II-III	Core-shell particles functionalized with steps I, II, and III
CS-I-II-III-IV	Core-shell particles functionalized with all the steps described
CS-I-IV	Core-shell particles functionalized with steps I and IV

Source: Author's elaboration

During the preparation of the supports, after each functionalization step, samples were taken to perform FTIR and ^1H NMR analyses to evaluate the incorporation of specific functional groups on the material's surface. FTIR analyses were performed using a Cary 600 series spectrometer (Agilent Technologies) equipped with a ZnSe crystal. The analysis was performed by transmittance in the $4000\text{-}600\text{ cm}^{-1}$ region, with a resolution of 4 cm^{-1} and 32 scans. The samples were previously ground in a coffee grinder (OMDR100 220V, Oester) and subsequently macerated with KBr to prepare the pellet for analysis.

^1H NMR spectroscopy analysis was performed using a Bruker AC-200F NMR, operated at 200 MHz. Chemical shifts were reported in ppm, relative to 0.01% (v/v) tetramethyl silane (TMS) ($\delta = 0.00$). For analysis, after each functionalization step, the polymer from the surface was separated by scraping with metal, and 25 mg was weighed to solubilize in 0.5 mL of DMSO ($\text{C}_2\text{H}_6\text{OS}$).

4.2.3. Laccase immobilization

Each prepared support was treated with 8 mL of laccase in acetate buffer solution (0.1 mol L^{-1} , pH 4.5) at a concentration of 0.25 mg mL^{-1} under stirring at 130 rpm and temperature of approximately 25° C (Shaker FWS-30 FAITHFUL). Initially, 0.85 grams of support was tested for these conditions. Immobilization tests were also performed with higher amount of support (1.25 grams). The supports that offered the best results in enzyme immobilization yield were immediately tested in other enzyme concentrations: 0.10, 0.15, 0.25, 0.35, 0.50, and 0.60 mg mL^{-1} . For all tests, the duration was 8 h, and immobilization kinetics were measured to monitor the time at which the highest immobilization yield was achieved. The following sampling times were used in all tests: 0.25, 0.75, 1, 2, 3, 4, 5, and 7 h. The time and concentrations

chosen to carry out the tests were extrapolated from the literature (VIEIRA *et al.*, 2023) to observe the behavior of the new support synthesized in this work. After immobilization, the heterogeneous catalyst was removed and washed thoroughly with ultrapure water. The immobilization yield was determined from the decay of enzymatic activity in the supernatant.

The laccase activity present in the supernatant was measured through the ABTS oxidation rate to calculate the laccase activity present in the supernatant. For laccase activity in the supernatant, 0.3 mL of aqueous ABTS (5 mmol/L) and 0.3 mL of enzyme solution at the desired concentration were added to 2.4 mL of phosphate-citrate buffer (0.1 mol L⁻¹, pH 6) in a glass cuvette. To read the blank, 0.3 mL of distilled water was used instead of the enzyme solution. The reaction occurred at approximately 23 °C for 2 min. To perform the reading, a UV/Vis spectrophotometer (U-1900, HITACHI) was used to measure the absorbance at 420 nm, and the ABTS molar extinction coefficient ($\epsilon_{420} = 3.6 \text{ L } \mu\text{mol}^{-1} \text{ cm}^{-1}$) was used to calculate the activity of laccase (PEREIRA, 2020; VIEIRA *et al.*, 2023), as presented by Equation 13:

$$C_{EA} = \frac{\Delta Abs. V}{\epsilon. d. t. v} \quad (13)$$

Where:

C_{EA} – enzymatic activity concentration (U/L);

ΔAbs – absorbance variation;

V – total reaction volume (L);

ϵ – molar extinction coefficient (L $\mu\text{mol}^{-1} \text{ cm}^{-1}$);

d – step length (cm);

t – reaction time (min);

v – sample volume (L).

One unit of laccase activity is defined as the amount of enzyme required to oxidize 1 μmol of substrate per minute. All analyses were performed in triplicate. Considering that the decrease of enzyme activity in the supernatant occurs due to the mass transfer of enzyme to the support, the immobilization yield can be calculated using the Equation 14.

$$Y (\%) = \frac{(EA_0 - EA_t)}{EA_0} \times 100 ; \quad (14)$$

Where:

Y – Immobilization Yield (%)

EA_0 – activity of the enzymatic solution in the supernatant at the beginning of the immobilization process ($t=0$);

EA_t – enzyme activity presents in the supernatant at any time of the immobilization process.

To evaluate whether the decay of the laccase activity present in the supernatant was not due to some loss of enzyme activity during the process, a study of the laccase activity over time was also carried out under the same conditions as the immobilization procedure, but without the presence of support.

4.2.4. Characterization of the enzyme derivative

In this section, the methodologies for characterizing the enzyme derivative are described. For the analyses, the support with immobilized laccase, which presented the best immobilization performance and the fewest possible functionalization steps, was chosen for the detailed characterization of performance indexes.

4.2.4.1. *Thermostability test*

The thermal stability of the enzyme derivative was evaluated by adding 0.2 g of the enzyme derivative to 2.4 mL of 0.1 mol L⁻¹ phosphate-citrate buffer solution (pH 6.0) and placing it at different temperatures (30, 50, 60, and 70 °C) in a water bath (MQBTC, Microquimica Equipamentos Ltda). The enzymatic activity of the derivative was measured according to the methodology described in the previous section in the following time intervals (0, 0.5, 0.75, 1, 2, 4, 6 and 8 h). In this case, the enzyme activity was directly measured with the enzymatic derivative in the cuvette to evaluate the oxidation rate of ABTS through the time. It was possible because the core-shell support floats in an aqueous medium and does not affect the passage of light in the cuvette during the UV-Vis analyses. Likewise, for comparison, 0.3 mL of free laccase solution at the same concentration was added to 2.4 mL of 0.1 mol L⁻¹ phosphate-citrate buffer solution (pH 6.0) and kept under the same conditions tested for immobilized laccase. Analyzes were performed in triplicate.

4.2.4.2. *pH stability test*

The stability of the catalyst at different pH values was carried out by adding 0.2 g of enzyme derivative in 2.4 mL of buffer solution with different pH values (3, 5, 6, and 8) and left at 25 °C for different periods. (0, 0.5, 0.75, 1, 2, 4, 6 and 8 h). The content was added to the cuvette at the set time, and its oxidation activity was evaluated using the methodology described in the previous sections. Likewise, the same procedure was applied to evaluate the stability of laccase in its free form, in which laccase solution at the same concentration was added to buffer solutions with the same pH values, and the activity was determined as previously described. Analyzes were performed in triplicate.

4.2.4.3. Storage stability test

Storage stability was monitored for 8 weeks. Immobilized laccase and free laccase were stored at 8 °C and 25 °C. Samples were collected every 7 days to monitor enzymatic activities for ABTS oxidation. Enzyme activity was determined as previously described. These analyses were carried out in duplicate, and storage stability was represented graphically as residual activity in percentage, considering the activity measured on the first day to be 100%.

4.2.4.4. Operational stability test

The operational stability of the laccase immobilized on the core-shell particles was determined by testing consecutive ABTS oxidation cycles. The residual activity assay was performed at 30 °C in a water bath (MQBTC, Microquimica Equipamentos Ltda) using 0.1 mol L⁻¹ phosphate-citrate buffer (pH 6) and was measured as previously described. The temperature and pH conditions used in these tests were chosen based on the best stability conditions of the enzymatic derivative (evaluated during the work as described previously), as well as conditions closest to typical wastewater and effluent treatment conditions. The enzymatic activity obtained at the first cycle was considered 100%. Then, the enzymatic derivative was washed seven times with 0.1 mol L⁻¹ phosphate-citrate buffer (pH 6), and the enzymatic activity present in the catalyst was determined again. Activity measures during reuse cycles continued until activity close to zero was noted. At each cycle, the residual activity was calculated according to Equation 15 (VIEIRA *et al.*, 2023; XU *et al.*, 2024).

$$EA_R = \left(\frac{C_n}{C_1} \right) \times 100 \quad (15)$$

Where:

EA_R – Residual enzyme activity (%)

C_{EA1} – Enzymatic activity concentration at the first cycle (U L⁻¹);

C_{EA_n} – Enzymatic activity concentration at the n^{th} cycle (U L⁻¹), $n > 1$.

4.2.4.5. Determination of kinetic parameters

The tests were carried out at the temperature of 30 °C and pH 6 in phosphate-citrate buffer (0.1 M), using concentrations of ABTS ranging from 0.5 to 30 mM to determine the maximum degradation rate (V_{max}) and the Michaelis-Menten constant (K_M). The oxidation assay for each concentration of ABTS (0.5, 1, 1.5, 2, 5, 10, 15, 20, and 30 mmol L⁻¹) was performed by adding 0.2 g of the enzymatic derivative, as described in other sections. To determine K_M and V_{max} in Michaelis-Menten equation (Eq. 16), the least squares function was minimized in the Origin software (KELBERT *et al.*, 2021; WU *et al.*, 2019; XU *et al.*, 2024).

$$V_0 = \frac{V_{max} C_S}{K_M + C_S} \quad (16)$$

Where V_0 is the initial reaction rate (mmol s⁻¹ L⁻¹) and C_S is the ABTS concentration (mmol L⁻¹).

4.2.5. Doxorubicin (DOX) degradation assays

Before carrying out DOX degradation tests, a calibration curve was build up to relate the fluorescence data obtained from the spectrophotometer with the

concentration values of the DOX solution. The equation obtained from the experimental data was:

$$Flu = 0.06155C_{DOX} + 1.7718 \quad (17)$$

where *Flu* is the fluorescence measure obtained by the spectrophotometer and C_{DOX} is the DOX concentration.

The doxorubicin degradation tests were carried out under conditions of temperature equal to 30 °C (Shaker FWS-30 FAITHFUL) and pH 6, in phosphate-citrate buffer (0.1 M), based on conditions close to those found in real effluents and, in addition, the best activity conditions of the catalyst obtained in the present study. DOX concentration was monitored using a fluorescence spectrophotometer (SpectraMax® Gemini™ EM, Molecular devices®). The excitation and emission wavelengths were 480 and 598 nm, respectively. For these tests, the degradation of DOX was evaluated in concentrations of 250 and 500 µg L⁻¹, as carried out by KELBERT *et al.* (2021) with laccase in its free form. The amount of enzyme derivative used in the tests was kept fixed at 1.5 grams.

In this case, some adaptations in protocol were required due to the relatively large size of the catalyst obtained in this study (~ 5mm in diameter). Thus, the amount of enzyme derivative was added to 8 mL of the DOX solution at the desired concentration. At each sampling time (0, 0.17, 0.33, 0.5, 0.75, 1, 1.5, 2, 3, 4 and 5 h), a 200 mL aliquot was removed and added to a well in a 96-well plate with a black bottom (Corning incorporated Costar®) and the fluorescence reading was immediately taken using a spectrophotometer. The same test was carried out with free laccase for

comparison, and the test time was determined based on the total degradation of the drug. These tests were carried out in 4 replications.

A standard curve was determined under pre-established pH and temperature conditions to eliminate any interference related to the analysis and monitor concentration values as a function of fluorescence values.

4.2.5.1. Operational stability in doxorubicin (DOX) degradation

The operational stability of the enzyme derivative in DOX degradation was monitored similarly to the procedure described in Section 4.2.4.4. However, in this case, the DOX concentration is evaluated after each cycle, and the drug concentration is determined using the fluorescence spectrophotometer. Each degradation cycle lasted 180 min in these tests, based on previous test, when the DOX degradation was achieved. Thus, in each cycle, the enzymatic derivative was washed seven times with pH 6 in phosphate-citrate buffer (0.1 M), and the procedure was repeated until it was noticed that the DOX concentration was no longer decreasing, indicating the total loss of enzyme activity.

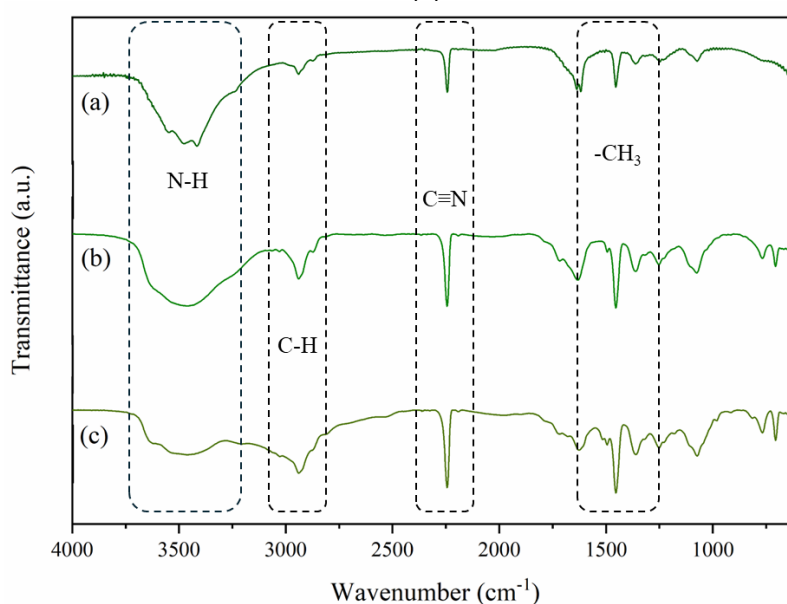
4.3. RESULTS AND DISCUSSION

In this section, the results obtained are presented. The information and data obtained from each analysis are also discussed. The results are organized and presented using graphs, tables, and other appropriate resources for visualizing the information. The discussions here provide a solid basis for the final discussions and considerations.

4.3.1. Functionalization of core-shell particles

The particles obtained as described in Chapter 3 with PAN shell were functionalized, and at each step, FTIR and ^1H NMR analysis of the particle surface was carried out. Figure 24 shows the FTIR spectra of each synthesized support after its functionalization.

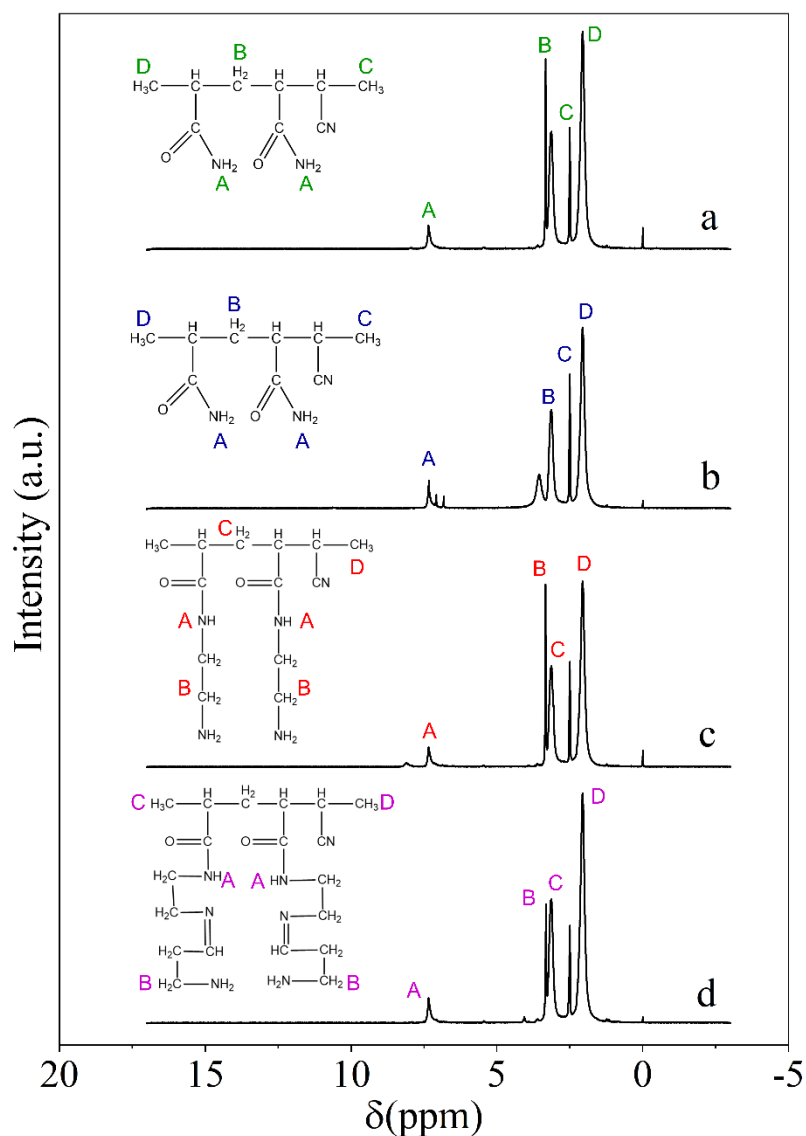
Figure 24: FTIR spectrum of surface samples of CS-I-II-III-IV (a), CS-I-II-III (b), and CS-I-IV (c)



Source: Author's elaboration

One can see from the spectra presented in Figure 24 that the transmittance peaks are very similar. It may happen due to the overlap of some peaks over others; therefore, the ^1H NMR results are more appropriate to provide a more detailed description of the chemical composition of each support after the functionalization steps. Through FTIR, the presence of the characteristic peak of acrylonitrile $\text{C}\equiv\text{N}$ was noticed; there is also the presence of $-\text{NH}$ group, indicated by the wave numbers of 2245 cm^{-1} and 3460 cm^{-1} , respectively (MOHAMED *et al.*, 2017). The results obtained with the ^1H NMR analysis are shown in Figure 25.

Figure 25: ^1H NMR results after (a) step 1, (b) step 2, (c) step 3 and (d) step 4 of support surface functionalization



Source: Author's elaboration

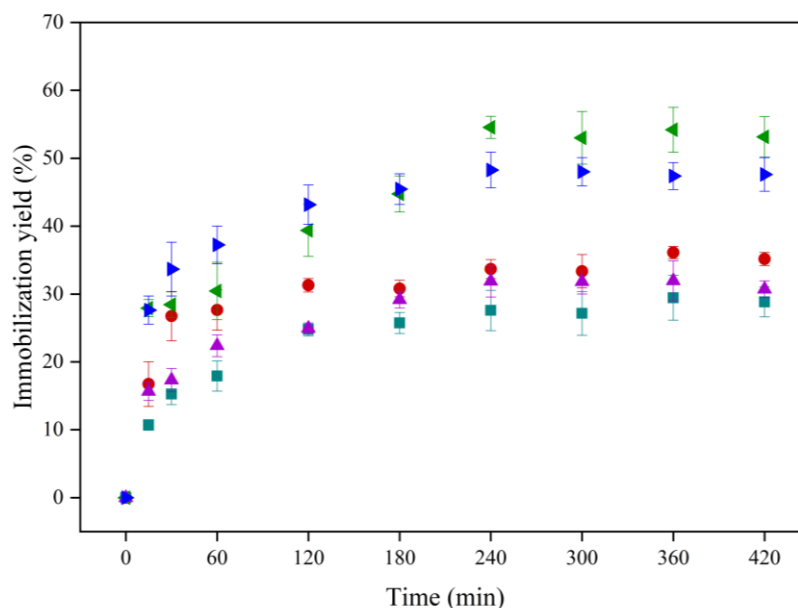
From the NMR analyses, one can observe that some functionalization steps did not add significant changes to the chemical structure of the support, and the groups identified by FTIR can be observed in the structures obtained by NMR. After the first functionalization step, the $-\text{NH}_2$ group appears in the structure, which was expected, according to VIEIRA *et al.* (2021). In the acid treatment, the appearance of the $-\text{OH}$

group was expected, but it did not appear in the results obtained. On the other hand, the third step is treatment with ethylenediamine, where -NH and NH₂ are present in the polymer chain, which was also expected. After treatment with glutaraldehyde, no new functional groups appear, but it is indicated that the polymer is cross-linked, which is desired in most enzyme immobilization processes. Despite the new groups added, what was observed was that there are still non-functionalized nitrile groups available, which was also observed in the FTIR spectra, which indicate the presence of peaks characteristic of the C≡N group.

4.3.2. Laccase immobilization

The kinetics of immobilization yield on each support using 0.85 g of support and 0.25 mg mL⁻¹ of laccase is shown in Figure 26.

Figure 26: Immobilization yield as a function of time for supports (using 0.25 g L⁻¹ initial concentration of laccase, 8 mL of volume and 0.85 g of support), where (●) CS-0, (■) CS-I-II, (▲) CS-I-II-III, (◀) CS-I-II-III-IV and (▶) CS-I-IV



Source: Author's elaboration

From Figure 26, it is observed that for all supports, the maximum immobilization yield is reached within 2 to 4 hours after the start of contact between the laccase solution and the CS particles. It is also possible to note that the supports functionalized with steps I and II (CS-I-II) or steps I, II, and III (CS-I-II-III), as shown in section 4.2.2, offered affinity with laccase similar to the support without any functionalization step (CS-0). These supports offered around 30% immobilization yield, while the supports that were treated by stage I and stage IV of functionalization reached 50% immobilization yield (supports CS-I-II-III-IV and CS-I-IV). The Table 11 below lists the maximum immobilization yield values for each support.

Table 9: Immobilization yield values for each support (tests carried out using 0.85 grams of support in 8 mL of laccase solution at a concentration of 0.25 mg/mL)

Support	Immobilization yield (%)	Enzyme concentration in the particle (mg of laccase/g of support)
CS-0	36.11 ± 0.91	0.847 ± 0.024
CS-I-II	29.45 ± 3.30	0.682 ± 0.089
CS-I-II-III	31.95 ± 2.95	0.752 ± 0.069
CS-I-II-III-IV	54.55 ± 1.62	1.283 ± 0.039
CS-I-IV	48.26 ± 2.62	1.135 ± 0.062

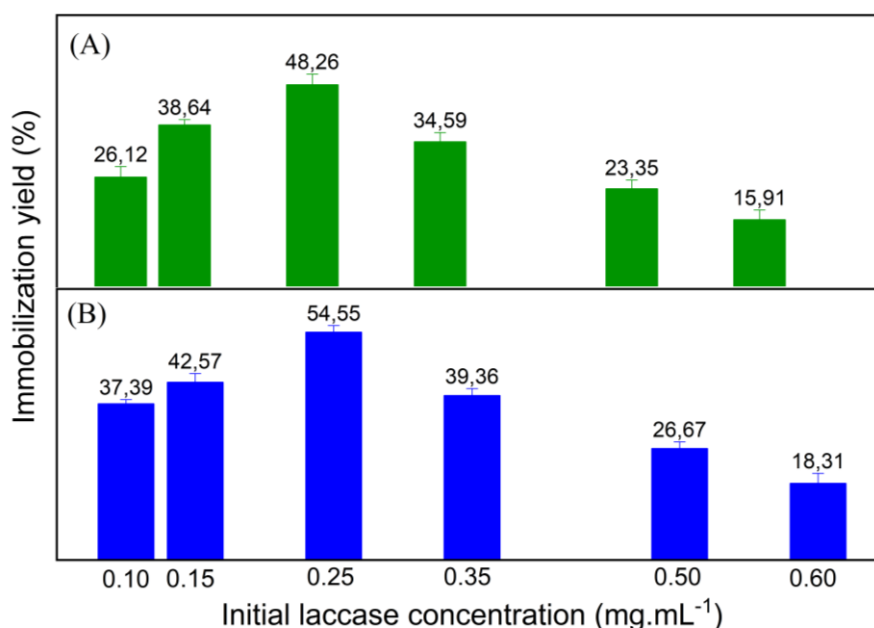
Source: Author's elaboration

In this sense, these results can be related with those obtained by ^1H NMR and FTIR in the previous section, which showed that the intermediate steps did not significantly affect the surface of the support. However, for laccase immobilization, treatment with glutaraldehyde (step IV) proved to be very important, since the immobilization yield improved by 20% with the addition of this step. Glutaraldehyde (GLU) is often used to immobilize enzymes on solid supports. GLU is a cross-linking agent that typically forms covalent bonds between amino groups of the enzyme and amino or hydroxyl groups on the surface of the support. In this way, the use of GLU in

the immobilization process is used to promote a stronger interaction between the enzymes and the surface of the solid support (ABELLANAS-PEREZ *et al.*, 2023; DAL MAGRO *et al.*, 2020).

From here, the supports that underwent treatment with 2% GLU (CS-I-II-III-IV and CS-I-IV) were selected to continue with the tests and other analyses regarding laccase immobilization. Thus, Figure 27 shows the maximum enzyme immobilization yields obtained for the different initial concentrations of laccase on the chosen supports.

Figure 27: Maximum laccase (LC) immobilization yield per initial LC concentration for CS-I-IV (A) and CS-I-II-III-IV (B) support, using 0.85 grams of support in a volume of 8 mL of laccase solution



Source: Author's elaboration

From the results, it was observed that the behavior of the laccase immobilization yield for different initial enzyme concentration is similar for the two supports. This behavior indicates a maximum capacity for laccase to bind to the supports in question. It may be related to several factors, including the availability of binding sites on the

support (functional groups on the surface of the particles), the structure and spatial conformation of the laccase (which may limit accessibility to some binding sites), and even some kinetic factors (DARONCH, 2020; KELBERT *et al.*, 2021). It will be shown in Table 12 that this maximum amount that can be immobilized on the support is equivalent to approximately 1.14 milligrams of laccase per gram of support for the CS-I-IV support and approximately 1.28 mg of laccase/g of support for the CS-I-II-III-IV support.

Table 10: Laccase immobilization data with different support mass (laccase concentration of 0.25 mg/mL and volume of 8 mL)

Support	Support mass (g)	Immobilization yield (%)	mg of laccase/g of support
CS-I-IV	0.85	48.26 ± 2.62	1.136
	1.25	71.12 ± 1.39	1.138
CS-I-II-III-IV	0.85	54.55 ± 1.62	1.283
	1.25	76.45 ± 1.24	1.223

Source: Author's elaboration

For the supports studied, the best initial concentration of laccase to achieve highest immobilization yield is 0.25 mg L⁻¹. Therefore, from now on, this laccase concentration was chosen to obtain the enzymatic derivative (support + enzyme) and kept fixed in the characterization tests. The immobilization yield was also measured when the amount of support in the laccase solution was increased, as shown in Table 12.

It can be stated that when the amount of support in contact with the enzyme solution is increased, this provides an increase in the functional groups (binding sites) amounts on the support for covalent bound or physical adsorption with the enzyme molecules. It also increases the likelihood of interactions between the enzyme molecules and the functional groups of the support that facilitate immobilization. It is

because there are a greater number of binding sites available, which can result in a greater immobilization yield, as more enzymes can be attached to the support.

However, increasing the enzyme per support will not necessarily increase the immobilization efficiency (mg of enzyme/g of support). This is because even if more active sites are available for each support, the total number of binding sites on the support may be limited. In this sense, there is a point at which saturation occurs, and adding more enzyme per support will not result in more efficient immobilization, as all binding sites may already be occupied.

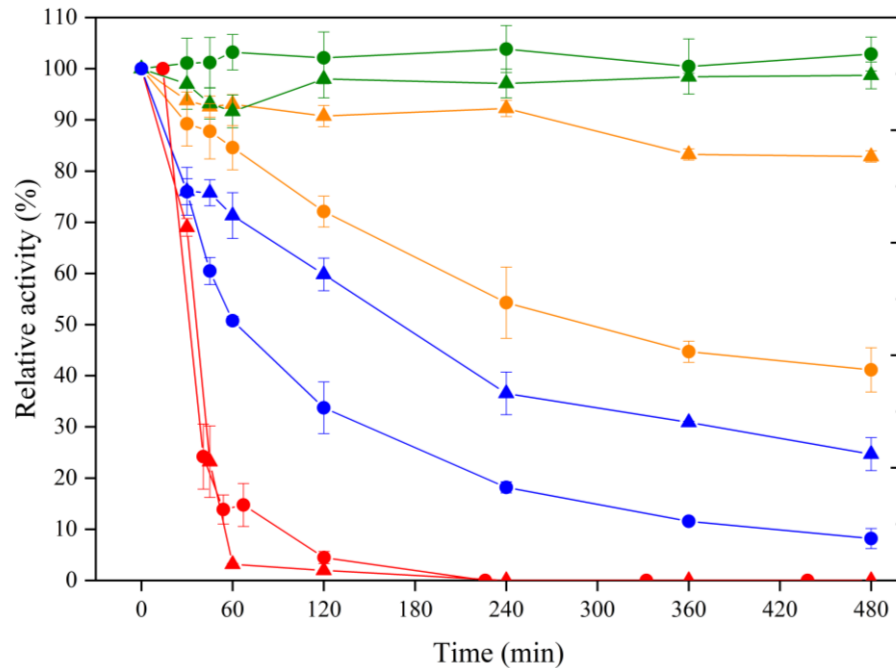
From that, the data obtained shows that the amount of laccase per support (mg g⁻¹) remains the same. Therefore, it is understood that the optimization of experimental conditions is needed to achieve maximum immobilization efficiency, but the ratio between the mass of enzyme and support is the same. There was a greater availability of active sites and functional groups (when the support mass was increased for the same amount of enzyme) for the laccase to bind to the support surface.

In this sense, to evaluate the characteristics of the enzymatic derivative, the enzymatic derivative obtained with 0.850 grams of the CS-I-IV support was chosen to reduce functionalization steps and, consequently, the costs involved in the process.

4.3.3. Characterization of the enzyme derivative

The thermal stability behavior of the free laccase and the laccase immobilized on the CS support at different temperatures are shown in Figure 28.

Figure 28: Thermal stability of the laccase immobilized (\blacktriangle) and free laccase (\bullet) at 30° C (\blacktriangle , \bullet), 50° C (\triangle , \circ), 60° C (\triangle , \bullet) and 70° C (\triangle , \bullet)



Source: Author's elaboration

The experimental results show that laccase presents a temperature range in which its activity and structure remain stable. Generally, laccase activity remains stable at lower temperatures, such as 30 °C. On the other hand, free laccase tends to denature at higher temperatures, as was noticed at temperatures of 50 and 60 °C. It happens due to the breakdown of the molecular interactions that keep its stability, resulting in the irreversible loss of enzymatic activity (ARICA *et al.*, 2017; ASGHER; NOREEN; BILAL, 2017; CHAUHAN *et al.*, 2019; KELBERT *et al.*, 2023).

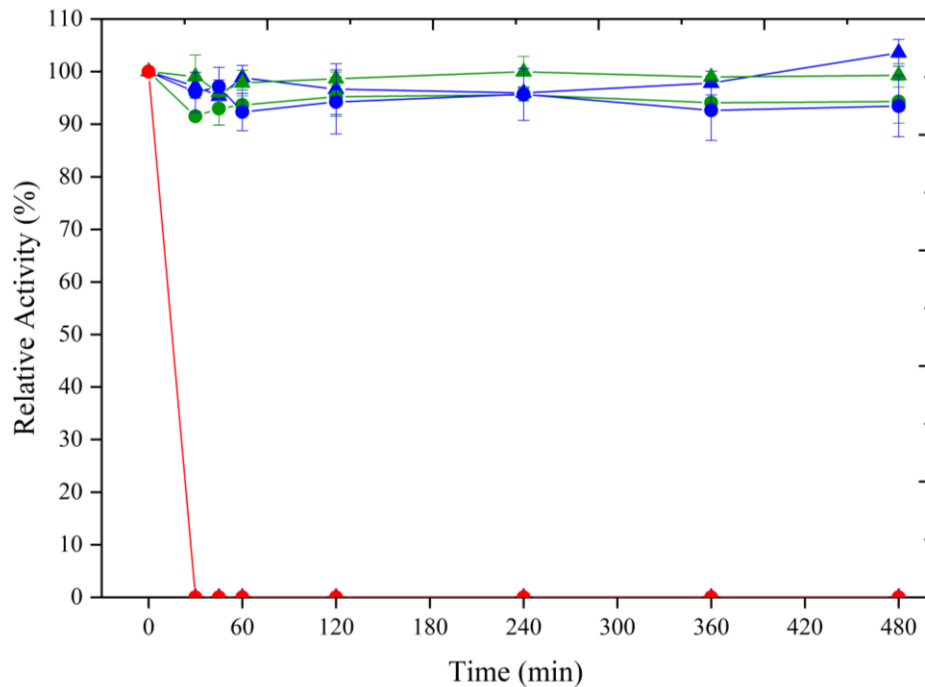
The specific case of the enzyme derivative obtained with the presented core-shell support demonstrated remarkable stability at higher temperatures, such as 50 °C. Even after 480 minutes, the immobilized enzyme maintained more than 80% (~83%) of its initial activity. This result contrasts with free laccase, which, at the same temperature after 480 minutes, showed only 41% of its residual activity. Immobilizing laccase on a solid support is a common strategy to increase its thermal stability and

functionality over a wide temperature range. Immobilization tends to offer physical protection to the enzyme structure, preventing its denaturation at higher temperatures (LADOLE *et al.*, 2020; TAHERAN *et al.*, 2017b; VIEIRA *et al.*, 2023).

The stability of the enzyme derivative at different pHs was also evaluated.

Figure 29 shows the residual activity as a function of time at each pH evaluated.

Figure 29: pH stability of the laccase immobilized and free laccase. Free laccase at pH 5.0 (●) and 6.0 (●); Immobilized laccase at pH 5.0 (▲) and 6.0 (▲); and Free and immobilized laccase at pHs 3.0 and 8.0 (●)



Source: Author's elaboration

Usually, pH is one of the main factors that influence the activity of enzymes, including (LIN *et al.*, 2017) (MORSI *et al.*, 2020; TAHERAN *et al.*, 2017b). Enzymatic activity depends on the environment in which the enzyme is added, and pH directly influences the three-dimensional structure and charge of protein molecules (LI *et al.*, 2020; WU *et al.*, 2019). From the data obtained, both free and immobilized laccase showed similar stability in the evaluated conditions of pH. At pH 3 and pH 8, a complete

loss of activity occurred in just 30 minutes, i.e., these pH extremes are unfavorable for the stability and functionality of the enzyme. This behavior happens because in very acidic or alkaline pH, the three-dimensional structure of laccase can be significantly altered, affecting the charges of the protein molecules and the ionic interactions that maintain the enzyme structure. These interactions can be disrupted, resulting in irreversible conformational changes in the laccase, which leads to the loss of its catalytic activity (LI *et al.*, 2020; WANG *et al.*, 2014).

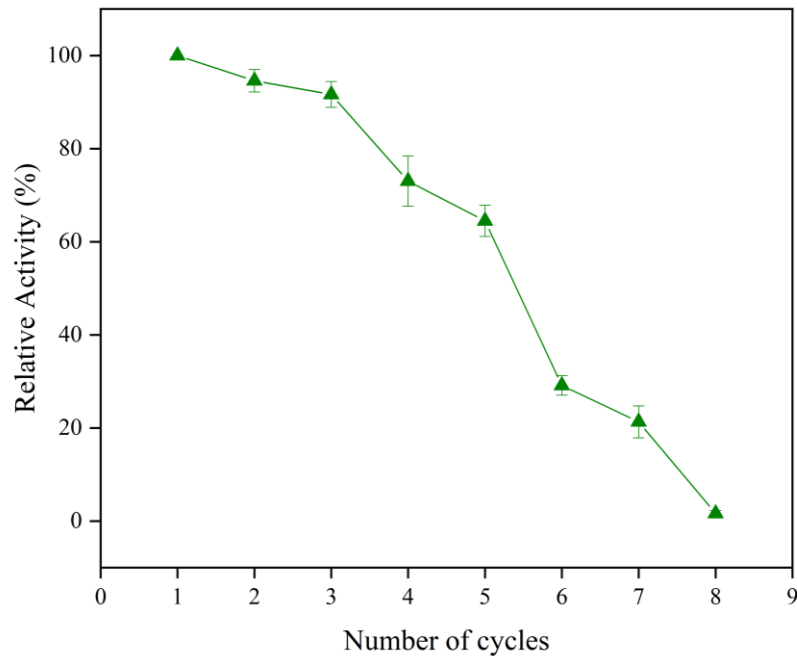
On the other hand, laccase maintains its activity throughout the entire time evaluated (480 minutes) at pHs 5 and 6. Therefore, these pH values are more suitable for enzyme stability and functionality. The ideal pH for laccase activity can vary depending on the origin of the enzyme (IMAM *et al.*, 2021; VIEIRA *et al.*, 2023), but neutral to slightly acidic pHs are often preferred to maintain optimal activity (KELBERT *et al.*, 2023; SHANMUGAM *et al.*, 2020). In these pH ranges, interactions between the enzyme amino acid residues and the surrounding environment are favorable, allowing laccase to maintain its three-dimensional structure and catalytic activity over time.

In addition to enzyme stability in different conditions of pH and temperature, the number of reuse cycles of immobilized enzymes, such as laccase, is a crucial aspect to be considered in the development of biotechnological processes, especially regarding economic viability and environmental sustainability. Figure 30 shows the results of residual activity by number of cycles.

The results indicate that the immobilized laccase maintains good activity after multiple reuse cycles. Up to five cycles, the enzyme activity was more than 60% of its initial activity, which is a promising result for practical application. The ability to maintain a significant fraction of activity over multiple reuse cycles is crucial for reducing

operating costs, as lower amounts of enzyme is required to be makeup for the process to recover the initial activity.

Figure 30: Reusability of laccase immobilized on CS-I-IV support



Source: Author's elaboration

After the fifth reuse cycle, a more pronounced decline in the activity of the immobilized laccase was observed. After the sixth and seventh cycles, residual activity decreased below 30%, suggesting that the stability of the enzyme and its ability to remain the activity throughout reuse cycles have limitations.

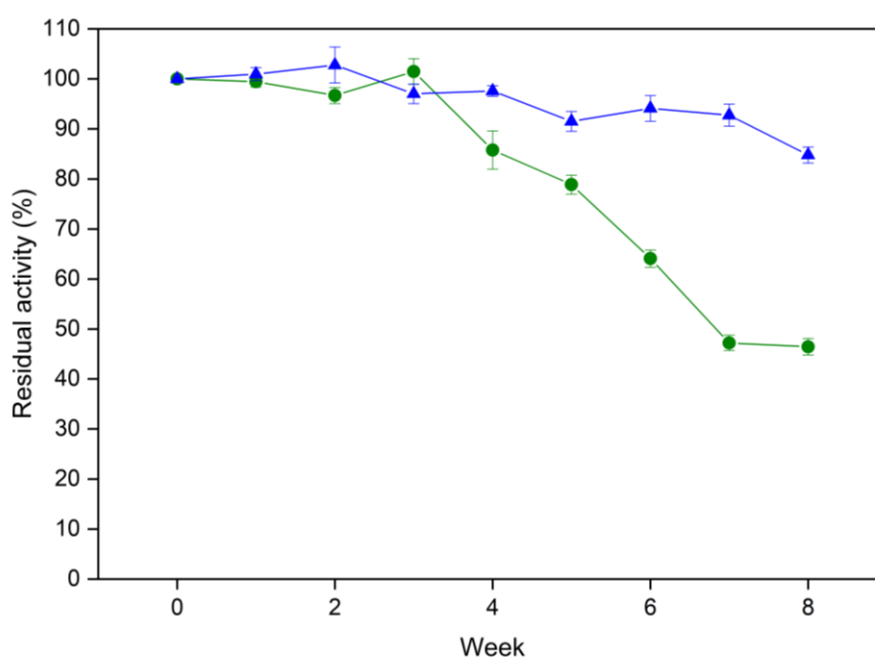
The decline in activity after multiple cycles of reuse can be attributed to several factors, including the possible deactivation of enzyme active sites due to changes in the structure of the polymeric support or the loss of enzyme stability over time due to degradation processes. Moreover, the enzyme concentration in support is also a factor to be considered in its stability in reuse cycles.

The results observed, where the activity of the immobilized laccase is maintained up to approximately six cycles of reuse, are in line with other studies found in the literature (IMAM *et al.*, 2021; SHANMUGAM *et al.*, 2020; VIEIRA *et al.*, 2023). It

suggests consistency in the results and stability of laccase immobilized on polymeric supports in different experimental conditions.

In addition to reuse, residual activity was also evaluated in storage conditions. The results obtained for residual activity for storage at refrigerator temperature ($\sim 8\text{ }^{\circ}\text{C}$) and at room temperature ($\sim 25\text{ }^{\circ}\text{C}$) are shown in Figure 31 below.

Figure 31: Residual activity for storage at refrigerator temperature ($\sim 8\text{ }^{\circ}\text{C}$) (\blacktriangle) and at room temperature ($\sim 25\text{ }^{\circ}\text{C}$) (\bullet)



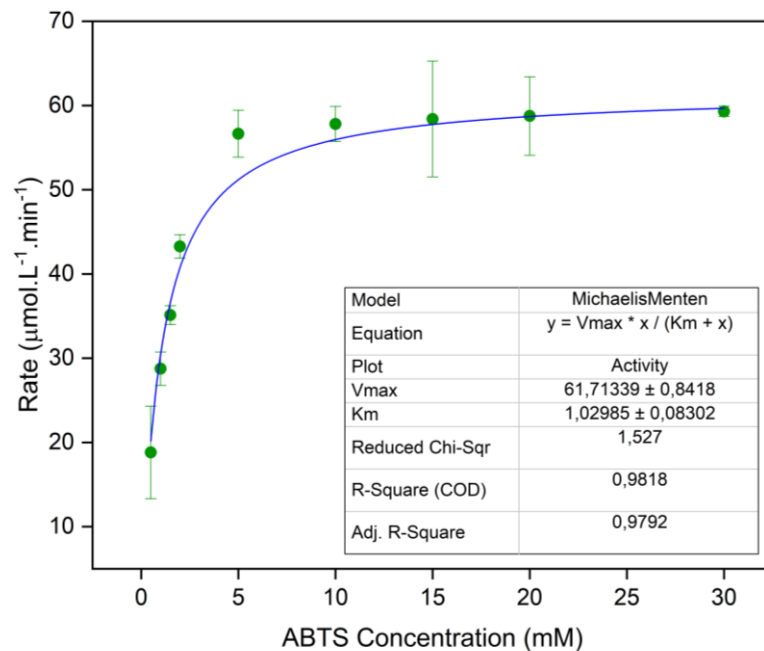
Source: Author's elaboration

It is noted that the stability of the biocatalyst is greater when stored in a refrigerator. In up to seven weeks, the catalytic activity is maintained above 90%, while for storage at a higher temperature (around $25\text{ }^{\circ}\text{C}$) the activity remains above 80% for up to four weeks, decreasing to below 60% after the fifth week. It was demonstrated that the shelf life at lower temperatures is longer. This behavior can be explained by some factors. Firstly, at lower temperatures, chemical reactions, including those that lead to the degradation of enzymes, occur at a slower rate. Enzymatic degradation can

be caused by processes such as thermal denaturation, oxidation or hydrolysis. At reduced temperatures, these reactions are less frequent and, therefore, enzymes maintain their structure and function for longer. Another factor is that enzymes can be degraded by microorganisms present in the storage environment. Lower temperatures inhibit the growth and activity of many of these microorganisms, reducing the likelihood of enzymatic degradation. Furthermore, at lower temperatures, the kinetic energy of molecules is reduced. This means there is less molecular agitation and less likelihood of collisions that can cause enzymes to denature (KUMAR *et al.*, 2023).

Figure 32 shows the substrate concentration on the ABTS enzymatic oxidation rate and the adjustment of Michaelis-Menten model.

Figure 32: Substrate concentration and the kinetic parameters, V_{max} (mmol L^{-1}) and K_M ($\mu\text{mol min}^{-1} \text{L}^{-1}$), obtained from the Michaelis-Menten model



Source: Author's elaboration

From the Michaelis-Menten model adjustment, it was possible to obtain K_M and V_{max} values, which were 1.03 mmol L^{-1} and $61.71 \mu\text{mol min}^{-1} \text{L}^{-1}$, respectively. Briefly, K_M and V_{max} are crucial parameters for enzyme kinetics, as they provide information

about the enzyme's affinity for the substrate (K_M) and its maximum capacity to catalyze the reaction (V_{max}). Furthermore, based on the curve obtained, below 5 mmol L^{-1} it is not possible to measure the activity as the speed is limited by the concentration of ABTS. Above this, the speed depends only on the amount of enzyme.

The Michaelis-Menten constant (K_M) represents the substrate concentration at which the enzymatic reaction rate is equal to half the maximum reaction rate (V_{max}). Thus, K_M is considered the measure of the enzyme affinity for the substrate. The lower the K_M value, the greater the enzyme affinity for the substrate. On the other hand, V_{max} is the maximum rate of an enzymatic reaction, when all active sites of enzyme are converted into enzyme-substrate intermediary complex and represents the maximum capacity of the enzyme to convert substrate into product in each experimental condition. This parameter can be affected by factors such as temperature, pH, and the presence of inhibitors (CORNISH-BOWDEN, 2015).

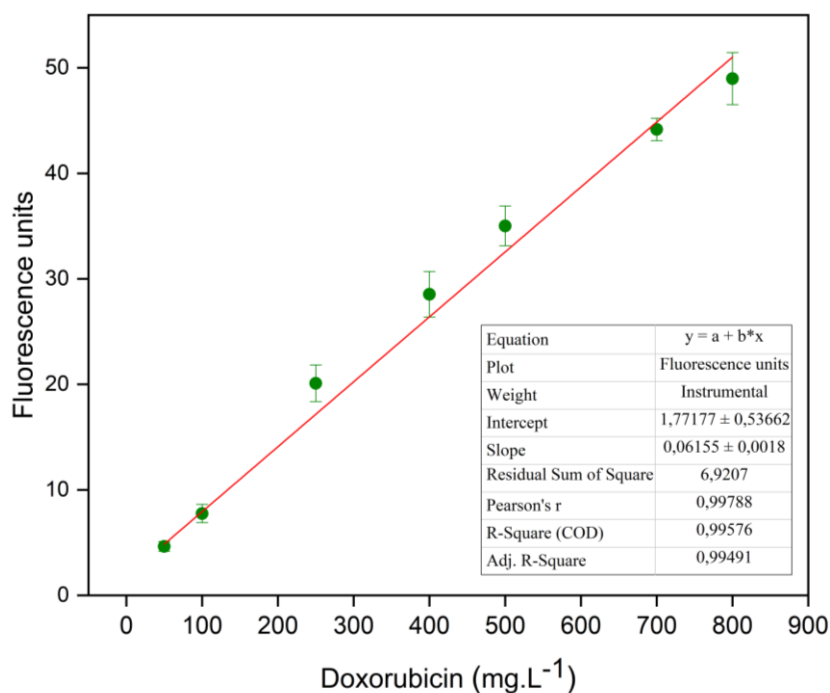
Compared with other works in the literature, around 2.67 mM (DARONCH, 2020), the K_M value found for the laccase immobilized in CS-I-IV offers an excellent value, indicating a high affinity between the derivative and the substrate (ABTS). The V_{max} value is within the expected range based on the enzymatic activity exhibited by the experimental results.

4.3.4. Doxorubicin (DOX) degradation assays

Figura 33 shows de calibration curve for fluorescent response as a function of DOX concentration. The concentration values in reference solutions are related to the data obtained by fluorescence through a straight-line equation. For example, when the $250 \text{ } \mu\text{g L}^{-1}$ DOX solution was analyzed, a fluorescence value of 17.448 ± 0.557 was measured. According to the equation, this data gives us an average DOX

concentration of $254.69 \mu\text{g L}^{-1}$. For the $500 \mu\text{g L}^{-1}$ solution, a fluorescence value of 34.125 ± 0.923 was obtained, which, according to the equation, gives an average DOX concentration of $525.64 \mu\text{g L}^{-1}$. Therefore, the calibration curve showed good agreement between experimental and theoretical data.

Figure 33: DOX concentration calibration curve by fluorescence data



Source: Author's elaboration

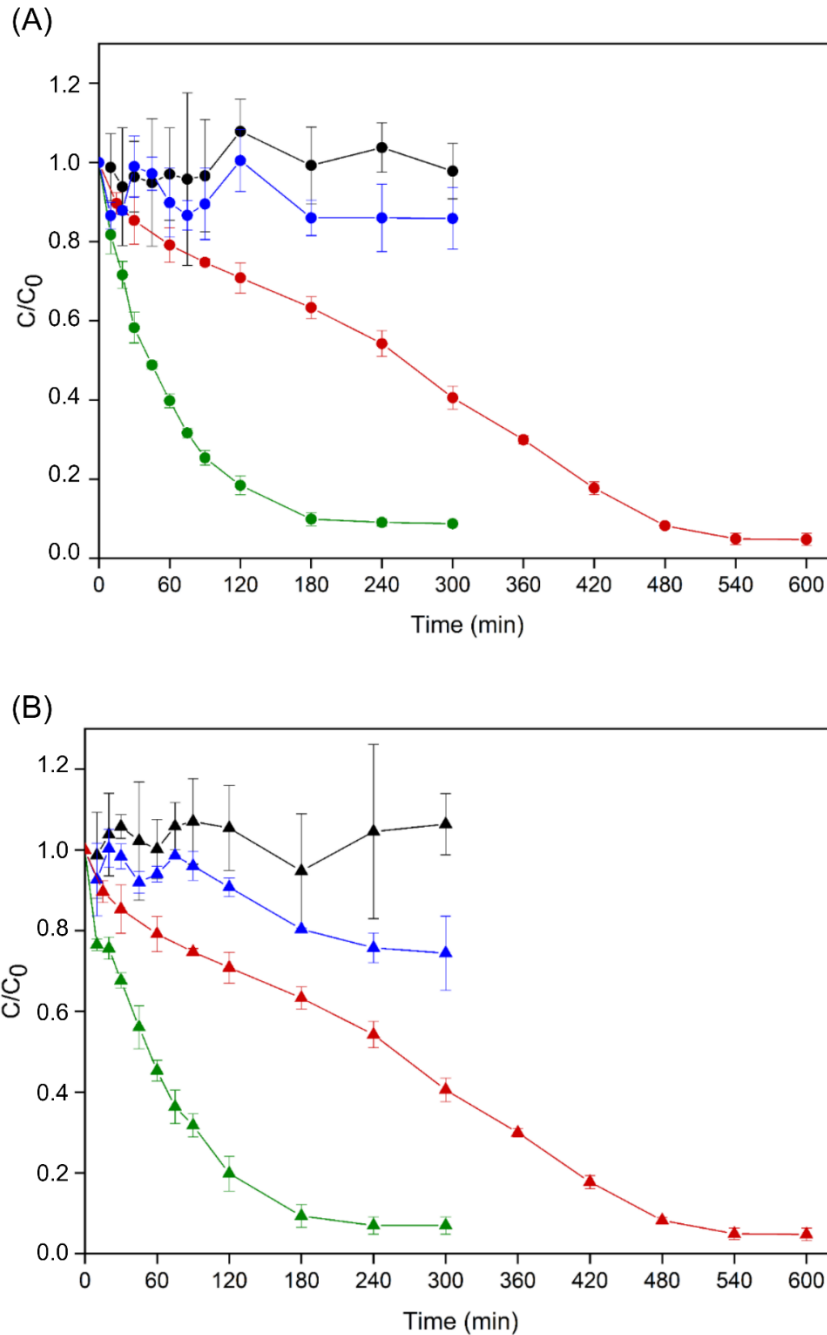
To evaluate the efficiency of the enzymatic derivative obtained by the immobilization of laccase in CS-I-IV, the degradation kinetic behavior of the anticancer drug DOX at concentrations of $250 \mu\text{g L}^{-1}$ and $500 \mu\text{g L}^{-1}$ was evaluated, as suggested by KELBERT *et al.* (2021), which investigated the degradation of DOX at the same concentrations but with free laccase. Figure 34 shows the following curves: (a) hydrolysis curve (measured only with the DOX solution, to check if there was any self-degradation during the time); (b) the adsorption curve (measured with the DOX solution in contact with the CS-I-IV support without the enzyme); (c) DOX degradation curve

measured with the enzymatic derivative (CS-I-IV + Lac + DOX); and (d) DOX degradation curve using free laccase.

From the adsorption curves, it is observed that at the concentration of $250 \mu\text{g L}^{-1}$, there was 10% removal and at a concentration of $500 \mu\text{g L}^{-1}$, there was 20% removal. Therefore, it can be stated that the support also has some DOX adsorption capacity, which is somewhat expected, considering that there is a specific area and functional groups on the support surface such as the nitrile group that can chemically interact with DOX. According to the FTIR results, there are unconverted nitrile groups on the surface and from this there may be a combined effect. However, as adsorption is minimal, the high degradation mainly comes from enzymatic action. Therefore, the results of DOX degradation using immobilized laccase are very promising, especially when compared with studies in the literature that used free laccase (JINGA; TUDOSE; IONITA, 2022; KELBERT *et al.*, 2021) and with the results obtained from free laccase.

For tests using a concentration of $250 \mu\text{g L}^{-1}$, the degradation of DOX was approximately 92% in 180 minutes when the immobilized laccase was used. For tests using $500 \mu\text{g L}^{-1}$ of DOX, the immobilized laccase showed results that are even more impressive. In 180 minutes, degradation was 91%, reaching up to 93% in 240 minutes. On other hand, one can see a lower reaction rates for DOX degradation, when free laccase was used.

Figure 34: DOX removal kinetic curves by: (A) Hydrolysis (●), Adsorption (●), Degradation with immobilized (●) and free laccase (●) at DOX concentration of $250 \mu\text{g L}^{-1}$; and (B) Hydrolysis (▲), Adsorption (▲), Degradation with immobilized (▲) and free laccase (▲) at DOX concentration of $500 \mu\text{g L}^{-1}$ (using 1.5 g of enzyme derivative and for the free enzyme assay an amount of 1.7 mg of laccase)



Source: Author's elaboration

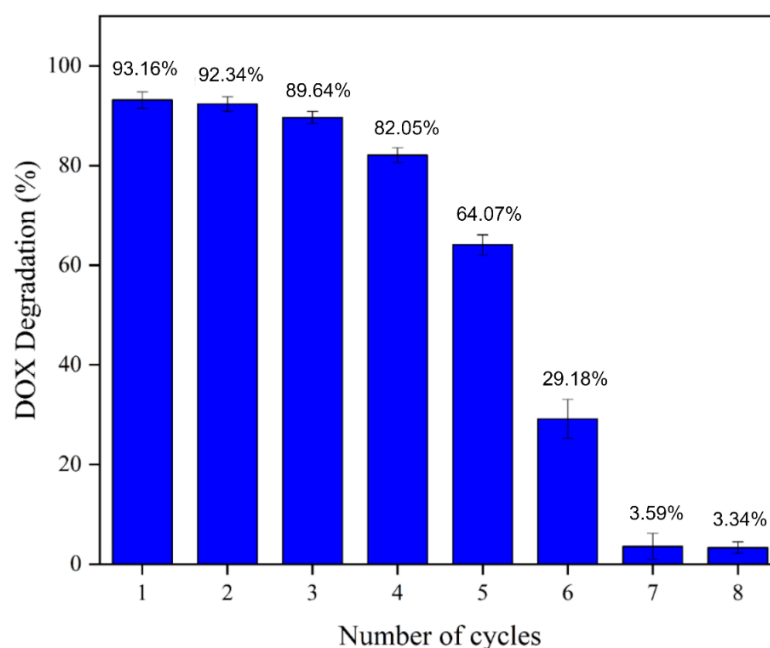
Regarding the degradation curves in presence of free laccase, the maximum DOX degradation at both concentrations ($250 \mu\text{g L}^{-1}$ and $500 \mu\text{g L}^{-1}$) was approximately

96.0% within 480 minutes. These results demonstrate the binding of the enzyme to the support enhances the degradation capacity of the anticancer drug by laccase. Immobilization can help stabilize the enzyme structure, protecting it against adverse conditions such as changes in pH, temperature, and the presence of inhibitors. Another factor is when the reaction product inhibits enzyme activity. In this case, immobilization can help reduce the concentration of the product near the enzyme sites, allowing the reaction to proceed at higher rate (ELMERHI *et al.*, 2023; GALODIYA; CHAKMA, 2024).

These results suggest some significant advantages of using immobilized laccase compared to the free form. Firstly, immobilized laccase is more efficient in DOX degradation than free laccase, requiring less time to reach high levels of degradation. Furthermore, the reusability of the immobilized laccase is an additional advantage. While free laccase cannot be reused, the immobilized form can be used multiple times, reducing costs, and increasing the efficiency of degradation process over time.

Therefore, the number of cycles in which the immobilized laccase could be reused to degrade DOX was also evaluated. Figure 35 presents the results obtained in reuse tests of the enzyme derivative with $500 \mu\text{g L}^{-1}$ of doxorubicin solution.

Figure 35: Reusability of the enzymatic derivative (CS-I-IV + Lac) in 500 $\mu\text{g L}^{-1}$ of DOX solution (Each cycle occurred for 180 min under conditions of pH 6.0 and temperature of 30 °C)



Source: Author's elaboration

Particularly, the immobilized laccase can be reused at least five times when it still maintains the DOX degradation at values above 60%. After the sixth reuse cycle, the derivative allowed only 29% DOX degradation. This is a good result and a pioneer in the literature since this work investigates the immobilized laccase in the degradation of DOX for the first time. The works found in the literature used free laccase; therefore, there is no possibility of reuse. However, the data are extremely promising when comparing these DOX degradation results with those obtained for ABTS oxidation.

In summary, the immobilization of laccase to the core-shell polymeric support provided significant advantages, including increased DOX degradation rates, greater stability, and ease of recovery and reuse, which allows cost reduction.

4.4. CONCLUSION AND FUTURE PERSPECTIVES

The present study investigated the immobilization of laccase on core-shell polymeric support and the characteristics and efficiency of the enzymatic derivative obtained. The results revealed that the functionalization of support surface was crucial for the efficient immobilization of laccase. Of the four steps performed, only two were necessary to achieve the best interaction with the enzyme. Notably, the reaction with glutaraldehyde emerged as the main step, highlighting its importance in the effectiveness of the immobilization process. Furthermore, the immobilized laccase demonstrated excellent stability, being reused more than five times in the process without significant loss of activity.

Additionally, immobilization provided the enzyme higher thermal resistance than its free form, which is promising for applications under different operating conditions. Doxorubicin degradation assays revealed that the immobilized laccase reached maximum degradation faster than the free enzyme, suggesting that the core-shell polymeric support contributed to a higher enzymatic degradation rate of the substrate in presence of laccase. In summary, this study demonstrated the efficiency of the enzyme system with laccase immobilized on a core-shell polymeric support. The results expand the understanding of enzyme immobilization processes and open doors to practical applications in biotechnology and degradation processes of aromatic compounds, including anticancer drugs.

5 CHAPTER 5 – FINAL CONSIDERATIONS

This chapter brings the main conclusions and future perspectives of the work, as well as all the references used during the development of this thesis, and these can be found in the QR Code below.



5.1. FINAL CONCLUSIONS AND FUTURE OUTLOOK

Particles with core-shell morphology were synthesized through polymerization processes in dispersed medium. During the study, the particles with a polypropylene core showed low swelling in styrene and, consequently, did not present homogeneous coverage of the polyacrylonitrile shell. At the same time, the particles produced with a polypropylene/polystyrene core (previously synthesized through seeded suspension polymerization) presented higher swelling rates. The swelling rates of core particles in styrene demonstrated a crucial role on formation of a uniform shell of polyacrylonitrile particles. In this context, the particles were produced with a core composed by low-cost polymers and a porous polyacrylonitrile shell, making the final particle surface chemically functionalizable and with desirable characteristics for enzyme immobilization.

In this sense, the work demonstrated that surface functionalization was crucial for the efficient immobilization of laccase. Of the four-functionalization steps carried out, the analysis of chemical composition and immobilization kinetics suggested that the reaction with glutaraldehyde acts as the main step, highlighting its importance in the effectiveness of the laccase immobilization process. Furthermore, the immobilized laccase showed excellent stability, being reused more than five times without significant loss of activity and giving the enzyme a higher temperature resistance compared to its free form. Doxorubicin degradation assays revealed that the immobilized laccase reached maximum degradation more quickly than the free enzyme, suggesting that the core-shell polymeric support contributed to a faster degradation rate. In summary, this study demonstrated the efficiency of the enzyme system with laccase immobilized on a core-shell polymeric support. The results open

the way for practical applications in biotechnology, aromatic compound degradation processes and anticancer drugs.

5.2. REFERENCES

ABELLANAS-PEREZ, P.; CARBALLARES, D.; FERNANDEZ-LAFUENTE, R.; ROCHA-MARTIN, J. Glutaraldehyde modification of lipases immobilized on octyl agarose beads: Roles of the support enzyme loading and chemical amination of the enzyme on the final enzyme features. **International Journal of Biological Macromolecules**, v. 248, n. July, p. 125853, 2023.

AGGARWAL, S.; CHAKRAVARTY, A.; IKRAM, S. A comprehensive review on incredible renewable carriers as promising platforms for enzyme immobilization & thereof strategies. **International Journal of Biological Macromolecules**, v. 167, p. 962–986, 2021.

AGRAWAL, K.; CHATURVEDI, V.; VERMA, P. Fungal laccase discovered but yet undiscovered. **Bioresources and Bioprocessing**, v. 5, n. 1, 2018.

AHANGARAN, F.; HAYATY, M.; NAVARCHIAN, A. H. Morphological study of polymethyl methacrylate microcapsules filled with self-healing agents. **Applied Surface Science**, v. 399, p. 721–731, 2017.

AL-SHALABI, E.; ALKHALDI, M.; SUNOQROT, S. Development and evaluation of polymeric nanocapsules for cirsiol isolated from Jordanian *Teucrium polium* L. as a potential anticancer nanomedicine. **Journal of Drug Delivery Science and Technology**, v. 56, n. October 2019, p. 101544, 2020.

ALMEIDA, F. L. C.; CASTRO, M. P. J.; TRAVÁLIA, B. M.; FORTE, M. B. S. Trends in lipase immobilization: Bibliometric review and patent analysis. **Process Biochemistry**, v. 110, n. July, p. 37–51, 2021.

ARICA, M. Y.; SALIH, B.; CELIKBICAK, O.; BAYRAMOGLU, G. Immobilization of laccase on the fibrous polymer-grafted film and study of textile dye degradation by MALDI–ToF-MS. **Chemical Engineering Research and Design**, v. 128, p. 107–119, 2017.

ASGHER, M.; NOREEN, S.; BILAL, M. Enhancing catalytic functionality of *Trametes versicolor* IBL-04 laccase by immobilization on chitosan microspheres. **Chemical Engineering Research and Design**, v. 119, p. 1–11, 2017.

BERG, C.; FU, L.; LIU, Y.; ENGQVIST, H.; XIA, W. Bulk nanobubbles as soft templates in the fabrication of inorganic core-shell particles. **Ceramics International**, v. 49, n. February, p. 16501–16513, 2023.

BESTETI, M. D.; CUNHA, A. G.; FREIRE, D. M. G.; PINTO, J. C. Core/shell polymer particles by semibatch combined suspension/emulsion polymerizations for enzyme immobilization. **Macromolecular Materials and Engineering**, v. 299, n. 2, p. 135–143, 2014a.

BESTETI, M. D.; JR., F. G. S.; FREIRE, D. M. G.; PINTO, J. C. Production of Core-Shell Polymer Particles-Containing Cardanol by Semibatch Combined Suspension/ Emulsion Polymerization. **Polymer Engineering and Science**, p. 1222–1229, 2014b.

BESTETI, M. D.; FREIRE, D. M. G.; PINTO, J. C. Production of Core-shell Particles by Combined Semibatch Emulsion/Suspension Polymerizations. **Macromolecular Reaction Engineering**, v. 5, n. 9–10, p. 518–532, 2011.

BHARDWAJ, P.; KAUR, N.; SELVARAJ, M.; GHRAMH, H. A.; AL-SHEHRI, B. M.; SINGH, G.; ARYA, S. K.; BHATT, K.; GHOTEKAR, S.; MANI, R.; CHANG, S. W.; RAVINDRAN, B.; AWASTHI, M. K. Laccase-assisted degradation of emerging recalcitrant compounds – A review. **Bioresource Technology**, v. 364, n. September, p. 128031, 2022.

BILAL, M.; ZHAO, Y.; RASHEED, T.; IQBAL, H. M. N. Magnetic nanoparticles as versatile carriers for enzymes immobilization: A review. **International Journal of Biological Macromolecules**, v. 120, p. 2530–2544, 2018.

BILAL, M.; RASHEED, T.; NABEEL, F.; IQBAL, H. M. N.; ZHAO, Y. Hazardous contaminants in the environment and their laccase-assisted degradation – A review. **Journal of Environmental Management**, v. 234, n. January, p. 253–264, 2019.

BOURGAT, Y.; TIERSCH, B.; KOETZ, J.; MENZEL, H. Enzyme Degradable Polymersomes from Chitosan-g-[poly-l-lysine-block- ϵ -caprolactone] Copolymer. **Macromolecular Bioscience**, v. 21, n. 1, p. 1–9, 2021.

CAI, D.; CHEN, H.; ZHANG, C.; TENG, X.; LI, X.; SI, Z.; LI, G.; YANG, S.; WANG, G.; QIN, P. Carbonized core-shell diatomite for efficient catalytic furfural production from corn cob. **Journal of Cleaner Production**, v. 283, n. 0959–6526, p. 125410, 2021.

CAO, S.; XU, P.; MA, Y.; YAO, X.; YAO, Y.; ZONG, M.; LI, X.; LOU, W. Recent advances in immobilized enzymes on nanocarriers. **Cuihua Xuebao/Chinese Journal**

of **Catalysis**, v. 37, n. 11, p. 1814–1823, 2016.

CAPELETTO, C. A.; DA ILVA, M. R.; SAYER, C.; DE ARAÚJO, P. H. H. Synthesis of core-shell particles with low molecular weight alkanes by miniemulsion polymerization. **Macromolecular Symposia**, v. 343, n. 1, p. 31–38, 2014.

CASTRO COELHO, S.; NOGUEIRO ESTEVINHO, B.; ROCHA, F. Encapsulation in food industry with emerging electrohydrodynamic techniques: Electrospinning and electrospraying – A review. **Food Chemistry**, v. 339, n. August 2020, p. 127850, 2021.

CATAPANE, M.; NICOLUCCI, C.; MENALE, C.; MITA, L.; ROSSI, S.; MITA, D. G.; DIANO, N. Enzymatic removal of estrogenic activity of nonylphenol and octylphenol aqueous solutions by immobilized laccase from *Trametes versicolor*. **Journal of Hazardous Materials**, v. 248–249, p. 337–346, 2013.

CHAPA GONZALEZ, C.; MARTÍNEZ PÉREZ, C. A.; MARTÍNEZ MARTÍNEZ, A.; OLIVAS ARMENDÁRIZ, I.; ZAVALA TAPIA, O.; MARTEL-ESTRADA, A.; GARCÍA-CASILLAS, P. E. Development of antibody-coated magnetite nanoparticles for biomarker immobilization. **Journal of Nanomaterials**, v. 2014, 2014.

CHAUHAN, P. S.; KUMARASAMY, M.; SOSNIK, A.; DANINO, D. Enhanced Thermostability and Anticancer Activity in Breast Cancer Cells of Laccase Immobilized on Pluronic-Stabilized Nanoparticles. **ACS Applied Materials and Interfaces**, v. 11, n. 43, p. 39436–39448, 2019.

CHEN, T.; PENG, Y.; QIU, M.; YI, C.; XU, Z. Heterogenization of homogeneous catalysts in polymer nanoparticles : From easier recovery and reuse to more efficient catalysis. **Coordination Chemistry Reviews**, v. 489, n. May, p. 215195, 2023.

CHEN, Z.; OH, W.; YAP, P. Chemosphere Recent advances in the utilization of immobilized laccase for the degradation of phenolic compounds in aqueous solutions : A review. **Chemosphere**, v. 307, n. P3, p. 135824, 2022.

CIPOLATTI, E. P.; VALÉRIO, A.; HENRIQUES, R. O.; MORITZ, D. E.; NINOW, J. L.; FREIRE, D. M. G.; MANOEL, E. A.; FERNANDEZ-LAFUENTE, R.; DE OLIVEIRA, D. Nanomaterials for biocatalyst immobilization-state of the art and future trends. **RSC Advances**, v. 6, n. 106, p. 104675–104692, 2016.

COMAN, C.; HĂDADE, N.; PESEK, S.; SILAGHI-DUMITRESCU, R.; MOȚ, A. C. Removal and degradation of sodium diclofenac via radical-based mechanisms using *S. sclerotiorum* laccase. **Journal of Inorganic Biochemistry**, v. 249, n. July,

2023.

CORDEIRO, A. L.; POMPE, T.; SALCHERT, K.; WERNER, C. Bioconjugation Protocols_2nd Edition (2011) 465-476.pdf. v. 751, p. 465–476, [s.d.].

CORNISH-BOWDEN, A. One hundred years of Michaelis–Menten kinetics. **Perspectives in Science**, v. 4, p. 3–9, 2015.

CUNHA, A. G.; BESTETI, M. D.; MANOEL, E. A.; DA SILVA, A. A. T.; ALMEIDA, R. V.; SIMAS, A. B. C.; FERNANDEZ-LAFUENTE, R.; PINTO, J. C.; FREIRE, D. M. G. Preparation of core-shell polymer supports to immobilize lipase B from *Candida antarctica*: Effect of the support nature on catalytic properties. **Journal of Molecular Catalysis B: Enzymatic**, v. 100, p. 59–67, 2014.

DAI, J.; WEN, X.; FENG, W.; CHENG, C.; HUANG, D. Correlation of the heat treatment feature and magnetic properties of the. **Materials Chemistry and Physics**, v. 276, n. May 2021, p. 125393, 2022.

DAL MAGRO, L.; KORNECKI, J. F.; KLEIN, M. P.; RODRIGUES, R. C.; FERNANDEZ-LAFUENTE, R. Pectin lyase immobilization using the glutaraldehyde chemistry increases the enzyme operation range. **Enzyme and Microbial Technology**, v. 132, n. June 2019, p. 109397, 2020.

DAMIN, B. I. S.; KOVALSKI, F. C.; FISCHER, J.; PICCIN, J. S.; DETTMER, A. Challenges and perspectives of the β -galactosidase enzyme. **Applied Microbiology and Biotechnology**, v. 105, n. 13, p. 5281–5298, 2021.

DARONCH, N. A.; KELBERT, M.; PEREIRA, C. S.; HENRIQUE, P.; ARAÚJO, H. DE; OLIVEIRA, D. DE. Elucidating the choice for a precise matrix for laccase immobilization: A review. **Chemical Engineering Journal**, v. 397, n. May, p. 125506, 2020.

DARONCH, N. A. **Polyurethane Foam as Matrix for One-Step Laccase Immobilization**. [s.l.] Universidade Federal de Santa Catarina, 2020.

DAS, R.; DWEVEDI, A.; KAYASTHA, A. M. Current and future trends on polymer-based enzyme immobilization. **Polymeric Supports for Enzyme Immobilization**, n. January, p. 1–25, 2021.

DE OLIVEIRA, A. L. B.; CAVALCANTE, F. T. T.; MOREIRA, K. S.; MONTEIRO, R. R. C.; ROCHA, T. G.; SOUZA, J. E. S.; DA FONSECA, A. M.; LOPES, A. A. S.; GUIMARÃES, A. P.; DE LIMA, R. K. C.; DE SOUZA, M. C. M.; DOS SANTOS, J. C. S. Lipases immobilized onto nanomaterials as biocatalysts in biodiesel production: Scientific context, challenges, and opportunities. **Revista Virtual de**

Quimica, v. 13, n. 4, p. 875–891, 2021.

DEHGHANIFARD, E.; JAFARI, A. J.; KALANTARY, R. R.; MAHVI, A. H.; FARAMARZI, M. A.; ESRAFILI, A. Biodegradation of 2,4-dinitrophenol with laccase immobilized on nano-porous silica beads. **Iranian Journal of Environmental Health Science and Engineering**, v. 10, n. 25, p. 1–9, 2013.

DENG, L.; TIAN, J.; XU, J.; WANG, F.; NIE, K.; TAN, T. A Core–Shell Structured Immobilized Lipase and Its Application in High-Temperature Reactions. **Applied Biochemistry and Biotechnology**, v. 189, n. 3, p. 774–786, 2019.

DENG, M.; ZHAO, H.; ZHANG, S.; TIAN, C.; ZHANG, D.; DU, P.; LIU, C.; CAO, H.; LI, H. High catalytic activity of immobilized laccase on core–shell magnetic nanoparticles by dopamine self-polymerization. **Journal of Molecular Catalysis B: Enzymatic**, v. 112, p. 15–24, 2015.

DOS SANTOS SILVA, J.; ALBUQUERQUE MELO, P.; MARINHO, R.; CASTRO DE JESUS, N. J.; MÁRCIO, M. H.; PINTO, J. C. Modeling of suspension polymerizations in continuous oscillatory baffled reactors (COBR) - Part I: Vinyl acetate polymerization. **Chemical Engineering Science**, v. 288, n. September 2023, p. 119845, 2024.

DUTRA, L.; OECHSLER, B. F.; BRANDÃO, A. L. T.; LIMA, R. C.; NELE, M.; PINTO, J. C. Preparation of Polymer Microparticles through Nonaqueous Suspension Polycondensations: Part V—Modeling and Parameter Estimation for Poly(butylene succinate) Polycondensations. **Macromolecular Reaction Engineering**, v. 14, n. 4, p. 1–16, 2020.

ELMERHI, N.; AL-MAQDI, K.; ATHAMNEH, K.; MOHAMMED, A. K.; SKORJANC, T.; GÁNDARA, F.; RAYA, J.; PASCAL, S.; SIRI, O.; TRABOLSI, A.; SHAH, I.; SHETTY, D.; ASHRAF, S. S. Enzyme-immobilized hierarchically porous covalent organic framework biocomposite for catalytic degradation of broad-range emerging pollutants in water. **Journal of Hazardous Materials**, v. 459, n. May, 2023.

EZZAHRA, F.; RAIHANE, M.; AMEDURI, B. Recent progress on core-shell structured BaTiO₃ @ polymer / fluorinated polymers nanocomposites for high energy storage : Synthesis , dielectric properties and applications. **Progress in Materials Science**, v. 113, n. April, p. 100670, 2020.

FAN, H.; YU, X.; LONG, Y.; ZHANG, X.; XIANG, H.; DUAN, C. Preparation of kapok – polyacrylonitrile core – shell composite microtube and its application as gold nanoparticles carrier. **Applied Surface Science**, v. 258, n. 7, p. 2876–2882, 2012.

FARHAN, M.; CHAUDHARY, D.; NÖCHEL, U.; BEHL, M.; KRATZ, K.; LENDLEIN, A. Electrical Actuation of Coated and Composite Fibers Based on Poly[ethylene-co-(vinyl acetate)]. **Macromolecular Materials and Engineering**, v. 306, n. 2, p. 1–8, 2021.

FERNÁNDEZ-FERNÁNDEZ, M.; SANROMÁN, M. Á.; MOLDES, D. Recent developments and applications of immobilized laccase. **Biotechnology Advances**, v. 31, n. 8, p. 1808–1825, 2013.

FERREIRA GARCIA, L.; GONÇALVES MORENO, E. K.; BARROSO BRITO, L.; RODRIGUES DE OLIVEIRA, G. A.; LINARES, J. J.; DE SOUZA GIL, E. Effective degradation of the antineoplastic doxorubicin by electrochemical oxidation on boron doped diamond. **Journal of Electroanalytical Chemistry**, v. 870, 2020.

GALODIYA, M. N.; CHAKMA, S. Immobilization of enzymes on functionalized cellulose nanofibrils for bioremediation of antibiotics: Degradation mechanism, kinetics, and thermodynamic study. **Chemosphere**, v. 349, n. August 2023, p. 140803, 2024.

GALOGAHI, F. M.; ZHU, Y.; AN, H.; NGUYEN, N. T. Core-shell microparticles: Generation approaches and applications. **Journal of Science: Advanced Materials and Devices**, v. 5, n. 4, p. 417–435, 2020.

GAO, H.; NING, S.; ZHOU, Y.; MEN, S.; KANG, X. Polyacrylonitrile-induced formation of core-shell carbon nanocages: Enhanced redox kinetics towards polysulfides by confined catalysis in Li-S batteries. **Chemical Engineering Journal**, v. 408, n. July 2020, p. 127323, 2021.

GIBSON, N.; KUCHENBECKER, P.; RASMUSSEN, K.; HODOROABA, V. D.; RAUSCHER, H. **Volume-specific surface area by gas adsorption analysis with the BET method**. [s.l.] Elsevier Inc., 2019.

GOKMEN, M. T.; DU PREZ, F. E. Porous polymer particles - A comprehensive guide to synthesis, characterization, functionalization and applications. **Progress in Polymer Science (Oxford)**, v. 37, n. 3, p. 365–405, 2012.

GONÇALVES, O. H.; ASUA, J. M.; DE ARAÚJO, P. H. H.; MACHADO, R. A. F. Synthesis of PS/PMMA core-shell structured particles by seeded suspension polymerization. **Macromolecules**, v. 41, n. 19, p. 6960–6964, 2008.

GONÇALVES, O. H.; MACHADO, R. A. F.; DE ARAÚJO, P. H. H.; ASUA, J. M. Secondary particle formation in seeded suspension polymerization. **Polymer**, v. 50, n. 2, p. 375–381, 2009.

GONZALEZ-ORTIZ, L. J.; ASUA, J. M. Development of Particle Morphology in Emulsion Polymerization . 1 . Cluster Dynamics. **Macromolecules**, v. 28, p. 3135–3145, 1995.

GONZÁLEZ-ORTIZ, L. J.; ASUA, J. M. Development of particle morphology in emulsion polymerization. 2. Cluster dynamics in reacting systems. **Macromolecules**, v. 29, n. 1, p. 383–389, 1996.

GURGEL, D.; VIEIRA, Y. A.; HENRIQUES, R. O.; MACHADO, R.; OECHSLER, B. F.; JUNIOR, A. F.; DE OLIVEIRA, D. A Comprehensive Review on Core-Shell Polymeric Particles for Enzyme Immobilization. **ChemistrySelect**, v. 7, n. 46, 2022.

GURGEL, D.; HENRIQUES, R. O.; CONRADI, V.; DE OLIVEIRA, D.; MACHADO, R. A. F.; PINTO, J. C.; JUNIOR, A. F.; OECHSLER, B. F. Preparation of functionalizable poly(propylene–styrene)/polyacrylonitrile millimeter-scale particles with core-shell morphology. **Journal of Applied Polymer Science**, n. March, p. 1–14, 2024.

HAYES, R.; AHMED, A.; EDGE, T.; ZHANG, H. Core–shell particles : Preparation, fundamentals and applications in high performance liquid chromatography. **Journal of Chromatography A**, v. 1357, p. 36–52, 2014.

HAYNE, S.; MARGEL, S. Thin coating of silica/polystyrene core-shell nano/microparticles with hierarchical morphology onto polymeric films for fabrication of superhydrophobic surfaces. **Materials Today Chemistry**, v. 30, p. 101497, 2023.

HE, C.; LIU, J.; XIE, L.; ZHANG, Q.; LI, C.; GUI, D.; ZHANG, G.; WU, C. Activity and thermal stability improvements of glucose oxidase upon adsorption on core-shell PMMA-BSA nanoparticles. **Langmuir**, v. 25, n. 23, p. 13456–13460, 2009.

HE, D.; ZHANG, C.; ZENG, G.; YANG, Y.; HUANG, D.; WANG, L.; WANG, H. A multifunctional platform by controlling of carbon nitride in the core-shell structure: From design to construction, and catalysis applications. **Applied Catalysis B: Environmental**, v. 258, n. May, p. 117957, 2019.

HE, L.; CUI, B.; LIU, J.; SONG, Y.; WANG, M.; PENG, D.; ZHANG, Z. Novel electrochemical biosensor based on core-shell nanostructured composite of hollow carbon spheres and polyaniline for sensitively detecting malathion. **Sensors and Actuators, B: Chemical**, v. 258, p. 813–821, 2018.

HO, K. M.; LI, W. Y.; WONG, C. H.; LI, P. Amphiphilic polymeric particles with core-shell nanostructures: Emulsion-based syntheses and potential applications.

Colloid and Polymer Science, v. 288, n. 16–17, p. 1503–1523, 2010.

HONG, S. H.; LAROCQUE, K.; JAUNKY, D. B.; PIEKNY, A.; OH, J. K. Dual disassembly and biological evaluation of enzyme/oxidation-responsive polyester-based nanoparticulates for tumor-targeting delivery. **Colloids and Surfaces B: Biointerfaces**, v. 172, p. 608–617, 2018.

HUANG, W.; MAO, Z.; XU, Z.; XIANG, B.; ZHANG, J. Synthesis and characterization of size-tunable core-shell structural polyacrylate-graft-poly(acrylonitrile-ran-styrene) (ASA) by pre-emulsion semi-continuous polymerization. **European Polymer Journal**, v. 120, n. 30, p. 109247, 2019.

IMAM, A.; SUMAN, S. K.; SINGH, R.; VEMPATAPU, B. P.; RAY, A.; KANAUIA, P. K. Application of laccase immobilized rice straw biochar for anthracene degradation. **Environmental Pollution**, v. 268, 2021.

İSPIRLI DOĞAÇ, Y.; TEKE, M. Urease immobilized core-shell magnetic Fe[NiFe]O₄/alginate and Fe₃O₄/alginate composite beads with improved enzymatic stability properties: removal of artificial blood serum urea. **Journal of the Iranian Chemical Society**, v. 18, n. 10, p. 2637–2648, 2021.

JAIN, S.; CHATTOPADHYAY, S.; JACKERAY, R.; ABID, C. K. V. Z.; SINGH, H. Novel functionalized fluorescent polymeric nanoparticles for immobilization of biomolecules. **Nanoscale**, v. 5, n. 15, p. 6883–6892, 2013.

JAYAWEERA, C. D.; NARAYANA, M. Multi-objective dynamic optimization of seeded suspension polymerization process. **Chemical Engineering Journal**, v. 426, n. December 2020, p. 130797, 2021.

JAYAWEERA, C. D.; WICKRAMASINGHE, C.; NARAYANA, M. Modeling seeded suspension polymerization of core-shell polymer particles using computational fluid dynamics. **Chemical Engineering Science**, v. 231, p. 116277, 2021.

JENJOB, R.; SEIDI, F.; CRESPIY, D. Recent advances in polymerizations in dispersed media. **Advances in Colloid and Interface Science**, v. 260, p. 24–31, 2018.

JENJOB, S.; SUNINTABOON, P.; INPRAKHON, P.; ANANTACHOKE, N.; REUTRAKUL, V. Chitosan-functionalized poly(methyl methacrylate) particles by spinning disk processing for lipase immobilization. **Carbohydrate Polymers**, v. 89, n. 3, p. 842–848, 2012.

JENSEN, A. T.; NETO, W. S.; FERREIRA, G. R.; GLENN, A. F.; GAMBETTA, R.; GONÇALVES, S. B.; VALADARES, L. F.; MACHADO, F. **Synthesis of**

polymer/inorganic hybrids through heterophase polymerizations. [s.l.] Elsevier Ltd, 2017.

JESIONOWSKI, T.; ZDARTA, J.; KRAJEWSKA, B. Enzyme immobilization by adsorption: A review. **Adsorption**, v. 20, n. 5–6, p. 801–821, 2014.

JEYARAMAN, S. N.; SLAUGHTER, G. Membranes, immobilization, and protective strategies for enzyme fuel cell stability. **Current Opinion in Electrochemistry**, v. 29, p. 100753, 2021.

JIN, X.; REN, N.; WU, X.; CHEN, R.; ZHU, X. Preparation, characterization and mechanism study of small size core-shell polymer nanoparticles dissociated from poly(N-isopropylacrylamide) ionic microgels. **Colloids and Surfaces A: Physicochemical and Engineering Aspects**, v. 559, n. August, p. 184–191, 2018.

JING, W.; DU, S.; ZHANG, Z. Synthesis of polystyrene particles with precisely controlled degree of concaveness. **Polymers**, v. 10, n. 4, p. 1–9, 2018.

JINGA, L. I.; TUDOSE, M.; IONITA, P. Laccase–TEMPO as an Efficient System for Doxorubicin Removal from Wastewaters. **International Journal of Environmental Research and Public Health**, v. 19, n. 11, 2022.

JUN, L. Y.; YON, L. S.; MUBARAK, N. M.; BING, C. H.; PAN, S.; DANQUAH, M. K.; ABDULLAH, E. C.; KHALID, M. An overview of immobilized enzyme technologies for dye and phenolic removal from wastewater. **Journal of Environmental Chemical Engineering**, v. 7, n. 2, p. 102961, 2019.

KARLSSON, O. J.; HASSANDER, H.; WESSLÉN, B. Influence of seed polymer molecular weight on polymerization kinetics and particle morphology of structured styrene-butadiene latexes. **Journal of Applied Polymer Science**, v. 77, n. 2, p. 297–311, 2000.

KARTSONAKIS, I. A.; VARDAKAS, P.; GOULIS, P.; PERKAS, N.; KYRIAZIS, I. D.; SKAPERDA, Z.; TEKOS, F.; CHARITIDIS, C. A.; KOURETAS, D. Toxicity assessment of core-shell and superabsorbent polymers in cell-based systems. **Environmental Research**, v. 228, n. August 2022, p. 115772, 2023.

KAUR, I.; GAUTAM, N.; KHANNA, N. D. Synthesis and Characterization of Polypropylene-Grafted Gelatin. **Journal of Applied Polymer Science**, v. 115, n. 5, p. 1226–1236, 2009.

KAUSAR, A. Polyacrylonitrile-based nanocomposite fibers: A review of current developments. **Journal of Plastic Film and Sheeting**, v. 35, n. 3, p. 295–316, 2019.

KELBERT, M.; PEREIRA, C. S.; DARONCH, N. A.; CESCA, K.; MICHELS, C.;

DE OLIVEIRA, D.; SOARES, H. M. Laccase as an efficacious approach to remove anticancer drugs: A study of doxorubicin degradation, kinetic parameters, and toxicity assessment. **Journal of Hazardous Materials**, v. 409, p. 124520, 2021.

KELBERT, M.; DARONCH, N. A.; PEREIRA, C. S.; CESCO, K.; MICHELS, C.; SOARES, H. M. Inhibitory impact of the anticancer drug doxorubicin on anaerobic microbial community. **Aquatic Toxicology**, v. 264, n. September, p. 106706, 2023.

KHANNA, N. D.; KAUR, I.; KUMAR, A. Starch-Grafted Polypropylene: Synthesis and Characterization. **Journal of Applied Polymer Science**, v. 119, n. 5, p. 602–612, 2010.

KOSKINEN, M.; CARL-ERIC WILÉN. Preparation of Core-Shell Latexes for Paper Coatings. **Journal of Applied Polymer Science**, v. 112, p. 1265–1270, 2009.

KUMAR, P.; KERMANSHAHI-POUR, A.; BRAR, S. K.; HE, Q. S.; RAINEY, J. K. Influence of elevated pressure and pressurized fluids on microenvironment and activity of enzymes. **Biotechnology Advances**, v. 68, n. February, p. 108219, 2023.

KURIAN, M.; THANKACHAN, S. Structural diversity and applications of spinel ferrite core - Shell nanostructures- a review. **Open Ceramics**, p. 100179, 2021.

LADOLE, M. R.; POKALE, P. B.; PATIL, S. S.; BELOKAR, P. G.; PANDIT, A. B. Laccase immobilized peroxidase mimicking magnetic metal organic frameworks for industrial dye degradation. **Bioresource Technology**, v. 317, n. June, p. 124035, 2020.

LANDFESTER, K.; BOEFFEL, C.; LAMBLA, M.; SPIESS, H. W. Characterization of interfaces in core-shell polymers by advanced solid-state NMR methods. **Macromolecules**, v. 29, n. 18, p. 5972–5980, 1996.

LE, T. T.; MURUGESAN, K.; LEE, C. S.; VU, C. H.; CHANG, Y. S.; JEON, J. R. Degradation of synthetic pollutants in real wastewater using laccase encapsulated in core-shell magnetic copper alginate beads. **Bioresource Technology**, v. 216, p. 203–210, 2016.

LENZI, M. K.; SILVA, F. M.; LIMA, E. L.; PINTO, C. Semibatch Styrene Suspension Polymerization Processes. **Journal of Applied Polymer Science**, v. 89, p. 3021–3038, 2002.

LI, X.; LI, S.; LIANG, X.; MCCLEMENTS, D. J.; LIU, X.; LIU, F. Applications of oxidases in modification of food molecules and colloidal systems: Laccase, peroxidase and tyrosinase. **Trends in Food Science and Technology**, v. 103, n. March, p. 78–93, 2020.

LIMA, A.; AZEREDO, A. P.; NELE, M.; LIBERMAN, S.; PINTO, J. C. Synthesis and characterization of diolefin/propylene copolymers by ziegler-natta polymerization. **Macromolecular Symposia**, v. 344, n. 1, p. 86–93, 2014.

LIMA, A. F. **Síntese e caracterização de polipropilenos modificados com diolefinas**. [s.l.] Universidade Federal do Rio de Janeiro, 2015.

LIN, J.; LAI, Q.; LIU, Y.; CHEN, S.; LE, X.; ZHOU, X. Laccase – methacryloyl functionalized magnetic particles: Highly immobilized, reusable, and efficacious for methyl red decolourization. **International Journal of Biological Macromolecules**, v. 102, p. 144–152, 2017.

LIN, W.; BIEGLER, L. T.; JACOBSON, A. M. Modeling and optimization of a seeded suspension polymerization process. **Chemical Engineering Science**, v. 65, n. 15, p. 4350–4362, 2010.

LIN, Y.; BILOTTI, E.; BASTIAANSEN, C. W. M.; PEIJS, T. Transparent semi-crystalline polymeric materials and their nanocomposites: A review. **Polymer Engineering and Science**, v. 60, n. 10, p. 2351–2376, 2020.

LOVELL, P. A.; SCHORK, F. J. Fundamentals of Emulsion Polymerization. **Biomacromolecules**, v. 21, n. 11, p. 4396–4441, 2020.

LU, L.; ZHANG, L.; YUAN, L.; ZHU, T.; CHEN, W.; WANG, G.; WANG, Q. Artificial Cellulosome Complex from the Self-Assembly of Ni-NTA-Functionalized Polymeric Micelles and Cellulases. **ChemBioChem**, v. 20, n. 11, p. 1394–1399, 2019.

LUO, H.; LIU, X.; YU, D.; YUAN, J.; TAN, J.; LI, H. Research Progress on Lignocellulosic Biomass Degradation Catalyzed by Enzymatic Nanomaterials. **Chemistry - An Asian Journal**, v. 17, n. 566, p. 1–20, 2022.

MA, J. Z.; LIU, Y. H.; BAO, Y.; LIU, J. L.; ZHANG, J. Research advances in polymer emulsion based on “core-shell” structure particle design. **Advances in Colloid and Interface Science**, v. 197–198, p. 118–131, 2013.

MA, Q.; ZUO, H.; XIA, H.; LIU, P.; ZHANG, G. Influence of dispersion on particle size-distribution based on multi-wavelength scattering measurement. **Optical Engineering**, v. 60, n. 03, p. 1–9, 2021.

MACHADO, R. A. F.; PINTO, J. C.; ARAÚJO, P. H. H.; BOLZAN, A. Mathematical modeling of polystyrene particle size distribution produced by suspension polymerization. **Brazilian Journal of Chemical Engineering**, v. 17, n. 4, p. 395–405, 2000.

MAGRO, M.; BARATELLA, D.; COLÒ, V.; VALLESE, F.; NICOLETTO, C.;

SANTAGATA, S.; SAMBO, P.; MOLINARI, S.; SALVIULO, G.; VENERANDO, A.; BASSO, C. R.; PEDROSA, V. A.; VIANELLO, F. Electrocatalytic nanostructured ferric tannate as platform for enzyme conjugation: Electrochemical determination of phenolic compounds. **Bioelectrochemistry**, v. 132, p. 107418, 2020.

MAKAN, A. C.; SPALLEK, M. J.; DU TOIT, M.; KLEIN, T.; PASCH, H. Advanced analysis of polymer emulsions: Particle size and particle size distribution by field-flow fractionation and dynamic light scattering. **Journal of Chromatography A**, v. 1442, p. 94–106, 2016.

MANOEL, E. A.; PINTO, M.; DOS SANTOS, J. C. S.; TACIAS-PASCACIO, V. G.; FREIRE, D. M. G.; PINTO, J. C.; FERNANDEZ-LAFUENTE, R. Design of a core-shell support to improve lipase features by immobilization. **RSC Advances**, v. 6, n. 67, p. 62814–62824, 2016.

MARTINOVÁ, L.; NOVÁK, J. Polymer nanofibrous material for enzyme immobilization. **Materials Science Forum**, v. 937 MSF, p. 129–135, 2018.

MELO, A.; PESSOA, F. L. P.; PINTO, J. C. Liquid–Liquid Equilibrium in Xylene Solubles (XS) Analysis of Polypropylene. **Macromolecular Reaction Engineering**, v. 17, n. 6, p. 1–14, 2023.

MENG, X.; XU, G.; ZHOU, Q. L.; WU, J. P.; YANG, L. R. Improvements of lipase performance in high-viscosity system by immobilization onto a novel kind of poly(methylmethacrylate-co-divinylbenzene) encapsulated porous magnetic microsphere carrier. **Journal of Molecular Catalysis B: Enzymatic**, v. 89, p. 86–92, 2013.

MIANDAD, R.; REHAN, M.; BARAKAT, M. A.; ABURIAZAIZA, A. S.; KHAN, H.; ISMAIL, I. M. I.; DHAVAMANI, J.; GARDY, J.; HASSANPOUR, A.; NIZAMI, A. S. Catalytic pyrolysis of plastic waste: Moving toward pyrolysis based biorefineries. **Frontiers in Energy Research**, v. 7, n. MAR, p. 1–17, 2019.

MINET, I.; HEVESI, L.; AZENHA, M.; DELHALLE, J.; MEKHALIF, Z. Preparation of a polyacrylonitrile/multi-walled carbon nanotubes composite by surface-initiated atom transfer radical polymerization on a stainless steel wire for solid-phase microextraction. **Journal of Chromatography A**, v. 1217, n. 17, p. 2758–2767, 2010.

MOHAMED, M. A.; JAAFAR, J.; ISMAIL, A. F.; OTHMAN, M. H. D.; RAHMAN, M. A. **Fourier Transform Infrared (FTIR) Spectroscopy**. [s.l.] Elsevier B.V., 2017.

MORSI, R.; BILAL, M.; IQBAL, H. M. N.; ASHRAF, S. S. Laccases and peroxidases: The smart, greener and futuristic biocatalytic tools to mitigate recalcitrant

emerging pollutants. **Science of the Total Environment**, v. 714, 2020.

NADERI, M. Surface Area: Brunauer-Emmett-Teller (BET). In: **Progress in Filtration and Separation**. [s.l.: s.n.]. p. 585–608.

NGUYEN, H. H.; KIM, M. An Overview of Techniques in Enzyme Immobilization. **Applied Science and Convergence Technology**, v. 26, n. 6, p. 157–163, 2017.

PAITAID, P.; H-KITTIKUN, A. Magnetic Cross-Linked Enzyme Aggregates of *Aspergillus oryzae* ST11 Lipase Using Polyacrylonitrile Coated Magnetic Nanoparticles for Biodiesel Production. **Applied Biochemistry and Biotechnology**, v. 190, p. 1319–1332, 2020.

PANDAY, R.; POUDEL, A. J.; LI, X.; ADHIKARI, M.; ULLAH, M. W.; YANG, G. Amphiphilic core-shell nanoparticles: Synthesis, biophysical properties, and applications. **Colloids and Surfaces B: Biointerfaces**, v. 172, n. July, p. 68–81, 2018.

PEDROCHE, J.; DEL MAR YUST, M.; MATEO, C.; FERNÁNDEZ-LAFUENTE, R.; GIRÓN-CALLE, J.; ALAIZ, M.; VIOQUE, J.; GUISÁN, J. M.; MILLÁN, F. Effect of the support and experimental conditions in the intensity of the multipoint covalent attachment of proteins on glyoxyl-agarose supports: Correlation between enzyme-support linkages and thermal stability. **Enzyme and Microbial Technology**, v. 40, n. 5, p. 1160–1166, 2007.

PEIXOTO, L. S.; MELO, P. A.; NELE, M.; PINTO, J. C. Expanded Core/Shell Poly(vinyl acetate)/Poly(vinyl alcohol) Particles for Embolization. **Macromolecular Materials and Engineering**, v. 294, n. 8, p. 463–471, 2009.

PEREIRA, C. S. **Enzymatic process as a potential treatment technology to remove anticancer drugs from wastewater: Laccase-assisted degradation of etoposide**. [s.l.] Universidade Federal de Santa Catarina, 2020.

PEREIRA, C. S.; KELBERT, M.; DARONCH, N. A.; MICHELS, C.; DE OLIVEIRA, D.; SOARES, H. M. Potential of enzymatic process as an innovative technology to remove anticancer drugs in wastewater. **Applied Microbiology and Biotechnology**, v. 104, n. 1, p. 23–31, 2020.

PEREIRA, C. S.; KELBERT, M.; DARONCH, N. A.; CORDEIRO, A. P.; CESCA, K.; MICHELS, C.; DE OLIVEIRA, D.; SOARES, H. M. Laccase-Assisted Degradation of Anticancer Drug Etoposide: By-Products and Cytotoxicity. **Bioenergy Research**, v. 16, n. 4, p. 2105–2114, 2023.

PERES, L. B.; PERES, L. B.; FARIA, T. J.; DE ASSIS, J. V.; DE ALMEIDA, M.

V.; GONÇALVES, O. H.; DE ARAÚJO, P. H. H.; SAYER, C. PLLA/PMMA blend in polymer nanoparticles: influence of processing methods. **Colloid and Polymer Science**, v. 295, n. 9, p. 1621–1633, 2017.

PINTO, M. C. C.; SANTOS, J. G. F.; MACHADO, F.; PINTO, J. C. Suspension Polymerization Processes. **Encyclopedia of Polymer Science and Technology**, n. 7, p. 1–31, 2013.

PINTO, M. C. C.; DE SOUZA E CASTRO, N. L.; CIPOLATTI, E. P.; FERNANDEZ-LAFUENTE, R.; MANOEL, E. A.; FREIRE, D. M. G.; PINTO, J. C. Effects of Reaction Operation Policies on Properties of Core–Shell Polymer Supports Used for Preparation of Highly Active Biocatalysts. **Macromolecular Reaction Engineering**, v. 13, n. 1, p. 1–14, 2019.

PINTO, M. C. C.; EVERTON, S. S.; CIRILO, L. C. M.; DE MELO, T. N.; CIPOLATTI, E. P.; MANOEL, E. A.; PINTO, J. C.; FREIRE, D. M. G. Effect of hydrophobicity degree of polymer particles on lipase immobilization and on biocatalyst performance. **Biocatalysis and Biotransformation**, v. 38, n. 4, p. 304–314, 2020.

RAMLI, R. A.; LAFTAH, W. A.; HASHIM, S. Core-shell polymers: A review. **RSC Advances**, v. 3, n. 36, p. 15543–15565, 2013.

RAN, F.; ZOU, Y.; XU, Y.; LIU, X.; ZHANG, H. Fe₃O₄@MoS₂@PEI-facilitated enzyme tethering for efficient removal of persistent organic pollutants in water. **Chemical Engineering Journal**, v. 375, n. June, 2019.

REN, D.; WANG, Z.; JIANG, S.; YU, H.; ZHANG, S.; ZHANG, X. Recent environmental applications of and development prospects for immobilized laccase: a review. **Biotechnology and Genetic Engineering Reviews**, v. 36, n. 2, p. 81–131, 2020.

RIBEIRO, L. F. B.; GONÇALVES, O. H.; MARANGONI, C.; MOTZ, G.; MACHADO, R. A. F. Chemical resistance of core-shell particles (PS/PMMA) polymerized by seeded suspension. **Polimeros**, v. 27, n. 3, p. 225–229, 2017.

RIVERA-ARMENTA, J. L.; SALAZAR-CRUZ, B. A.; ESPINDOLA-FLORES, A. C.; VILLARREAL-LUCIO, D. S.; DE LEÓN-ALMAZÁN, C. M.; ESTRADA-MARTINEZ, J. Thermal and Thermomechanical Characterization of Polypropylene-Seed Shell Particles Composites. **Applied Sciences (Switzerland)**, v. 12, n. 16, 2022.

RODRIGUES, R. C.; BERENQUER-MURCIA, Á.; CARBALLARES, D.; MORELLON-STERLING, R.; FERNANDEZ-LAFUENTE, R. Stabilization of enzymes via immobilization: Multipoint covalent attachment and other stabilization strategies.

Biotechnology Advances, v. 52, n. 0734–9750, p. 107821, 2021.

RODRIGUEZ-ABETXUKO, A.; SÁNCHEZ-DEALCÁZAR, D.; MUÑUMER, P.; BELOQUI, A. Tunable Polymeric Scaffolds for Enzyme Immobilization. **Frontiers in Bioengineering and Biotechnology**, v. 8, n. August, 2020.

RUDAKIYA, D. M.; GUPTA, A. Laccases in nano-biotechnology: Recent trends and advanced applications. **Recent Advances in Biotechnology**, n. August, p. 39–62, 2019.

RUDIN, A.; CHOI, P. Dispersion and Emulsion Polymerizations. In: **The Elements of Polymer Science & Engineering**. [s.l.: s.n.]. p. 427–447.

SARNELLO, E.; LIU, Y.; PALEN, B.; SUN, E.; ZUO, X.; XU, T.; LI, T. Synthesis and Characterization of Bio-Active GFP-P4VP Core–Shell Nanoparticles. **Catalysts**, p. 28–30, 2020.

SARNELLO, E.; LI, T. Synthesis and advanced characterization of polymer-protein core-shell nanoparticles. **Catalysts**, v. 11, n. 6, p. 1–8, 2021.

SAYER, C.; HENRIQUE, P.; ARAÚJO, H. DE. Synthesis of Polymer Particles with Core-Shell Morphologies. In: **Advanced Polymer Nanoparticles: Synthesis and Surface Modifications**. [s.l.: s.n.]. p. 31–64.

SELVARAJ, V.; SAKTHIVEL, P.; RAJENDRAN, V. Ultrasonics Sonochemistry Effect of ultrasound in the free radical polymerization of acrylonitrile under a new multi-site phase-transfer catalyst – A kinetic study. **Ultrasonics - Sonochemistry**, v. 22, p. 265–271, 2015.

SENICHEV, V. Y.; TERESHATOV, V. V. **General principles governing dissolution of materials in solvents**. Second Edition. [s.l.] ChemTec Publishing, 2014. v. 1

SHANMUGAM, S.; KRISHNASWAMY, S.; CHANDRABABU, R.; VEERABAGU, U.; PUGAZHENDHI, A.; MATHIMANI, T. Optimal immobilization of *Trichoderma asperellum* laccase on polymer coated Fe₃O₄@SiO₂ nanoparticles for enhanced biohydrogen production from delignified lignocellulosic biomass. **Fuel**, v. 273, n. January, p. 117777, 2020.

SHARMA, A.; THATAI, K. S.; KUTHIALA, T.; SINGH, G.; ARYA, S. K. Employment of polysaccharides in enzyme immobilization. **Reactive and Functional Polymers**, v. 167, n. May, p. 105005, 2021.

SILVA, J. C. DA; SANTOS, L. J. DA C.; LUSTOSA, S. M. C.; SILVA, G. DE A.; PAZ, G. M. DA; VIANA, D. DOS S. F.; VIANA, V. G. F. Thermal and toxicological

analysis of commercial polystyrene with recycled polystyrene. **Society and Development**, v. 11, n. January, p. 1–9, 2022.

STUBBS, J. M.; SUNDBERG, D. C. Nonequilibrium morphology development in seeded emulsion polymerization. V. The effect of crosslinking agent. **Journal of Applied Polymer Science**, v. 102, n. 3, p. 2043–2054, 2006.

SU, H.; TIAN, Q.; PRICE, C. H.; XU, L.; QIAN, K. Nanoporous core@shell particles: Design, preparation, applications in bioadsorption and biocatalysis. **Nano Today**, v. 31, p. 100834, 2020.

SUN, H.; WEI, Y.; KONG, X. Z.; JIANG, X. Preparation of uniform polyurea microspheres at high yield by precipitation polymerization and their use for laccase immobilization. **Polymer**, v. 216, n. November 2020, p. 123432, 2021.

SUNDBERG, D. C.; DURANT, Y. G. Latex particle morphology, fundamental aspects: A review. **Polymer Reaction Engineering**, v. 11, n. 3, p. 379–432, 2003.

TAHERAN, M.; NAGHDI, M.; BRAR, S. K.; KNYSTAUTAS, E. J.; VERMA, M.; SURAMPALLI, R. Y. Covalent Immobilization of Laccase onto Nano fibrous Membrane for Degradation of Pharmaceutical Residues in Water. **ACS Sustainable Chemistry & Engineering**, v. 5, p. 10430–10438, 2017a.

TAHERAN, M.; NAGHDI, M.; BRAR, S. K.; KNYSTAUTAS, E. J.; VERMA, M.; SURAMPALLI, R. Y. Degradation of chlortetracycline using immobilized laccase on Polyacrylonitrile-biochar composite nanofibrous membrane. **Science of the Total Environment**, v. 605–606, p. 315–321, 2017b.

TAHERI, S.; CLARK, S. M. Preparation of Self-healing Additives for Concrete via Miniemulsion Polymerization: Formulation and Production Challenges. **International Journal of Concrete Structures and Materials**, v. 15, n. 1, 2021.

TAKUYA TANAKA, REIKO NAKATSURU, YOSHIMI KAGARI, NAOHIKO SAITO, AND M. O. Effect of Molecular Weight on the Morphology of Polystyrene/ Poly(methyl methacrylate) Composite Particles Prepared by the Solvent Evaporation Method†. **Langmuir**, v. 24, n. 1, p. 12267–12271, 2008.

TKACHENKO, V.; VIDAL, L.; JOSIEN, L.; SCHMUTZ, M.; POLY, J. Characterizing the Core-Shell Architecture of Block Copolymer Nanoparticles with Electron Microscopy: A Multi-Technique Approach. **Polymers**, 2020.

ULIANA, N. R.; MACHADO, R. A. F.; SAYER, C.; ARAÚJO, P. H. H. SB-S core-shell particles in semicontinuous seeded emulsion polymerization and their use as impact modifier. **Macromolecular Symposia**, v. 344, n. 1, p. 28–32, 2014.

URREA-QUINTERO, J. H.; HERNANDEZ, H.; OCHOA, S. Towards a controllability analysis of multiscale systems: Application of the set-theoretic approach to a semi-batch emulsion polymerization process. **Computers and Chemical Engineering**, v. 138, p. 106833, 2020.

VAES, D.; VAN PUYVELDE, P. Semi-crystalline feedstock for filament-based 3D printing of polymers. **Progress in Polymer Science**, v. 118, p. 101411, 2021.

VATANKHAH, Z.; DEGHANI, E.; SALAMI-KALAJAHI, M.; ROGHANI-MAMAQANI, H. Seed's morphology-induced core-shell composite particles by seeded emulsion polymerization for drug delivery. **Colloids and Surfaces B: Biointerfaces**, v. 191, n. April, p. 111008, 2020.

VERMETTE, M. L.; HICKS, M. R.; KHOROUSH, K.; TEO, M. Y.; GATES, B. D. Wipe sampling of antineoplastic drugs from workplace surfaces: A review of analytical methods and recommendations. **Hygiene and Environmental Health Advances**, v. 9, n. January, p. 100089, 2024.

VIEIRA, Y. A.; GURGEL, D.; HENRIQUES, R. O.; MACHADO, R. A. F.; DE OLIVEIRA, D.; OECHSLER, B. F.; FURIGO JUNIOR, A. A Perspective Review on the Application of Polyacrylonitrile-Based Supports for Laccase Immobilization. **Chemical Record**, p. 1–16, 2021.

VIEIRA, Y. A.; HENRIQUES, R. O.; GURGEL, D.; HARTMANN, D.; MACHADO, R. A. F.; OECHSLER, B. F.; JR, A. F. Functionalized polyacrylonitrile particles as a promising support for the immobilization of laccase from *Trametes versicolor*. **Journal of Applied Polymer Science**, n. March, p. 1–14, 2023.

VIVALDO-LIMA, E.; WOOD, P. E.; HAMIELEC, A. E.; PENLIDIS, A. An Updated Review on Suspension Polymerization. **Industrial and Engineering Chemistry Research**, v. 36, n. 4, p. 939–965, 1997.

WAN, M.; XIANG, F.; LIU, Z.; GUAN, D.; SHAO, Y.; ZHENG, L.; JIN, M.; SHE, Y.; CAO, L.; JIN, F.; CHEN, R.; WANG, S.; WU, Y.; ABD EL-ATY, A. M.; WANG, J. Novel Fe₃O₄@metal-organic framework@polymer core-shell-shell nanospheres for fast extraction and specific preconcentration of nine organophosphorus pesticides from complex matrices. **Food Chemistry**, v. 365, n. January, p. 130485, 2021.

WANG, H.; PENG, X.; ZHANG, H.; YANG, S.; LI, H. Microorganisms-promoted biodiesel production from biomass: A review. **Energy Conversion and Management: X**, v. 12, n. 2590–1745, p. 100137, 2021a.

WANG, H.; PENG, X.; LI, H.; GIANNIS, A.; HE, C. Recent Biotechnology

Advances in Bio-Conversion of Lignin to Lipids by Bacterial Cultures. **Frontiers in Chemistry**, v. 10, n. April, p. 1–8, 2022.

WANG, J.; PAN, K.; GIANNELIS, E. P.; CAO, B. Polyacrylonitrile/polyaniline core/shell nanofiber mat for removal of hexavalent chromium from aqueous solution: Mechanism and applications. **RSC Advances**, v. 3, n. 23, p. 8978–8987, 2013a.

WANG, Q.; CUI, J.; LI, G.; ZHANG, J.; LI, D.; HUANG, F.; WEI, Q. Laccase Immobilized on a PAN/Adsorbents Composite Nanofibrous Membrane for Catechol Treatment by a Biocatalysis/Adsorption Process. **Molecules**, p. 3376–3388, 2014.

WANG, S.; YUE, K.; LIU, L.; YANG, W. Photoreactive, core-shell cross-linked/hollow microspheres prepared by delayed addition of cross-linker in dispersion polymerization for antifouling and immobilization of protein. **Journal of Colloid and Interface Science**, v. 389, n. 1, p. 126–133, 2013b.

WANG, Y.; KE, Y.; LI, J.; DU, S.; XIA, Y. Dispersion behavior of core-shell silica-polymer nanoparticles. **China Particuology**, v. 5, n. 4, p. 300–304, 2007.

WANG, Z. Y.; JU, C. J.; ZHANG, R.; HUA, J. Q.; CHEN, R. P.; LIU, G. X.; YIN, K.; YU, L. Acceleration of the bio-reduction of methyl orange by a magnetic and extracellular polymeric substance nanocomposite. **Journal of Hazardous Materials**, v. 420, n. July, p. 126576, 2021b.

WOLF, B.; ECKELT, A.; ECKELT, J. **Encyclopedia of Polymer Science and Technology**. [s.l: s.n.].

WU, E.; LI, Y.; HUANG, Q.; YANG, Z.; WEI, A.; HU, Q. Laccase immobilization on amino-functionalized magnetic metal organic framework for phenolic compound removal. **Chemosphere**, v. 233, p. 327–335, 2019.

WU, Q.; XU, Z.; DUAN, Y.; ZHU, Y.; OU, M.; XU, X. Immobilization of tyrosinase on polyacrylonitrile beads: biodegradation of phenol from aqueous solution and the relevant cytotoxicity assessment. **RSC Advances**, v. 7, p. 28114–28123, 2017.

XIAO, Z.; SUN, N. Crystallization behavior for metallocene-catalyzed isotactic polypropylene in alkane solvents of various molecular sizes. **Journal of Thermal Analysis and Calorimetry**, v. 124, n. 1, p. 295–303, 2016.

XU, W.; YANG, W.; GUO, H.; GE, L.; TU, J.; ZHEN, C. Constructing a TiO₂/PDA core/shell nanorod array electrode as a highly sensitive and stable photoelectrochemical glucose biosensor. **RSC Advances**, v. 10, n. 17, p. 10017–10022, 2020.

XU, X.; CHEN, T.; XU, L.; LIN, J. Immobilization of laccase on magnetic nanoparticles for enhanced polymerization of phenols. **Enzyme and Microbial Technology**, v. 172, n. October 2023, p. 110331, 2024.

XU, X. J.; GAN, L. M. Recent advances in the synthesis of nanoparticles of polymer latexes with high polymer-to-surfactant ratios by microemulsion polymerization. **Current Opinion in Colloid and Interface Science**, v. 10, n. 5–6, p. 239–244, 2005.

YADAV, A.; YADAV, P.; KUMAR SINGH, A.; KUMAR, V.; CHINTAMAN SONAWANE, V.; MARKANDEYA; NARESH BHARAGAVA, R.; RAJ, A. Decolourisation of textile dye by laccase: Process evaluation and assessment of its degradation bioproducts. **Bioresource Technology**, v. 340, n. June, p. 125591, 2021.

YANG, X.; XIE, Y. Recent advances in polymeric core – shell nanocarriers for targeted delivery of chemotherapeutic drugs. **International Journal of Pharmaceutics**, v. 608, n. July, p. 121094, 2021.

YASSIN, M. A.; GAD, A. A. M. Immobilized Enzyme on Modified Polystyrene Foam Waste: A Biocatalyst for Wastewater Decolorization. **Journal of Environmental Chemical Engineering**, v. 8, n. 5, p. 104435, 2020.

YILDIZ, U.; CAPEK, I. Microemulsion polymerization of styrene in the presence of macroinimer. **Polymer**, v. 44, n. 8, p. 2193–2200, 2003.

YUAN, Y.; WANG, J.; NI, X.; CAO, Y. A biosensor based on hemoglobin immobilized with magnetic molecularly imprinted nanoparticles and modified on a magnetic electrode for direct electrochemical determination of 3-chloro-1, 2-propandiol. **Journal of Electroanalytical Chemistry**, v. 834, n. September 2018, p. 233–240, 2019.

ZETTLEMOYER, A. C. **Hydrophobic Surfaces**. [s.l.] ACADEMIC PRESS, INC., 1968.

ZHANG, H. Controlled/"living" radical precipitation polymerization: A versatile polymerization technique for advanced functional polymers. **European Polymer Journal**, v. 49, n. 3, p. 579–600, 2013.

ZHANG, S.; ZHANG, Q.; SHANG, J.; MAO, Z.; YANG, C. Measurement methods of particle size distribution in emulsion polymerization. **Chinese Journal of Chemical Engineering**, v. 39, p. 1–15, 2021a.

ZHANG, S.; BILAL, M.; ZDARTA, J.; CUI, J.; KUMAR, A.; FRANCO, M.; FERREIRA, L. F. R.; IQBAL, H. M. N. Biopolymers and nanostructured materials to

develop pectinases-based immobilized nano-biocatalytic systems for biotechnological applications. **Food Research International**, v. 140, n. June 2020, p. 109979, 2021b.

ZHANG, S.; MA, X.; ZHU, Y.; GUO, R. Colloids and Surfaces A: Physicochemical and Engineering Aspects Dispersion polymerization of styrene / acrylonitrile in polyether stabilized by macro-RAFT agents. **Colloids and Surfaces A: Physicochemical and Engineering Aspects**, v. 647, n. February, p. 129166, 2022.

ZHAO, C.; LI, C.; CHEN, M.; NIU, T.; ZHAO, Q.; NI, T.; YAN, D.; WU, W.; LIU, D. Effective removal of antineoplastic doxorubicin by 0D Nb₂O₅ quantum dots embed 3D porous C-doped g-C₃N₄: Degradation mechanism, pathway and toxicity assessment. **Applied Surface Science**, v. 612, n. November 2022, p. 155861, 2023.

ZHAO, W.; KUMAR KUNDU, C.; LI, Z.; LI, X.; ZHANG, Z. Flame retardant treatments for polypropylene: Strategies and recent advances. **Composites Part A: Applied Science and Manufacturing**, v. 145, n. October 2020, p. 106382, 2021.

ZHOU, W.; ZHANG, W.; CAI, Y. Laccase immobilization for water purification: A comprehensive review. **Chemical Engineering Journal**, v. 403, n. April 2020, p. 126272, 2021.

ZHU, S.; HAMIELEC, A. **Polymerization Kinetic Modeling and Macromolecular Reaction Engineering**. [s.l.] Elsevier B.V., 2012. v. 4

ZOFAIR, S. F. F.; AHMAD, S.; HASHMI, M. A.; KHAN, S. H.; KHAN, M. A.; YOUNUS, H. Catalytic roles, immobilization and management of recalcitrant environmental pollutants by laccases: Significance in sustainable green chemistry. **Journal of Environmental Management**, v. 309, n. January, p. 114676, 2022.

